PHOSPHONATE AND BISPHOSPHONATE-FUNCTIONALIZED POLY(β-AMINO ESTER)S AND POLYETHYLENIMINES FOR BIOMEDICAL APPLICATIONS

by

Mirac Tatlıyüz

B.S., Chemistry, Boğaziçi University, 2014

Submitted to the Institute for Graduate Studies in
Science and Engineering in partial fulfillment of
The requirements for the degree of
Master of Science

Graduate Program in Chemistry

Boğaziçi University

2017

PHOSPHONATE AND BISPHOSPHONATE-FUNCTIONALIZED POLY(β-AMINO ESTER)S AND POLYETHYLENIMINES FOR BIOMEDICAL APPLICATIONS

APPROVED BY:

Prof. Duygu Avcı Semiz (Thesis Supervisor)	.....
Assoc. Prof. Ersin Acar	.....
Assoc. Prof. Havva Funda Yağcı Acar	.....

DATE OF APPROVAL: 03.08.2017

Dedicated to my family...

ACKNOWLEDGEMENTS

First of all, I would like to deeply thank my supervisor Prof. Duygu Avcı Semiz for her valuable guidance, advices, attention and encouragement throughout my research. I gained lots of experience thanks to her and I am very appreciated to do master's degree under her supervision.

I want to express my thanks to my committee members Assoc. Prof. Ersin Acar and Assoc. Prof. Havva Funda Yağcı Acar for politely giving their valuable time for reviewing the final manuscript and for their constructive comments and recommendations.

I would like to thank my dear friends Tayfun Kamit, Ömer Pehlivan and Ömer Çorbacı for their friendship and advices. I would also like to thank my dear group friends Melek Naz Güven, Ece Akyol, Tuğçe Nur Eren, Betül Bingöl, Seçkin Altuncu and Türkan Gençoğlu for their help and supportive friendship.

I would also like to thank all members of Chemistry Department for their help.

I want to express my gratitude to my mother, father, sister and brother for their endless love, support and encouragement throughout my whole life.

This research has been financially supported by The Scientific and Technological Research Council of Turkey (TÜBİTAK) [114Z926].

ABSTRACT

PHOSPHONATE AND BISPHOSPHONATE-FUNCTIONALIZED POLY(β-AMINO ESTER)S AND POLYETHYLENIMINES FOR BIOMEDICAL APPLICATIONS

In the first part of this study, phosphonate/bisphosphonate end-modified poly(β-amino ester)s (PBAEs) are synthesized and their pH sensitivity and drug delivery properties are investigated. Synthesis of the polymers involves two steps: i) preparation of acrylate-terminated polymers from reactions of poly(ethylene glycol) diacrylate (PEGDA, M_n=575) and 1,6-hexanediol diacrylate (HDDA) with propyl amine (PA) or 5-amino-1-pentanol (HP) and ii) reaction of these polymers with a phosphonate or a bisphosphonate-functionalized amine to give phosphonate/bisphosphonate end-modified PBAEs. The pH sensitivity of the polymers are determined, the pK_b values ranging 4.90 to 7.50. Two of the micelle forming PBAEs were investigated for the delivery of the chemotherapy drug Doxorubicin (DOX). The micelles released DOX slowly at pH 7.4 (less than 20% in 120 hours). However, DOX release at pH 5.5 was fast (60% in 120 hours) because of the dissolution of the micelles at the acidic pH. Results of this study demonstrated the potential of the tested polymers as drug delivery systems.

In the second part, phosphonate/bisphosphonate functionalized polyethylenimines (PEIs) (branched, M_n= 1.8 and 10 kDa) are synthesized for possible gene transfer applications. Synthesis of polymers involved Michael Addition reactions of diethyl vinylphosphonate (P1), tetraethyl vinylidene bisphosphonate (P2) and PEIs. Preliminary examinations showed some transfection efficiencies for P2 substituted PEIs. Moreover, P2 substitution decreased the toxicity of the polymers *in vitro*.

ÖZET

BİYOMEDİKAL UYGULAMALAR İÇİN FOSFONAT VE BİFOSFONAT FONKSİYONLU POLİ (β-AMİNO ESTER) VE POLİETİLENİMİNLER

Bu çalışmanın ilk kısmında, sonları fosfonat ve bifosfonat ile modifiye edilmiş poli(β-amino ester)ler (PBAE) sentezlendi ve bunların pH ve ilaç salınım özellikleri araştırıldı. Polimerlerin sentezi iki aşamada gerçekleşti: i) poli(etilen glikol) diakrilat (PEGDA, M_n=575) ve 1,6-hekzan diol diakrilat (HDDA)ın propil amin (PA) veya 5-amino-1-pentanol (HP) ile reaksiyonlarından akrilat sonlu polimerler hazırlanması ve ii) sonları fosfonat/bifosfonat ile modifiye edilmiş (PBAE)ler elde etmek için ilk basamakta sentezlenen polimerlerin fosfonat ya da bifosfonat fonsiyonlu aminler ile reaksiyonu. Polimerlerin pH duyarlılıkları belirlendi ve pK_b değerlerinin 4.90 ile 7.50 arasında değiştiği bulundu. İki tane misel yapabilen PBAE, kanser ilacı olan Doksorubisin'in salınımı için araştırıldı. pH 7.4'de miseller DOX'u yavaşca saldı (120 saat içinde %20 den daha az). Ancak, miselerin asidik ortamda bozulmasından dolayı pH 5.5'de DOX daha fazla salındı (120 saat içinde %60). Bu çalışmanın sonuçları test edilen polimerlerin ilaç salınım sistemlerinde kullanılma potensiyelleri olduğunu gösterdi.

İkinci kısımda, fosfonat ve bifosfonat ile fonsiyonlu polietileniminler (PEI) (dallı, M_n= 1.8 ve 10 kDa) gen transfer uygulamaları için sentezlendi. Polimerler, dietil vinil fosfonat (P1), tetraetil viniliden bifosfonat (P2) ve PEI'in Michael katılma reaksiyonuyla sentezlendi. Önsonuçlar P2 eklenmiş polimerlerin bir miktar gen taşıyabildiklerini gösterdi. Ayrıca, P2 eklenmesi in vitro toksisiteyi azalttı.

TABLE OF CONTENTS

ACKNOWLEDGEMENTS iv

ABSTRACT v

ÖZET vi

LIST OF FIGURES ix

LIST OF TABLES xii

LIST OF SYMBOLS xiv

TABLE OF CONTENTS vii

LIST OF ACRONYMS/ABBREVIATIONS xvi

1. INTRODUCTION 1

1.1. Poly(β-amino ester)s 1

1.1.1. Gene Delivery Applications 1

1.1.2. Drug Delivery Applications 4

1.1.3. Tissue Engineering Applications 7

1.2. Phosphorous Based Biomaterials 15

1.3. Polyethylenimines 16

1.3.1. Gene Delivery Applications 17

1.3.2. CO_2 Capture Applications 19

1.3.3. Antiviral Microbicide Applications 21

2. OBJECTIVES 23

3. EXPERIMENTAL WORK 24

3.1. Materials 24

3.2. Characterization 24

3.3. Synthesis of Starting Materials 25

3.3.1. Synthesis of diethyl 2-aminoethylphosphonate (A1) 25

3.3.2. Synthesis of bisphosphonate-functionalized 4,9-dioxa-1,12 dodecanediamine (A2) 25
3.4. PBAEs 26
3.4.1. Synthesis of PBAEs Macromers 26
3.4.1.1. HDDA:PA 26
3.4.1.2. HDDA:HP. 26
3.4.1.3. PEGDA:PA 27
3.4.1.4. PEGDA:HP 27
3.4.2. Synthesis of Phosphonate and Bisphosphonate-Functionalized PBAEs 27
3.4.2.1. [HDDA:PA]-A1. 27
3.4.2.2. [HDDA:HP]-A1. 28
3.4.2.3. [PEGDA:PA]-A1 28
3.4.2.4. [PEGDA:HP]-A1 28
3.4.2.5. [HDDA:PA]-A2. 29
3.4.3. Measurement of pK_b 29
3.4.4. pH-Dependent Light Transmittance 29
3.4.5. Preparation of Micelles 29
3.4.6. Characterization of Micelles 30
3.4.7. DOX Encapsulation and Release 30
3.5. Polyethylenimines 31
3.5.1. Synthesis of Phosphonated PEIs 31
3.5.1.1. PEI-P1 31
3.5.1.2. PEI-P2 31
3.5.1.3. PEI-(HDDA:A1) 31
3.5.2. In Vitro Uptake of Synthesized Polymers/pDNA Complexes 32
4. RESULTS AND DISCUSSION 33
4.1. PBAEs 33

4.1.1. Synthesis of Phosphonate and Bisphosphonate-Functionalized Amines 33
4.1.2. Synthesis of PBAE Macromers 36
4.1.3. Synthesis of Phosphonate and Bisphosphonate Functionalized PBAEs 40
4.1.4. pH Sensitivity of PBAEs 44
4.1.5. Synthesis and Characterization of Micelles 48
4.1.6. DOX Encapsulation and Release 52
4.2. Polyethylenimines 54
4.2.1. Synthesis of Phosphonate and Bisphosphonate-Functionalized PEIs 54
4.2.2. Cellular Uptake and Transfection Efficiency of Polymers 56
5. CONCLUSIONS 59
REFERENCES 60

LIST OF FIGURES

Figure 1.1. Synthesis of poly(β-amino ester)s 1

Figure 1.2. (A) Synthesis of acrylate-terminated C32 polymer (C32-Ac). (B) Synthesis of end-modified C32 polymers (C32-X). (C) Amine capping molecules [2]. 2

Figure 1.3. Synthesis of HPAEs for gene delivery via an "A2+B3+C2" type Michael addition reaction [3]. 3

Figure 1.4. Preparation of PEI−PBAE (C16) polymer [4]. 4

Figure 1.5. Preparation of PBAEs, PEG-PBAE block copolymers and titration curves of some of PBAEs [7]. 5

Figure 1.6. (a) Chemical structure of MPEG-PAE block copolymer (MPEG-PAE). (b) Schematic diagram of pH-responsive MPEG-PEG micelles at weakly pH condition. (c) Size distribution of MPEG-PAE micelles in PBS [8]. 6

Figure 1.7. Schematic diagram of the preparation of PDNs and the triggered-release behavior of shRNA and DOX from PDNs [9]. 7

Figure 1.8. (A) Load'ng, release, and dissociation of DOX from micelles upon changes of pH value, DTT concentration or dual factors. (B) Synthesis routine of reducible PBAE-PEG copolymers [10]. 8

Figure 1.9. General synthesis scheme and chemical structures of used amines and diacrylates [15]. 10

Figure 1.10. Degradation behavior of polymers synthesized from one amine and four acrylates [15]. 11

Figure 1.11. Schematic illustration of macromer synthesis, network formation and degradation [16]. 11

Figure 1.12. Tensile and compressive moduli initially and with degradation for networks formed with different monomer ratios [16]. 12

Figure 1.13. Effect of macromer molecular weight on tensile and compressive modulus [17]. 13

Figure 1.14. Network mass loss with degradation for the various MMW of J6 (A) [17]. .. 14

Figure 1.15. Synthesis schematic for PBAE crosslinkers, network formation with PBAE and MMA. As degradation occurs, PBAE leaves networks and thus overall MMA content increases which increases T_g [19]. 14

Figure 1.16. Structures of methacrylamides and bismethacrylamide monomers [22]. 15

Figure 1.17. Hydrolysis of camdronate prodrug under physiological conditions [23]. 16

Figure 1.18. Proposed mechanism of release of tryptophan [23]. 16

Figure 1.19. Relative atomic % of (a) Ca and (b) P on inner and outer surface of normal and phosphonated scaffold [24]. 17

Figure 1.20. Shapes of (A) linear PEI and (B) branched PEI [26]. 18

Figure 1.21. Schematic representation of proton sponge effect of PEI [30]. 18

Figure 1.22. Schematic illustration of the structure of used groups to modify PEI [33]. 19

Figure 1.23. Cytotoxicity of PEI-Cys derivatives determined by MTT assays [34]. 20

Figure 1.24. Schematic diagram of PEI status in MCM-41 at (A) low T and (B) high T [40]. 20

Figure 1.25. Effect of cationic degree on bactericidal ratio of QPEI [42]. 21

Figure 1.26. Bacterial growth rate of Streptococcus mutans and Lactobacillus casei following direct contact with aged glass ionomer cements (Fuji I and Ketac-Cem) incorporating 0 and 1% w/w QPEI [41]. 22

Figure 4.1. Structures of phosphonate and bisphosphonate-functionalized amines. 33

Figure 4.2. Synthesis of A1. 33

Figure 4.3. ^{1}H NMR spectrum of A1. 34

Figure 4.4. FTIR spectrum of A1. 34

Figure 4.5. Synthesis of A2. 35

Figure 4.6. ^{1}H NMR spectrum of A2. 35

Figure 4.7. Synthesis route of macromers and structures of diacrylates and amines. 37

Figure 4.8. ^{1}H-NMR spectrum of HDDA:PA macromer (diacrylate to amine ratio is 1.2:1 mol). 38

Figure 4.9. ^{1}H-NMR spectrum of HDDA:HP macromer (diacrylate to amine ratio is 1.2:1 mol). 38

Figure 4.10. ^{1}H-NMR spectrum of PEGDA:PA macromer (diacrylate to amine ratio is 1.2:1 mol). 39

Figure 4.11. ^{1}H-NMR spectrum of PEGDA:HP macromer (diacrylate to amine ratio is 1.2:1 mol). 39

Figure 4.12. FTIR spectra of PEGDA:HP and HDDA:HP macromers. 40

Figure 4.13. Structures of A1-based polymers. 41

Figure 4.14. ^{1}H-NMR spectrum of [HDDA:HP]-A1 polymer. 42

Figure 4.15. ^{1}H-NMR spectrum of [PEGDA:PA]-A1 polymer. 42

Figure 4.16. FTIR spectra of [HDDA:PA]-A1 and [PEGDA:PA]-A1. 43

Figure 4.17. FTIR spectra of [HDDA:HP]-A1 and [PEGDA:HP]-A1. 43

Figure 4.18. FTIR spectrum of [HDDA:PA]-A2. 44

Figure 4.19. Structure of [HDDA:PA]-A2. 44

Figure 4.20. pH titration curve of macromers (1:1 ratio). 45

Figure 4.21. pH titration curve of macromers (1.2:1 ratio). 46

Figure 4.22. pH titration curve of polymers (1:1 ratio). 46

Figure 4.23. pH titration curve of polymers (1.2:1 ratio). 47

Figure 4.24. Transmittance curves of HDDA-based polymers. 48

Figure 4.25. Structure of phosphonate and bisphosphonate end functionalized polymers.. 49

Figure 4.26. DLS result of DOX-loaded [HDDA(1.2):PA(1)]-A1 micelles. 50

Figure 4.27. DLS result of unloaded [HDDA(1.2):PA(1)]-A1 micelles. 50

Figure 4.28. DLS result of DOX-loaded [HDDA(1.2):PA(1)]-A2 micelles. 51

Figure 4.29. SEM image of DOX-loaded [HDDA(1.2):PA(1)]-A1 micelles. 51

Figure 4.30. SEM image of DOX-loaded [HDDA(1.2):PA(1)]-A2 micelles. 52

Figure 4.31. Release profiles of DOX-loaded [HDDA(1.2):PA(1)]-A1 micelles in different pH buffer solutions. 53

Figure 4.32. Release profiles of DOX-loaded [HDDA(1.2):PA(1)]-A2 micelles in different pH buffer solutions. 53

Figure 4.33. ^{1}H-NMR spectrum of PEI-P1(0.5). 55

Figure 4.34. ^{1}H-NMR spectrum of PEI-P2(0.13). 55

Figure 4.35. FTIR spectra of PEI-P1-0.5 and PEI-P2-0.5. 56

Figure 4.36. Transfection effieciencies of PEI (25 kDa) and the synthesized polymers at a DNA:polymer ratio of 1:5 and 1:10. 58

LIST OF TABLES

Table 4.1. Solubilities of macromers. 37

Table 4.2. Repeating units (n) of macromers. 37

Table 4.3. pK_b values of macromers and polymers. 47

Table 4.4. Synthesized phosphonate and bisphosphonate-substituted 1.8 kDa PEIs. 56

LIST OF SYMBOLS

M_n	Number average molecular weight
pK_b	Base dissociation constant
T	Transmittance
T_g	Glass transition temperature

LIST OF ACRONYMS/ABBREVIATIONS

A1	Diethyl 2-aminoethylphosphonate
A2	Bisphosphonated 4,9-dioxa-1,12-dodecanediamine
DOX	Doxorubicin
DLS	Dynamic Light Scattering
HDDA	1,6-Hexane diol diacrylate
HP	5-amino-1-pentanol
FT-IR	Fourier Transform Infrared Spectroscopy
MWCO	Molecular weight cut off
NMR	Nuclear Magnetic Resonance spectroscopy
P1	Diethyl vinylphosphonate
P2	Tetraethyl vinylidene bisphosphonate
PA	Propyl amine
PBAE	Poly β-amino ester
PBS	Phosphate buffered saline
PEGDA	Poly(ethylene glycol) diacrylate
PEI	Polyethylenimine
UV	Ultraviolet
SEM	Scanning electron microscope

1. INTRODUCTION

1.1. Poly(β-amino ester)s

Poly(β-amino ester)s (PBAEs) are very important polymers for biomaterials because of their pH-sensitivity, biodegradability and high biocompatibility. They are synthesized by the aza-Michael Addition reaction of primary or secondary amines and diacrylates without solvents or catalysts (Figure 1.1). Their backbones consist of amine and ester groups and they can be degraded under physiological conditions into small molecules such as diols and poly(acrylic acid)s. Their degraded products have no or low toxicity, so they can be used in some biomedical applications such as drug and gene delivery vehicles and tissue engineering scaffolds, for example.

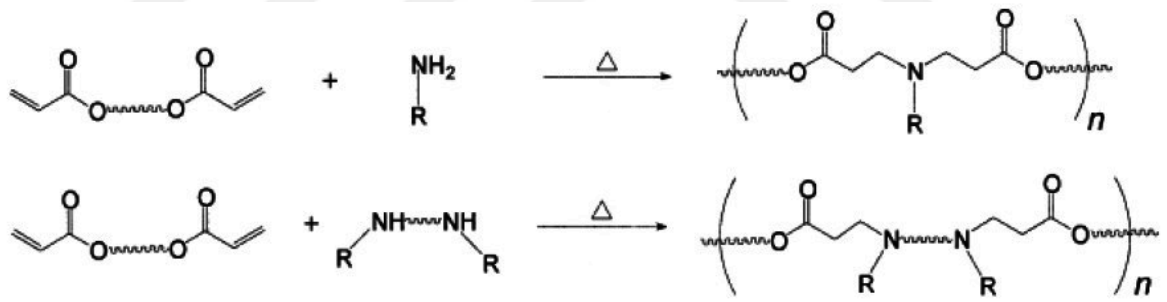

Figure 1.1. Synthesis of poly(β-amino ester)s

1.1.1. Gene Delivery Applications

PBAEs are biodegradable cationic polymers, have shown low cytotoxicity compared to polyethylenimine (PEI) which is a widely studied polymer for gene delivery and so they are developed as non-viral gene delivery vehicles [1]. They have ability to bind negatively charged nucleotides and form polyplexes by electrostatic interactions. Because of biophysical properties of PBAE polyplexes, they can overcome critical barriers to gene delivery at the cellular level, including cellular uptake and endosomal escape via pH buffering.

Some research showed that transfection efficiency and biocompatibility were affected by changing the end-groups of the polymer, its molecular weight or branching. For example, a recent study showed that variations in the terminal amine structure have large effects on the physical properties of polymer-DNA complexes, their cellular uptake, and subsequent transfection (Figure 1.2) [2].

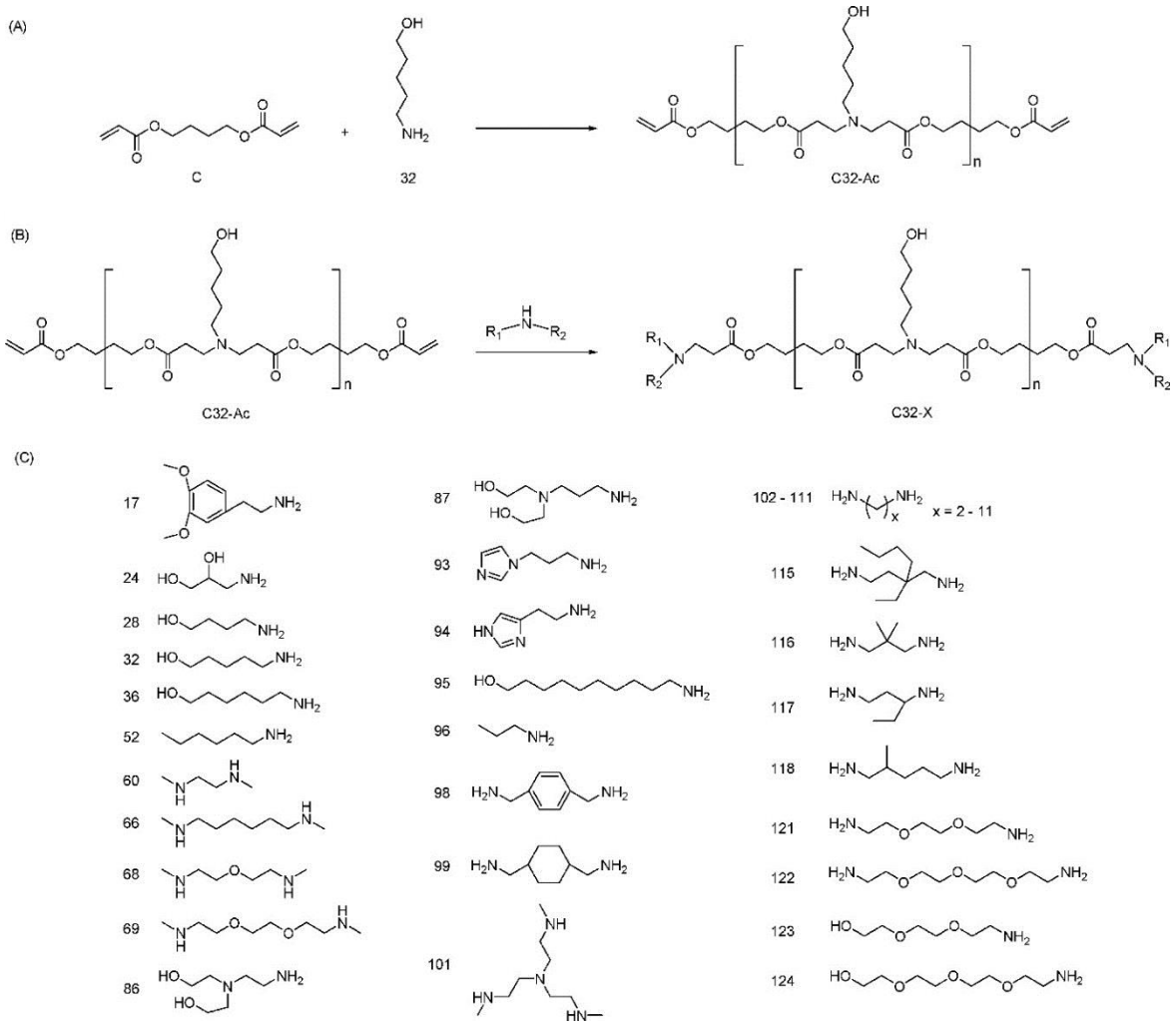

Figure 1.2. (A) Synthesis of acrylate-terminated C32 polymer (C32-Ac). (B) Synthesis of end-modified C32 polymers (C32-X). (C) Amine capping molecules [2].

Another study investigated the effects of molecular weight and configuration of highly branched PBAEs on gene transfection biocompatibility and efficiency. Higher gene transfection efficiency and low cytotoxicity were achieved by highly branched PBAEs with high molecular weight. The interactions of highly branched PBAE/DNA polyplexes

with cell membrane account for the favorable correlation between biocompatibility and molecular weight (Figure 1.3) [3].

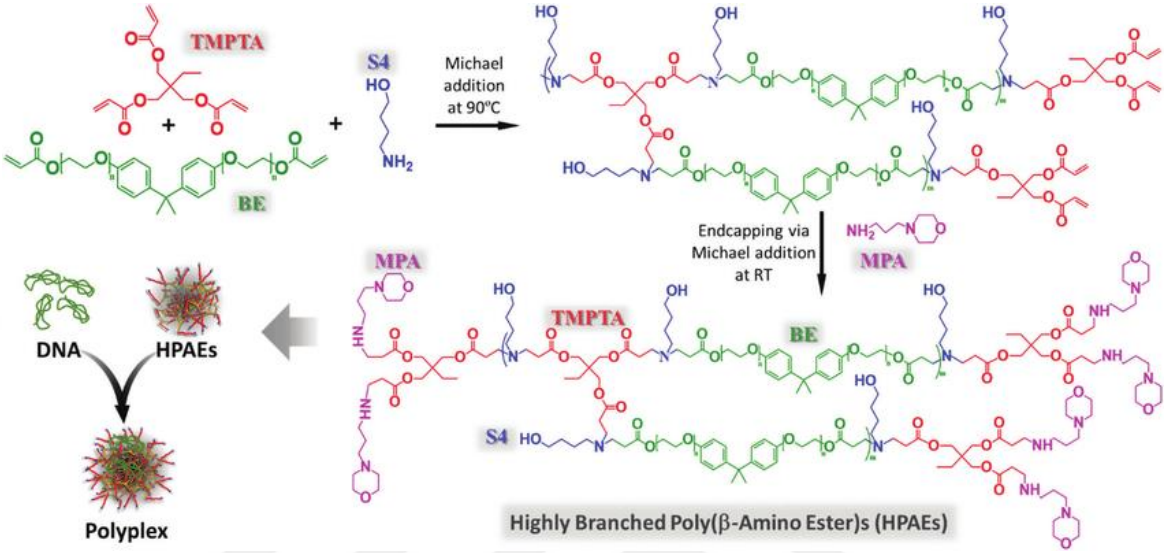

Figure 1.3. Synthesis of HPAEs for gene delivery via an "A2+B3+C2" type Michael addition reaction [3].

Gene therapy has shown great potential for treating some serious diseases but building efficient and non-toxic gene delivery systems is a major challenge for clinical therapy. Minicircle DNA (mcDNA) is an enhanced non-viral DNA vector which shows important profiles in biosafety. A study reported a novel amphiphilic polymer containing PEI modified PBAE for efficient mcDNA delivery in vivo. This polymer could condense mcDNA into a nanoscaled structure and showed good transfection efficiency without any cytotoxicity (Figure 1.4) [4].

PBAEs with high molecular weight show good transfection efficiency but they show considerable toxicities. In order to solve this problem, trigger-responsive PBAEs were developed. Photo-responsive PBAEs can be rapidly cleaved upon external UV light triggering intracellular DNA release as well as decreased material toxicity [5].

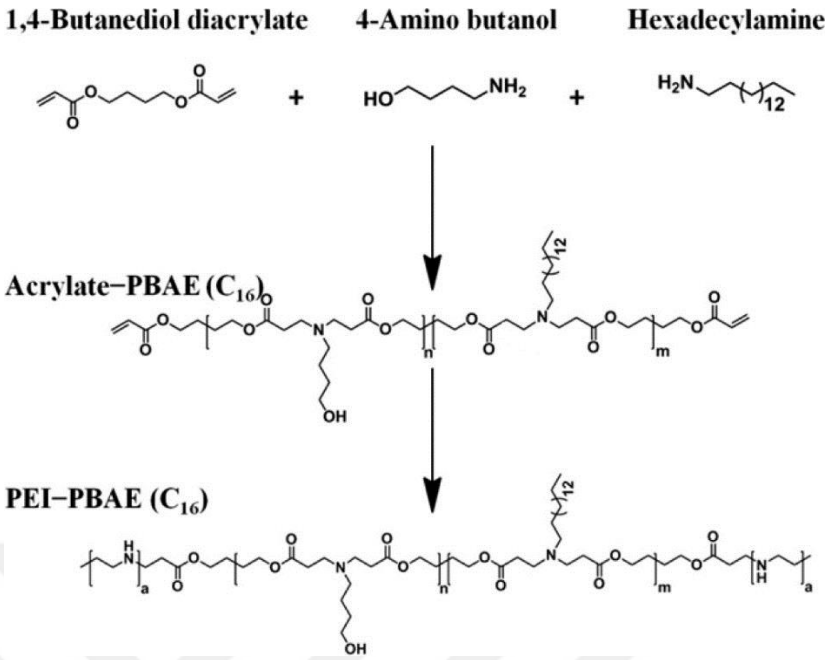

Figure 1.4. Preparation of PEI−PBAE (C16) polymer [4].

1.1.2. Drug Delivery Applications

PBAEs are biodegradable polymers and they can be formed as nanoparticles because of their amphiphilic characteristics. Due to their tertiary amine structures, they have higher buffer capacity. They are insoluble at physiological pH (7.4) because of their unprotonated structures but they are soluble if pH of the medium is less than 6.5. It is known that cancer cells have lower pH medium compared to normal cells because of less oxygen and this property can be used for drug delivery strategies [6].

pH sensitivity of PBAEs can be modulated by changing alkyl groups of diacrylates and amines [7] (Figure 1.5). Generally, pK_b value of polymers can be increased by decreasing alkyl chain length of amines and increasing alkyl chain length of acrylates. PBAEs constitute the hydrophobic part of amphiphilic copolymers and poly(ethylene glycol) (PEG) in the main chain is the hydrophilic segment. For instance, camptothecin release was investigated from pH responsive polymeric micelles of MPEG-poly(β-amino ester) block copolymer [8] (Figure 1.6).

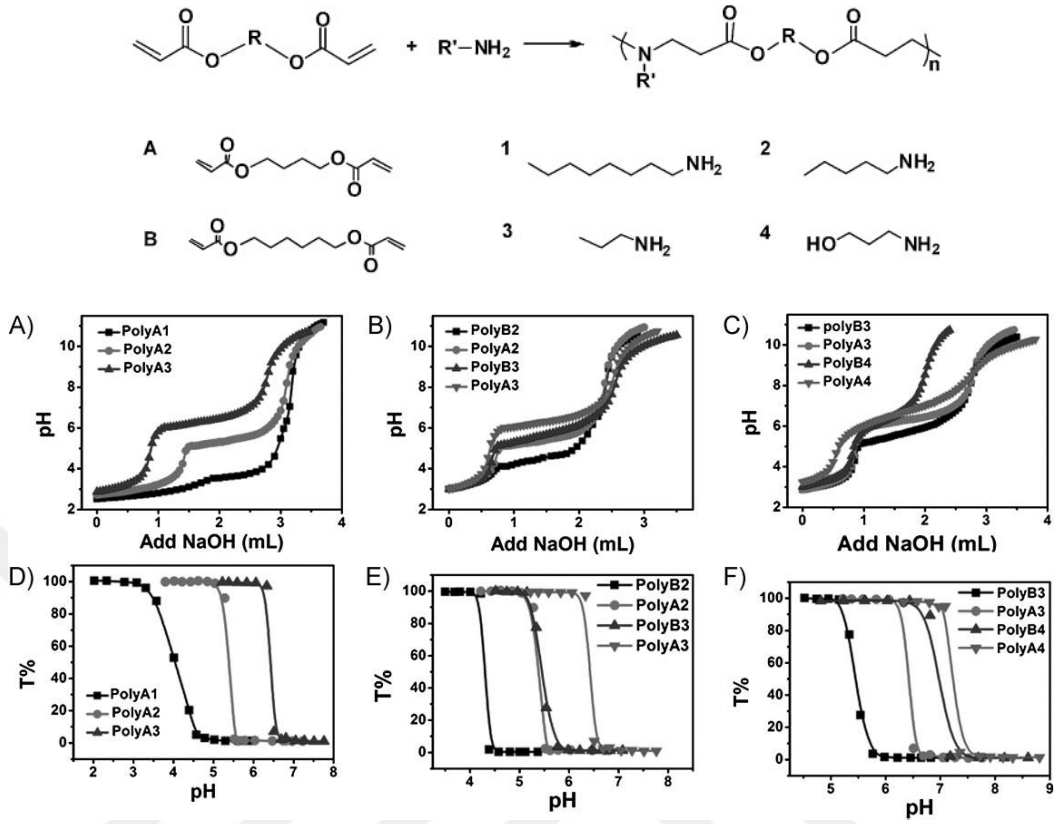

Figure 1.5. Preparation of PBAEs, PEG-PBAE block copolymers and titration curves of some of PBAEs [7].

Multidrug resistance (MDR) is one of the main obstacles to the successful chemotherapy of breast cancer. In order to reverse MDR more efficiently, co-delivery systems of chemotherapeutic drugs and nucleic acid were developed. A new amphiphilic PBAE was synthesized and doxorubicin (DOX) and survivin-targeting shRNA co-loading nanoparticles were prepared [9] (Figure 1.7).

Redox responsive polymers are another important class for drug delivery systems because of the existence of high amounts of reducing agent in the tumor cells. pH and reduction dual-sensitive micelles were prepared for intracellular DOX delivery owing to the fact that the tumor tissues show low pH and high reduction environment [10] (Figure 1.8).

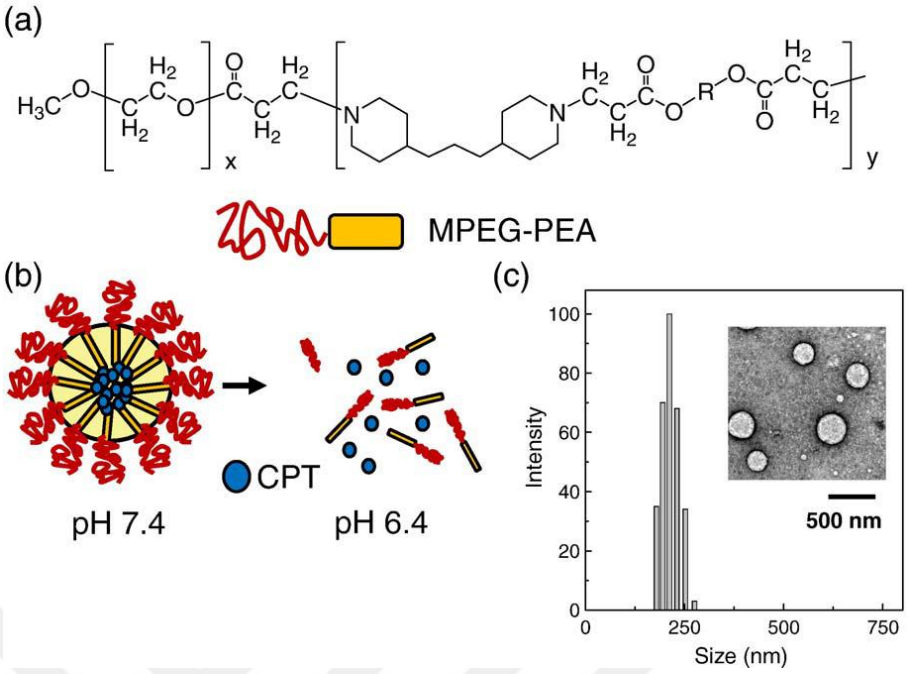

Figure 1.6. (a) Chemical structure of MPEG-PAE block copolymer (MPEG-PAE). (b) Schematic diagram of pH-responsive MPEG-PEG micelles at weakly pH condition. (c) Size distribution of MPEG-PAE micelles in PBS [8].

Hyperthermia which is the heating of cancer tissues up to the 45 ^{o}C has been proven to provide a more efficient way of treating some kinds of cancer in combination of with well-developed procedures such as chemotherapy and radiation therapy. Biodegradable PBAE hydrogels containing iron oxide and paclitaxel were investigated for chemotherapy and heat delivery in the synergistic treatment of cancer [11].

pH-sensitive polymeric micelles were developed for co-delivery of docetaxel (DTX) and proapoptotic peptide for synergistic cancer therapy. With the help of the peptide, these nanoparticles can identify tumor blood vessels and can be endocytosed by the cancer cells selectively [12].

Positively charged PBAE was used as a drug carrier in order to deliver dexamethasone (DEX) to cartilage which has negatively charged glycosaminoglycan. DEX was covalently bound to both ends of PBAE chains or electrostatically linked to the PBAE chain and PBAE could deliver DEX to negatively charged cartilage [13].

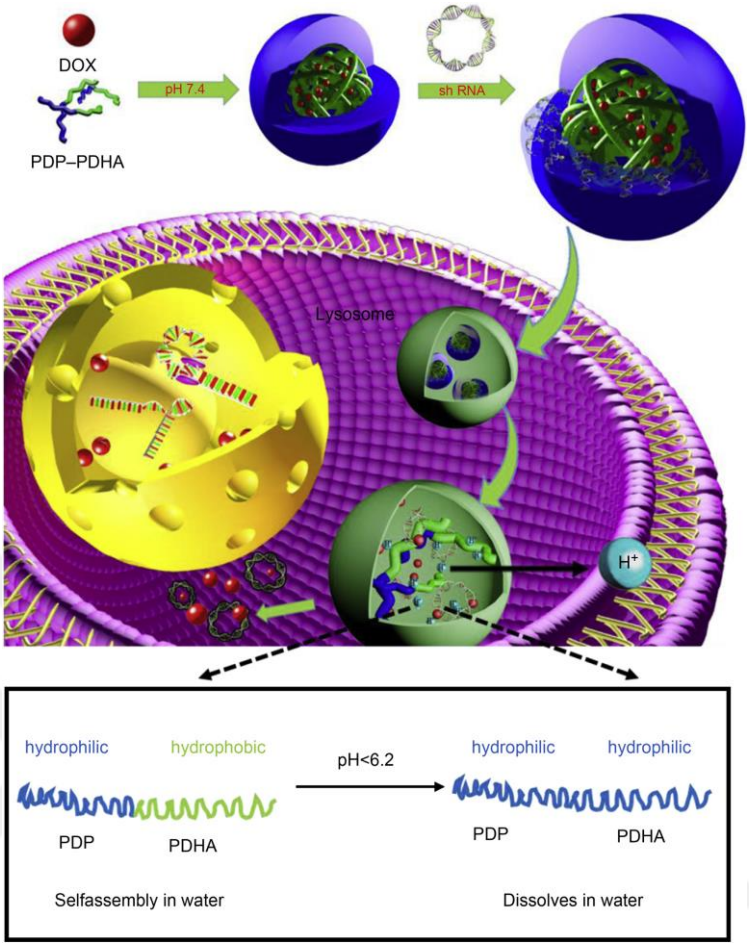

Figure 1.7. Schematic diagram of the preparation of PDNs and the triggered-release behavior of shRNA and DOX from PDNs [9].

Triger-responsive PBAE macromers were synthesized via Michael addition reaction between primary amines and stimuli-responsive monomers and were used in the preparation of the protein encapsulated hydrogel. The synthesized hydrogel showed good controlled release of the cargo in response to external conditions [14].

1.1.3. Tissue Engineering Applications

Biodegradable and photocrosslinkable polymers have potential use in tissue engineering applications due to diverse chemistries available, controllable degradation rate and broad range of mechanical properties. Degradation is important for tissue engineering. It allows tissue growth into the material as the polymer degrades and does away with the need of second surgery to remove device. Mechanical properties are also crucial because

very hard material may be desirable for some applications like orthopedics whereas soft materials are necessary for other applications such as tissue adhesives.

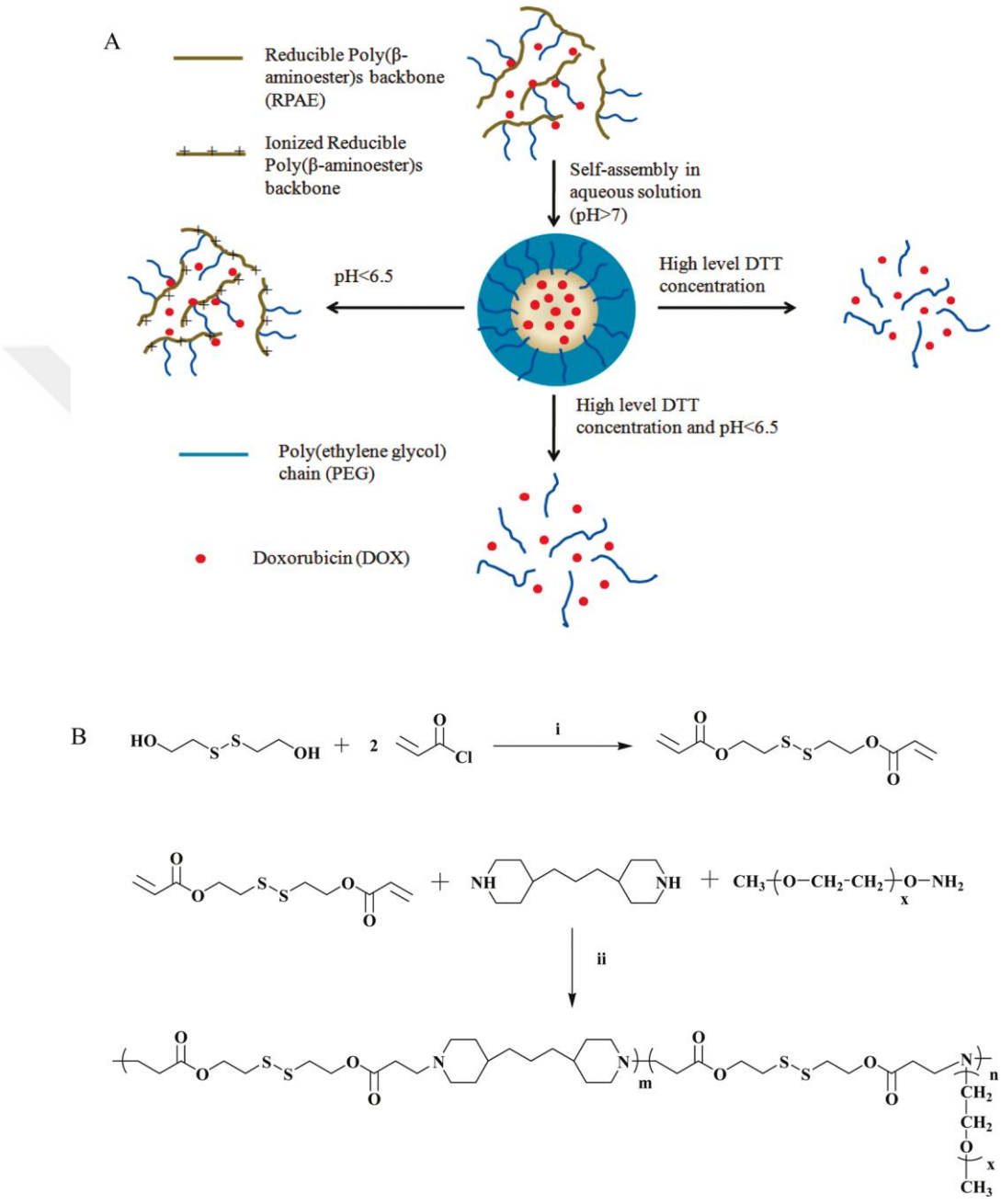

Figure 1.8. (A) Loading, release, and dissociation of DOX from micelles upon changes of pH value, DTT concentration or dual factors. (B) Synthesis routine of reducible PBAE-PEG copolymers [10].

Molecular weight of PBAEs can be controlled by changing the molar ratio of diacrylate/amine monomers, it increases with decreasing diacrylate to amine ratio. Acrylate end group macromers can be easily prepared by using the diacrylate monomer in higher than the amine monomer. After that these macromers can be photopolymerized and give crosslinked and degradable network structures which can be utilized for tissue engineering applications.

Using different acrylates and amines, 120 different PBAEs were synthesized and the effect of the structure of amines and diacrylates were investigated [15] (Figure 1.9). Results showed that hydrophilicity of the monomers affected degradation properties of the polymers. Polymers obtained from more hydrophilic monomers degraded more rapidly than more hydrophobic ones [15] (Figure 1.10).

The effect of macromer branching on network properties was also determined (Figure 1.11). Adding tri functional acrylate increased initial tensile and compressive modulus of network polymers [16] (Figure 1.12).

Molecular weight of macromers can affect network properties. One investigation showed that tensile and compressive moduli increase with increasing diacrylate to amine ratio (Figure 1.13). Besides, mass loss is related with molar ratio of the diacrylate to amine [17] (Figure 1.14).

Another study found that the rubbery modulus was affected by the macromer molecular weight and the acrylate end group conversion [18]. Glass transition temperature of the networks were dependent on the structure of the monomers. T_g of the PBAE networks were increased by using high T_g methyl methacrylate [19] (Figure 1.15).

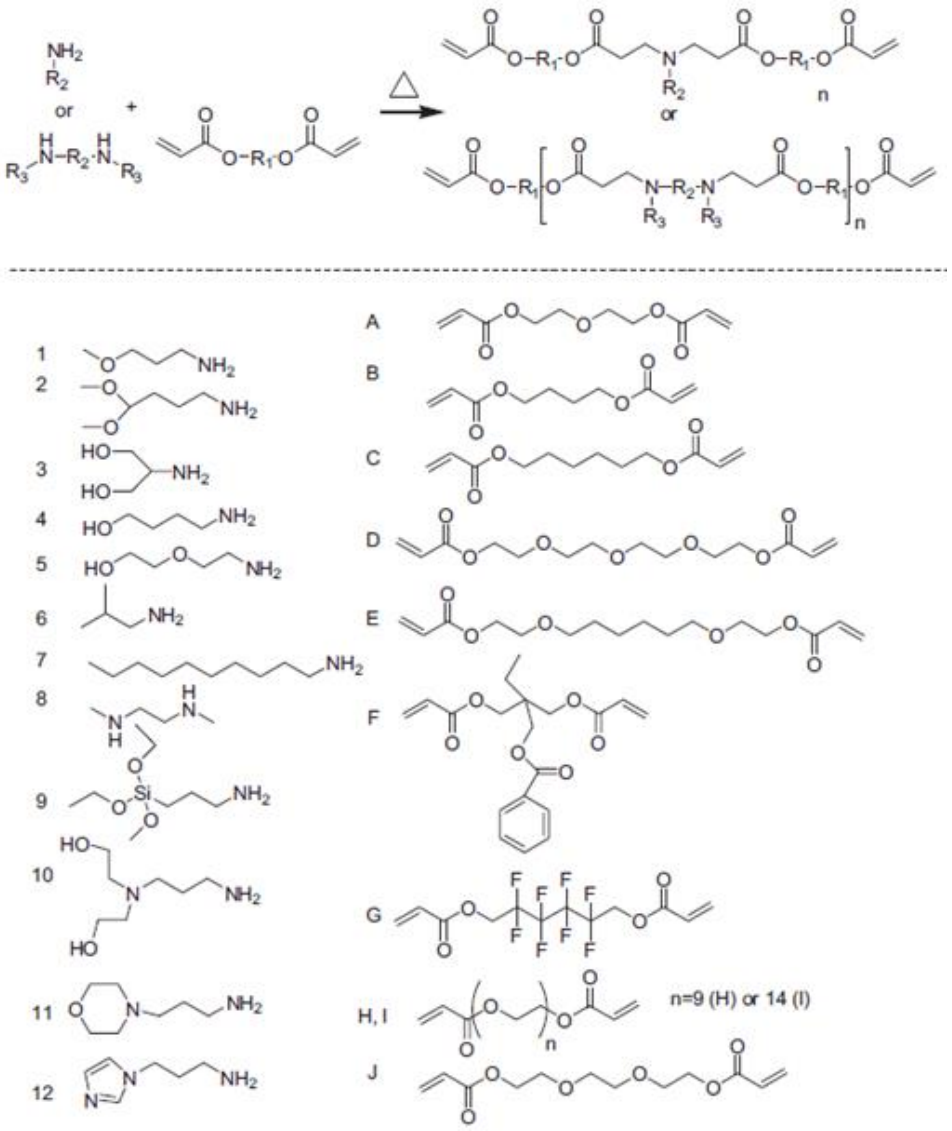

Figure 1.9. General synthesis scheme and chemical structures of used amines and diacrylates [15].

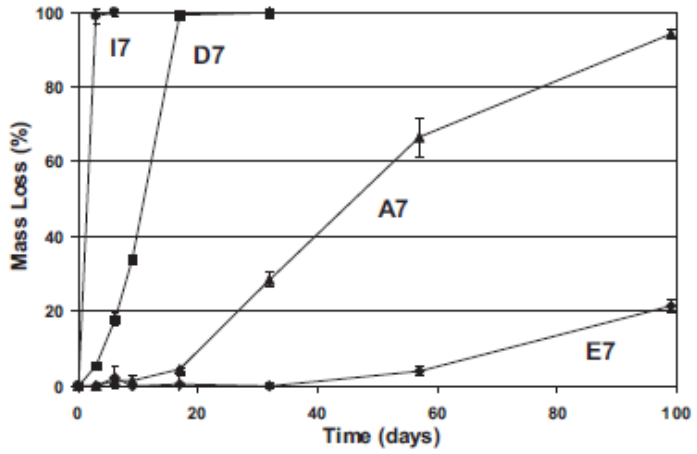

Figure 1.10. Degradation behavior of polymers synthesized from one amine and four acrylates [15].

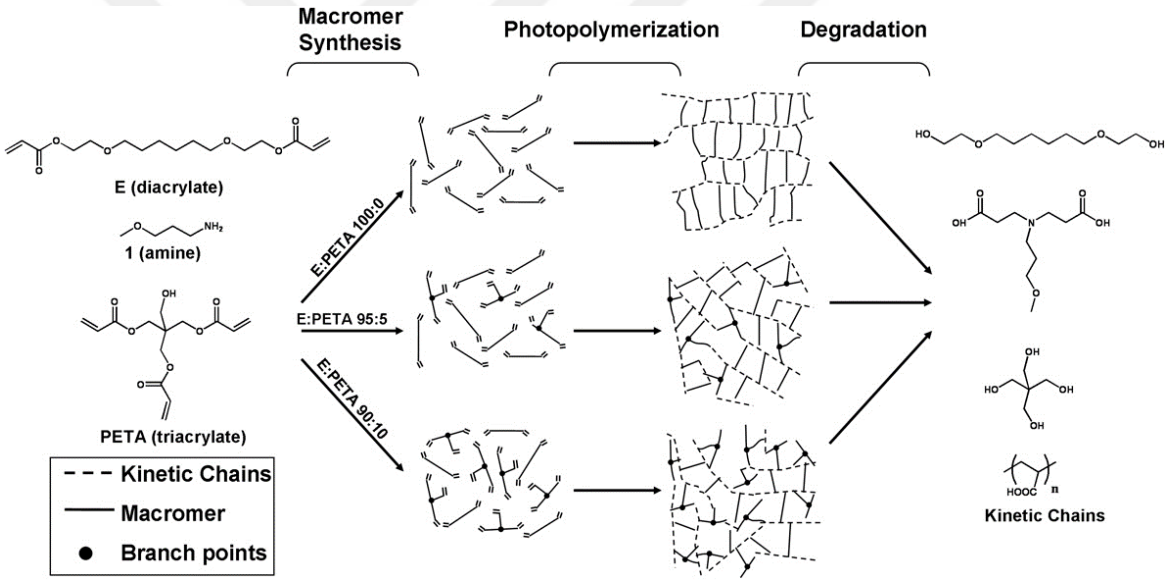

Figure 1.11. Schematic illustration of macromer synthesis, network formation and degradation [16].

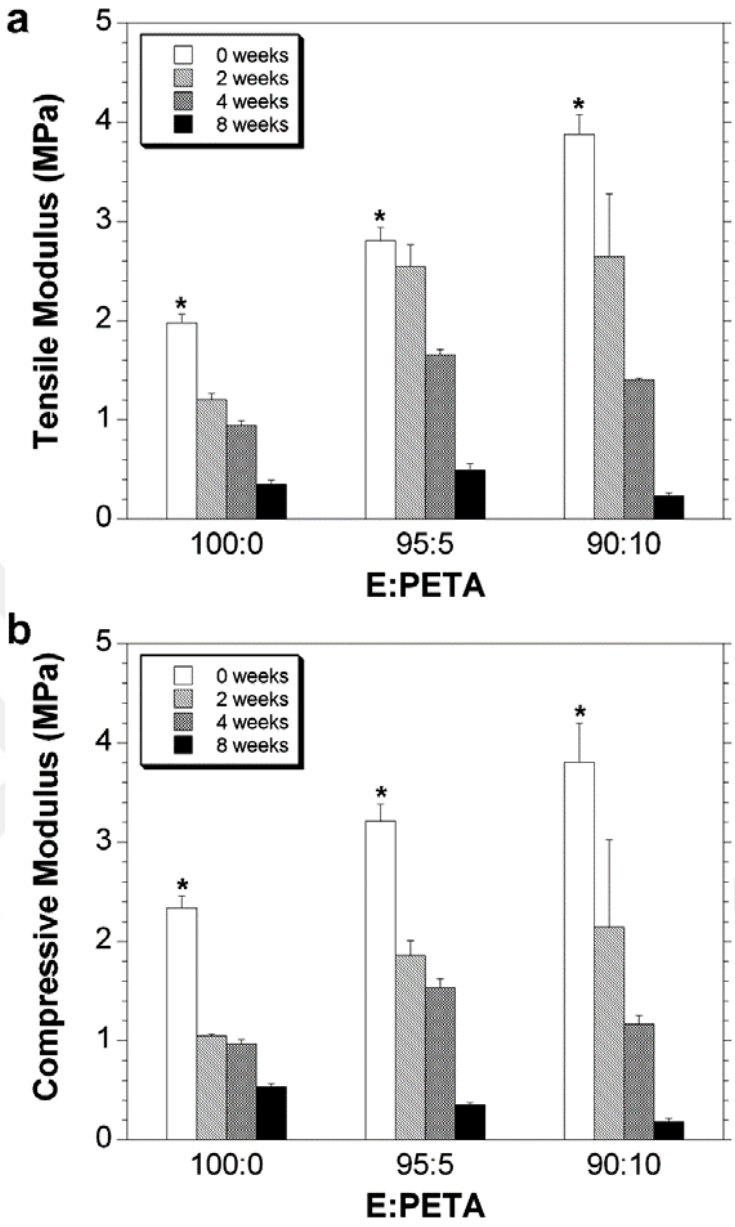

Figure 1.12. Tensile and compressive moduli initially and with degradation for networks formed with different monomer ratios [16].

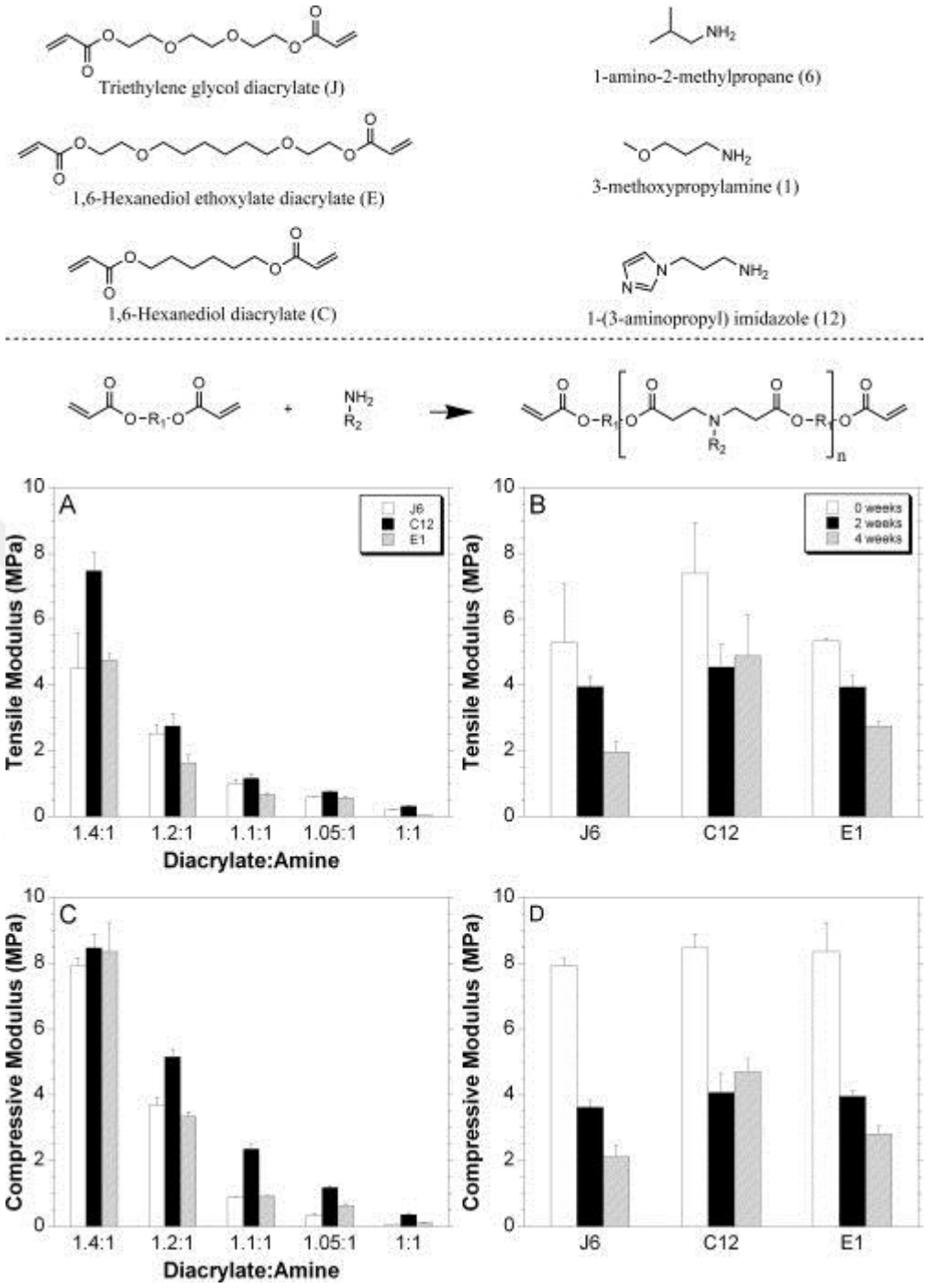

Figure 1.13. Effect of macromer molecular weight on tensile and compressive modulus [17].

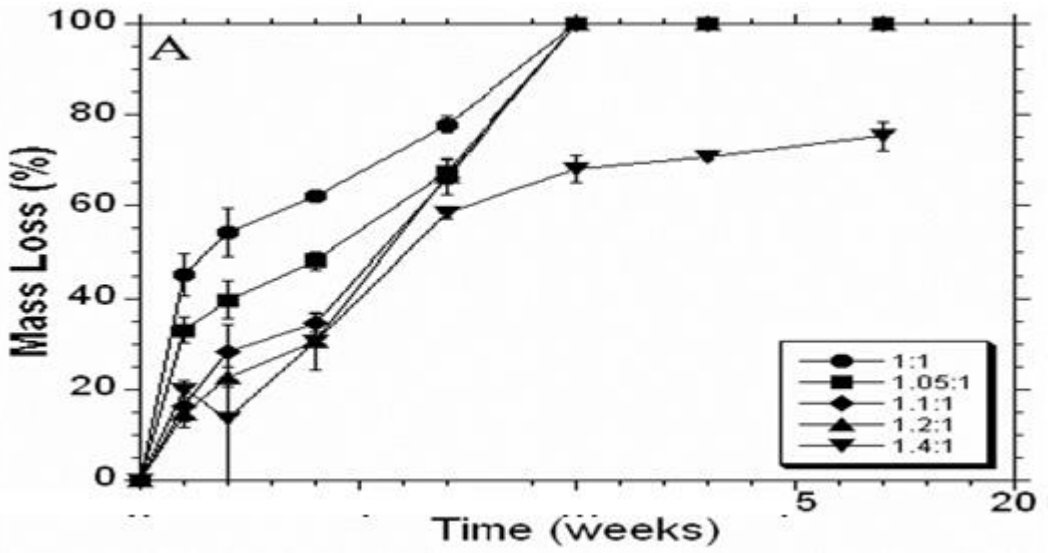

Figure 1.14. Network mass loss with degradation for the various MMW of J6 (A) [17].

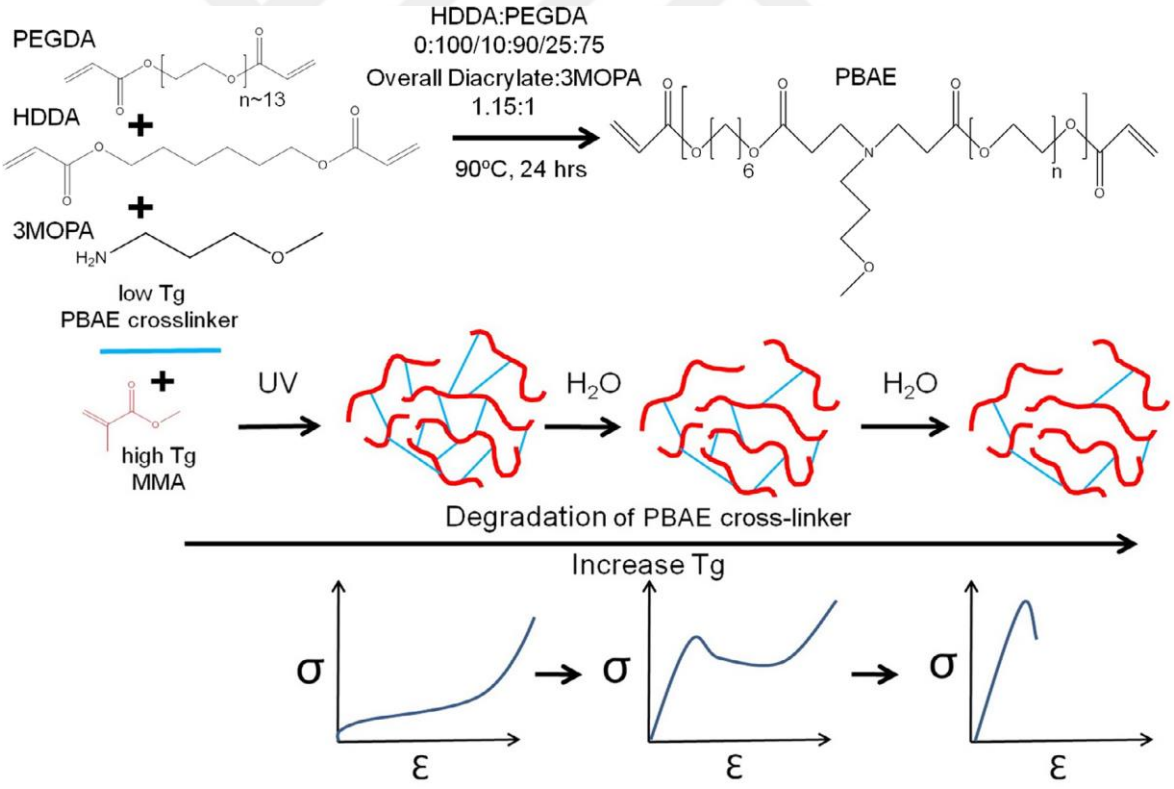

Figure 1.15. Synthesis schematic for PBAE crosslinkers, network formation with PBAE and MMA. As degradation occurs, PBAE leaves networks and thus overall MMA content increases which increases T_g [19].

1.2. Phosphorous Based Biomaterials

The interest of phosphorus-based materials such as polyphosphates, polyphosphonates, phosphonated poly(meth)acrylates, polyphosphoesters is increasing rapidly in the biomedical field because of their biodegradability, hemocompatibility, reduced protein adsorption and ability to make strong interactions with dentin, enamel, or bones [20]. Phosphonic and phosphoric acids can form chelates with calcium ions on the tooth surface so they are important for dental adhesives and composites [21]. Also, it was found that methacrylamides and bismethacrylamides with bisphosphonate or bisphosphonic acid functional groups (Figure 1.16) show improved properties such as hydrolytic stability, ability to form bonds with and high rate of copolymerization with dental monomers [22].

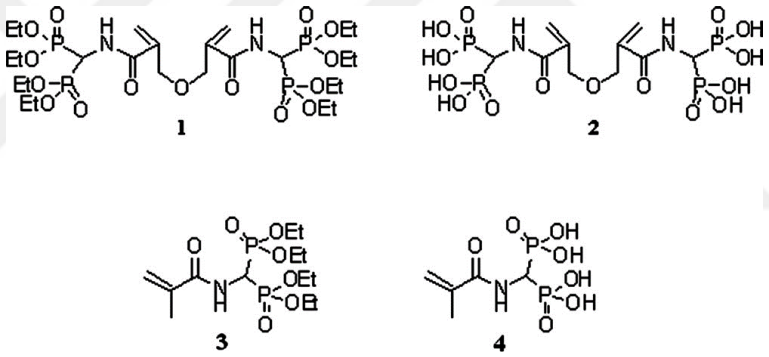

Figure 1.16. Structures of methacrylamides and bismethacrylamide monomers [22].

Osseous tissues are considered to be limited as therapeutic target sides because they mainly consist of hydroxyapatite (HAP) so the flow rate of blood in bones is very low. In order to overcome this problem, bisphosphonate containing prodrugs were synthesized (Figure 1.17 and Figure 1.18). They showed important binding capability to HAP and were hydrolytically activated under physiological conditions [23].

Polyesters are commonly used as a scaffold in bone tissue engineering. However, their surface is not very ideal for cell adhesion and growth because of their hydrophobicity and lack of functionalities. In order to improve polyester scaffold efficiencies, they were functionalized with phosphonate groups. The results showed that more calcium-containing

minerals were deposited and cell viability/metabolic activity were increased [24] (Figure 1.19).

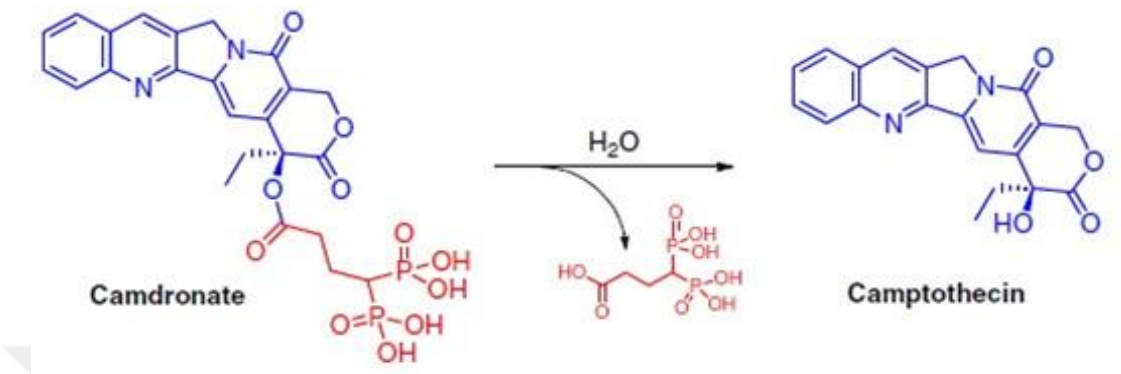

Figure 1.17. Hydrolysis of camdronate prodrug under physiological conditions [23].

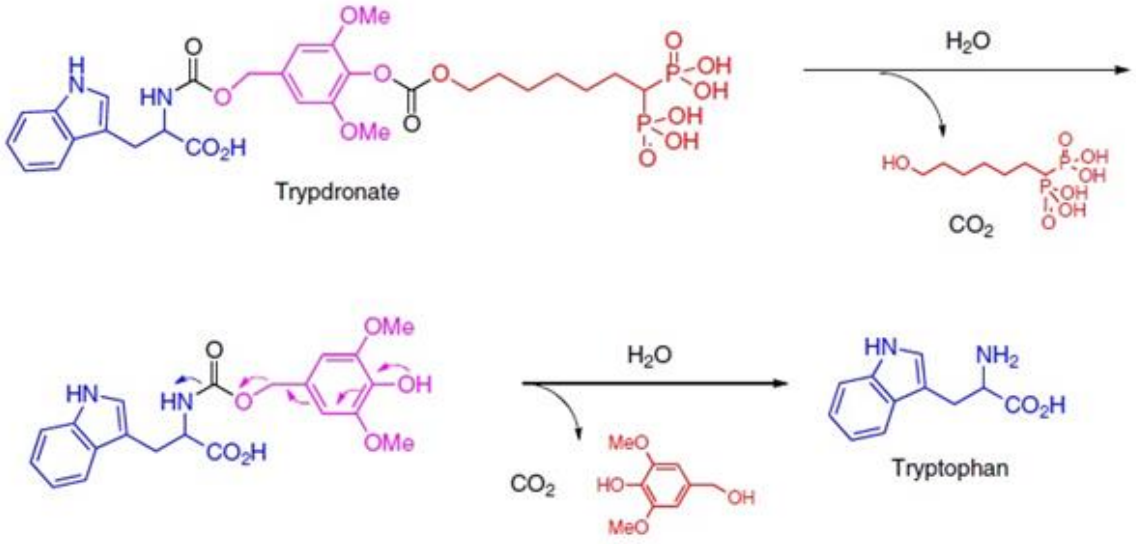

Figure 1.18. Proposed mechanism of release of tryptophan [23].

1.3. Polyethylenimines

Polyethylenimines (PEIs) are polymeric molecules which are composed of repeating units of amine groups and two aliphatic carbons. They can be synthesized from acid-catalyzed aziridine ring opening reaction that leads to branched PEI or from hydrolysis of poly(2-ethyl-2oxazolium) that results in linear PEI [25]. A branched

polyethylenimine (BPEI) may have primary, secondary, and tertiary amino groups while a linear polyethylenimine (LPEI) includes only secondary amino groups in the backbone and primary amino groups at the end of the chains [26] (Figure 1.20). BPEIs are liquid at room temperature while LPEIs are solid at all molecular weights [27]. Because of polycationic character of PEI, it has many application areas such as gene delivery, CO_2 capture, and antiviral microbicides. However, PEIs are cytotoxic [28].

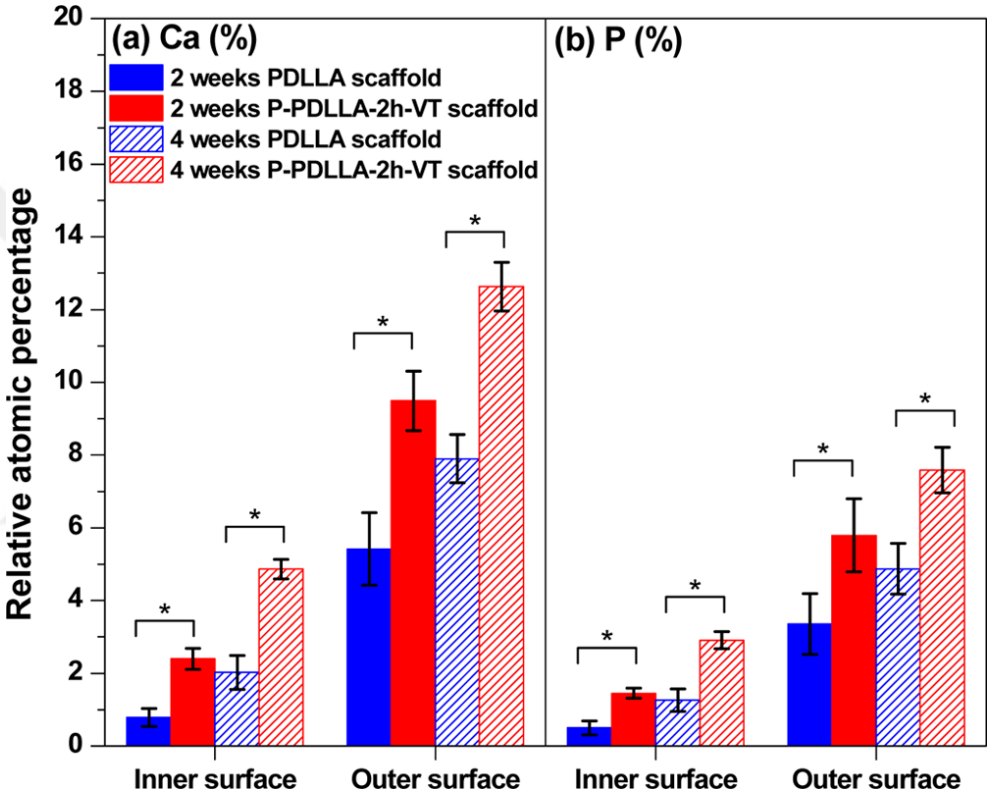

Figure 1.19. Relative atomic % of (a) Ca and (b) P on inner and outer surface of normal and phosphonated scaffold [24].

1.3.1. Gene Delivery Applications

PEI was the second polymeric reagent discovered among various kind of cationic polymers [29]. However, it has been the most widely investigated because it has strong DNA condensation capacity, intrinsic endosomal activity and unique buffering capacity which is called proton sponge effect [30] (Figure 1.21). The transfection efficiency of PEI/DNA complexes depends mostly on the molecular weight of PEI. 25 kDa PEI showed excellent transfection efficiency in comparison with low molecular weight of PEI [31].

However, high molecular weight PEI (25 kDa) lacks degradable linkages and shows some toxicity in therapeutic applications [32]. PEIs with different surface functionalities were synthesized and they showed improved biocompatibility [33] (Figure 1.22).

Another study showed that modification of 25 kDa PEI with reductively cleavable cystamine periphery (PEI-Cys) to a certain extent could significantly improve its transfection and decrease cytotoxic effects [34] (Figure 1.23).

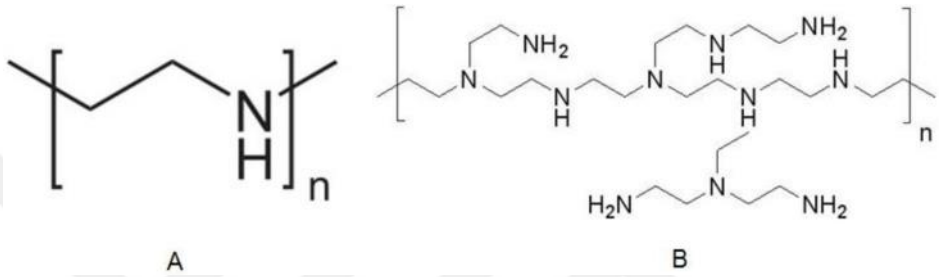

Figure 1.20. Shapes of (A) linear PEI and (B) branched PEI [26].

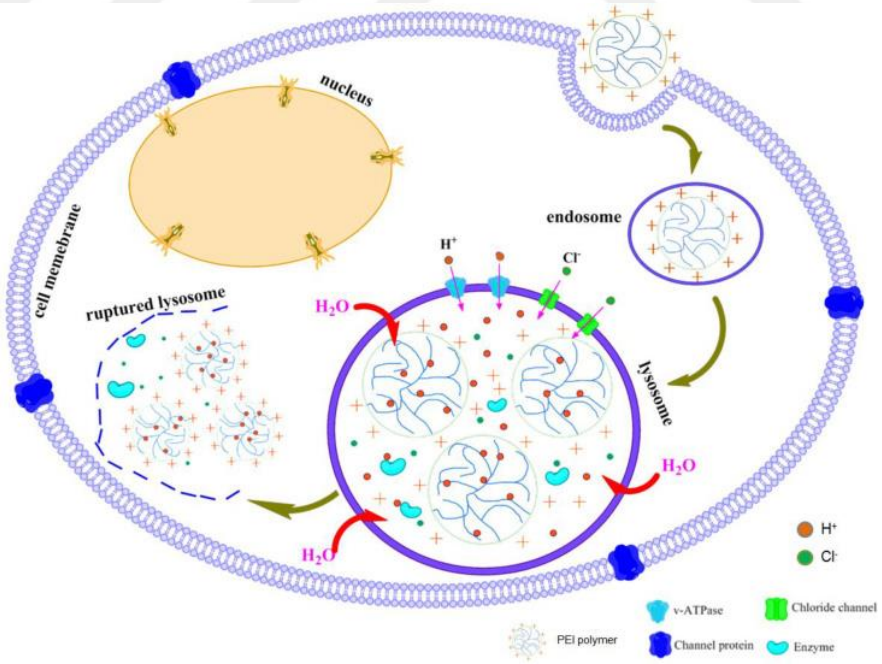

Figure 1.21. Schematic representation of proton sponge effect of PEI [30].

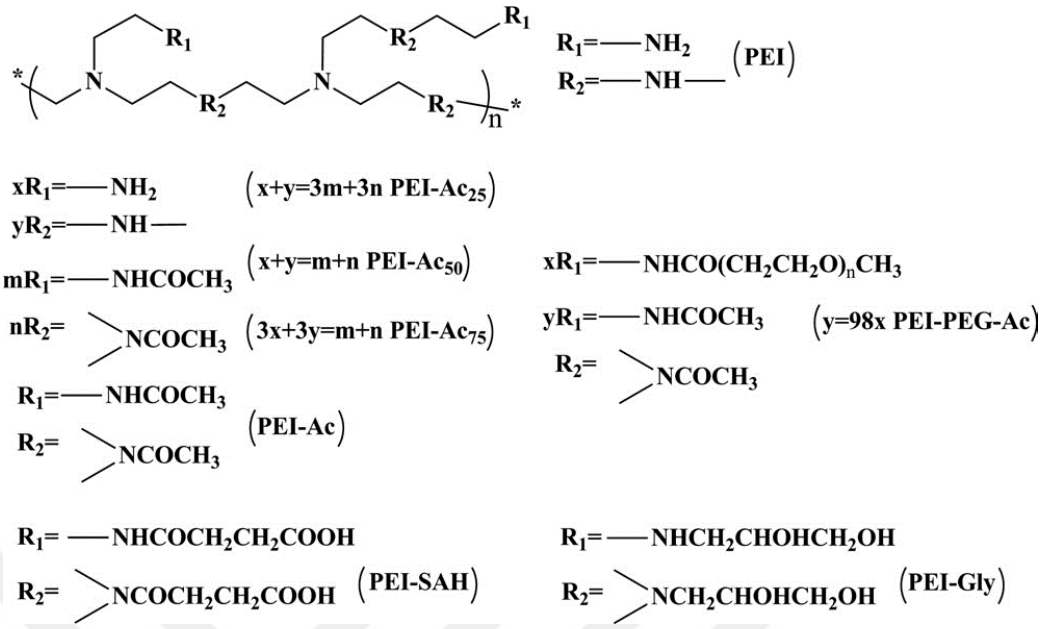

Figure 1.22. Schematic illustration of the structure of used groups to modify PEI [33].

1.3.2. CO_2 Capture Applications

Increased CO_2 concentration in the atmosphere because of the emissions of CO_2 from fossil fuel combustion has caused concerns about global warming so CO_2 capture and sequestration are receiving significant attention [35,36]. Adsorption is one of the promising methods and there are various adsorbents such as activated carbons, pillared clays, metal oxides, and zeolites [37,38]. Branched PEIs impregnated over porous materials have been used for CO_2 adsorption. First use of PEI in CO_2 capture was in the regenerable CO_2 removal system of the space shuttle, to remove CO_2 from crew compartment [39]. Another study showed that mesoporous molecular sieve of MCM-41 type was modified with PEI and its adsorption capacity was significantly increased (Figure 1.24) [40].

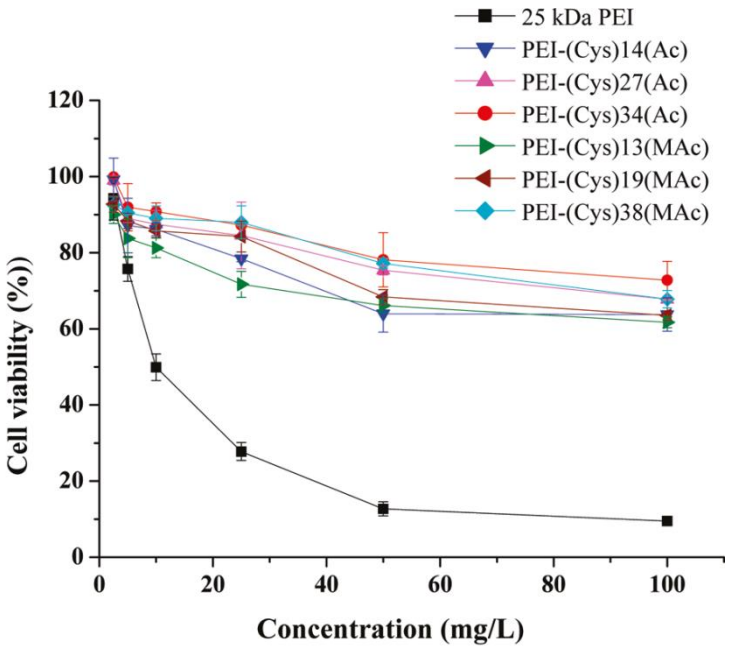

Figure 1.23. Cytotoxicity of PEI-Cys derivatives determined by MTT assays [34].

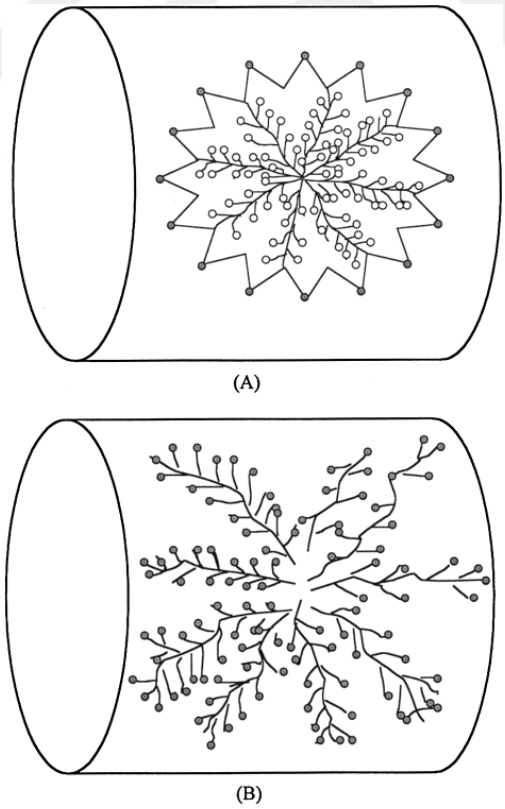

Figure 1.24. Schematic diagram of PEI status in MCM-41 at (A) low T and (B) high T [40].

1.3.3. Antiviral Microbicide Applications

Cationic polymers developed with quaternary ammonium groups can be used as efficient antimicrobials. Bacteria do not appear to develop resistance to cationic polymers because of their cationic structures [41]. Quaternized PEI (QPEI) was synthesized and the antibacterial efficiency of it was significantly dependent on its cationization degree. (Figure 1.25) [42]. Cross-linked QPEI was incorporated in glass ionomer cements (GICs) and exhibited a strong antibacterial effect against Streptococcus mutans and Lactobacillus casei (Figure 1.26) [41].

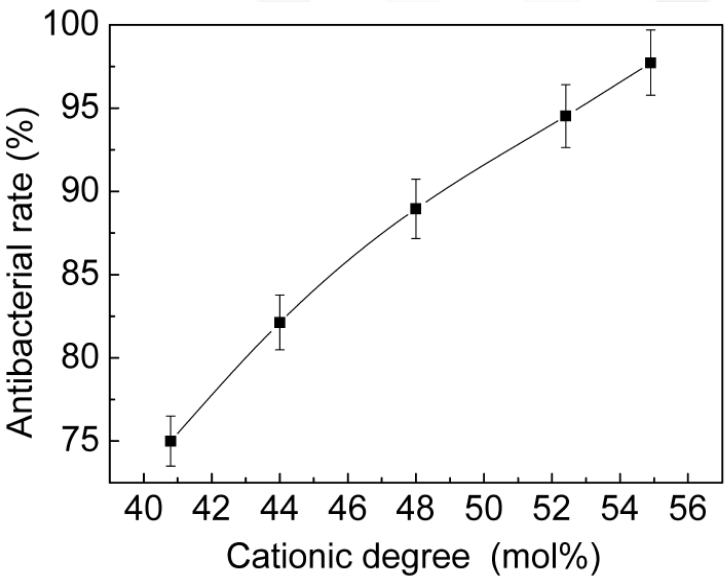

Figure 1.25. Effect of cationic degree on bactericidal ratio of QPEI [42].

The multilayer of PEI and carrageenan were formed by layer-by-layer assembly adsorption technique for potential use as coating on biomaterial surfaces and the multilayer exhibited antibacterial activity against Enterobacter cloaceae, Staphylococcus aureus and Enterococcus faecalis [43]. Another study showed that preincubation of cells with PEI blocked primary attachment of human papillomaviruses and human cytomegaloviruses to cells and caused a decrease in infection [44].

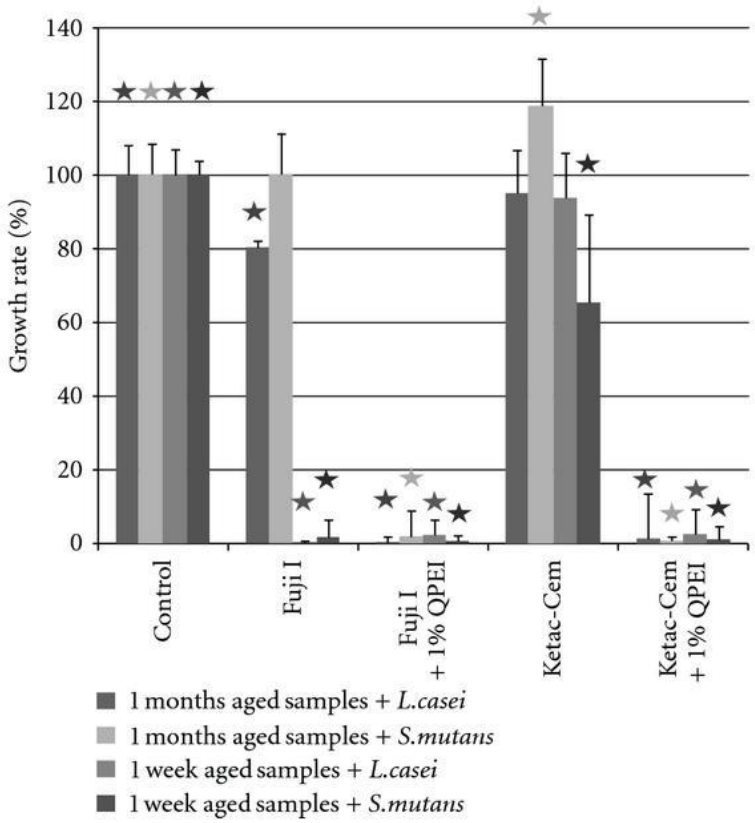

Figure 1.26. Bacterial growth rate of Streptococcus mutans and Lactobacillus casei following direct contact with aged glass ionomer cements (Fuji I and Ketac-Cem) incorporating 0 and 1% w/w QPEI [41].

2. OBJECTIVES

In this study, the aim is to synthesize novel phosphonate and bisphosphonate functionalized PBAEs and PEIs for biomedical applications.

The effect of PBAE structure on the pH sensitivities is studied. Furthermore, micelle forming PBAEs are expected to have potential for drug delivery, and two such candidates are investigated.

The addition of phosphonate and bisphosphonates to PEI is expected to decrease the toxicity of PEI which is an important vehicle for gene delivery and therefore produce much more usable systems.

3. EXPERIMENTAL WORK

3.1. Materials

1,6-hexane diol diacrylate (HDDA), poly(ethylene glycol) diacrylate (PEGDA, M_n = 575), propyl amine (PA), diethyl vinylphosphonate, 5-amino-1-pentanol (HP), 4,9-dioxa-1,12-dodecanediamine, paraformaldehyde, diethyl amine, triethyl amine (TEA), tetraethyl methylene bisphosphonate, p-toluenesulfonic acid monohydrate (p-TsOH), and all other reagents were purchased from Aldrich and used as received. Polyethylenimine (M_n = 1.8 and 10 kDa) was purchased from Polysciences Inc. Ammonia solution, methanol, toluene, dimethyl sulfoxide (DMSO) and all other solvents were purchased from Merck. Toluene was dried over molecular sieves. Doxorubicin (DOX) was a gift from Deva Holding. Dialysis membranes (1000 molecular weight cutoff (MWCO)) were purchased from Spectrum Labs.

3.2. Characterization

^{1}H NMR spectra were recorded on a Varian Gemini (400 MHz) spectrometer by using $CDCl_3$ or D_2O as solvent. NICOLET 6700 Fourier transform infrared (FTIR) spectrophotometer was used for recording IR spectra. The morphology of micelles was investigated by using a scanning electron microscope (SEM) (ESEM-FEG) (FEI-Philips XL30). Drug release studies were performed using a VWR Incubating Mini Shaker. UV-VIS spectra were measured on a TU-1880 Double Beam UV-Vis spectrophotometer. The pK_b values of the polymers were determined using a pH meter (Jenco 6173). Dynamic light scattering (DLS) studies were performed with Zetasizer Nano ZS (Malvern). MDA-231 cells were observed by Laser Scanning Confocal Microscopy (LSM710, Carl Zeiss AG, Oberkochen, Germany). Mn values of macromers were determined by gel permeation chromatography (GPC) with THF solvent using polystyrene standards.

3.3. Synthesis of Starting Materials

3.3.1. Synthesis of diethyl 2-aminoethylphosphonate (A1)

This amine was synthesized according to the literature procedure [45]. Briefly, ammonia solution (15 mL) was reacted with diethyl vinyl phosphonate (1.64 g, 0.01 mol) at room temperature.

The reaction was continued for three days and then extracted with $CHCl_3$ (3x15 mL). The organic layer was dried over anhydrous Na_2SO_4, filtered and evaporated under reduced pressure. After that, the residue was distilled under reduced pressure to give pure product as a colorless liquid in 30% yield.

^{1}H-NMR (400 MHz, $CDCl_3$, TMS): δ = 1.32 (CH_3), 2.03 (CH_2-P), 2.87 (CH_2-N), 3.3 (NH_2), 4.11 (CH_2-O) ppm.

FT-IR (ATR): 3289 (N-H), 1162 (C-O), 1229 (P=O), 1021, 954 (P-O) cm^{-1}

3.3.2. Synthesis of bisphosphonate-functionalized 4,9-dioxa-1,12 dodecanediamine (A2)

This amine was synthesized in two steps according to literature procedures [46]. First, tetraethyl vinylidene bisphosphonate was synthesized. Paraformaldehyde (0.26 g, 8,7 mmol), diethylamine (0.18 mL, 1,7 mmol) and methanol (5 mL) were mixed in vial and stirred for 50 minutes at 37 °C. Then tetra ethyl methylene bisphosphonate (0.43 mL, 1.17 mmol) was added and refluxed for 24 h at 68 °C. After that methanol was removed under reduced pressure. Also toluene (2x2.5 mL) was added and removed under reduced pressure. Then p-TsOH (2 mg) and dry toluene (2.5mL) were added to reaction medium and refluxed for 17 h. After that $CHCl_3$ (2.5 mL) was added and then extracted with H_2O (2x4 mL). Organic phased was dried with Na_2SO_4 and $CHCl_3$ was removed under reduced pressure. In the second step, 4,9-dioxa-1,12- dodecanediamine (0.7 g, 3.48 mmol) and tetraethyl vinylidene bisphosphonate (2.5 g, 8.37 mmol) in dry DMF (25 mL) were mixed at room temperature for 2 days. After removal of DMF under reduced pressure, the residue

was washed with petroleum ether and residual product was obtained light yellow viscous liquid in 80-90% yield.

^{1}H NMR (400 MHz, $CDCl_3$, TMS): δ = 1.27 (CH_3), 1.54 (CH_2- N), 1.67 (CH_2), 2.60 (CH_2-N), 2.62 CH-P), 3.08 (CH_2-CH-P), 3.34 (CH_2-O), 3.39 (CH_2-O), 4.12 (CH_2- O-P) ppm.

FTIR (ATR): 3309 (N-H), 2981, 2933, 2860 (C-H), 1245 (P=O), 1016, 955 (P-O) cm^{-1}.

3.4. PBAEs

3.4.1. Synthesis of PBAEs Macromers

The acrylates (HDDA and PEGDA) and amines (PA or HP) were mixed at molar ratios of 1.2:1 (2.4 mmol:2 mmol) and 1:1 (2 mmol:2 mmol) in vials at 90 °C 24 h while stirring. After reaction completed, resultant mixtures were washed with petroleum ether to remove unreacted monomers and dried under reduced pressure. Macromers were obtained as yellowish viscous liquids in 75-80% yield.

3.4.1.1. HDDA:PA.

^{1}H-NMR (400 MHz, $CDCl_3$, TMS): δ = 0.85 (CH_3), 1.39 (CH_2), 1.42 (CH_2), 1.62 (CH_2), 2.35 (CH_2-N), 2.45 (CH_2-C=O), 2.75 (CH_2-N), 4.04 (CH_2-O), 4.14 (CH_2-O), 5.80 (CH=CH-*H*), 6.11 (C*H*=CH_2), 6.40 (CH=CH-*H*) ppm.

FTIR (ATR): 2934 (C-H), 1727 (C=O), 1613 (C=C) cm^{-1}.

3.4.1.2. HDDA:HP.

^{1}H-NMR (400 MHz, $CDCl_3$, TMS): δ = 1.12 (CH_2), 1.19 (CH_2), 1.23 (CH_2), 1.32 (CH_2), 1.45 (CH_2), 2.23 (CH_2-N, CH_2-C=O), 2.57 (CH_2-N), 3.39 (CH_2-OH), 3.86 (CH_2-O), 3.96 (CH_2-O), 5.63 (CH=CH-*H*), 5.91 (C*H*=CH_2), 6.19 (CH=CH-*H*) ppm.

FTIR (ATR): 3433 (O-H), 2934, 2860 (C-H), 1729 (C=O), 1627 (C=C) cm^{-1}.

3.4.1.3. PEGDA:PA.

^{1}H-NMR (400 MHz, $CDCl_3$, TMS): δ = 0.8 (CH_3), 1.41 (CH_2), 2.35 (CH_2-N), 2.55 (CH_2-C=O), 2.75 (CH_2-N), 3.65 (CH_2-O), 3.70 (CH_2-O), 4.21 (CH_2-O), 4.31 (CH_2-O), 5.83 (CH=CH-*H*), 6.15 (C*H*=CH_2), 6.42 (CH=CH-*H*) ppm.

FTIR (ATR): 2869 (C-H), 1721 (C=O), 1635 (C=C) cm^{-1}.

3.4.1.4. PEGDA:HP.

^{1}H-NMR (400 MHz, $CDCl_3$, TMS): δ = 1.32 (CH_2), 1.43 (CH_2), 1.54 (CH_2), 2.39 (CH_2-N), 2.46 (CH_2-O), 2.74 (CH_2-N), 3.65 (CH_2-O), 3.65 (CH_2-O), 3.65 (CH_2-O), 4.21 (CH_2-O), 4.31 (CH_2-O), 5.83 (CH=CH-*H*), 6.15 (C*H*=CH_2), 6.42 (CH=CH-*H*) ppm.

FTIR (ATR): 3503 (O-H), 2864 (C-H), 1730 (C=O), 1631 (C=C) cm^{-1}.

3.4.2. Synthesis of Phosphonate and Bisphosphonate-Functionalized PBAEs

The macromers (HDDA:PA, HDDA:HP, PEGDA:PA or PEGDA:HP) and A1 were mixed at macromer:amine ratio of 1:2.4 (2 mmol: 4.8 mmol) in vials at room temperature for three days. Then, polymers were washed with ether or petroleum ether to ether to remove unreacted A1 and dried under reduced pressure. Yield of the polymers was about 90-95%.

The macromer (HDDA:PA) and A2 were mixed at macromer:amine ratio of 1:1 (2 mmol:2 mmol) in a vial at room temperature for five days.

3.4.2.1. [HDDA:PA]-A1.

^{1}H-NMR (400 MHz, $CDCl_3$, TMS): δ = 0.85 (CH_3), 1.29 (CH_3), 1.35 (CH_2), 1.41 (CH_2), 1.62 (CH_2), 1.92 (CH_2-P), 2.34 (CH_2-N), 2.41 (CH_2-C=O), 2.41 (CH_2-C=O), 2.46 (CH_2-N), 2.73 (CH_2-N), 2.84 (CH_2-N), 4.04 (CH_2-O), 4.04 (CH_2-O), 4.04 (CH_2-O-P) ppm.

FTIR (ATR): 2935 (C-H), 1729 (C=O), 1242 (P=O), 1026, 966 (P-O) cm^{-1}.

3.4.2.2. [HDDA:HP]-A1.

^{1}H-NMR (400 MHz, $CDCl_3$, TMS): δ = 1.30 (CH_3), 1.32 (CH_2), 1.36 (CH_2), 1.43 (CH_2), 1.54 (CH_2), 1.62 (CH_2), 1.92 (CH_2-P), 2.42 (CH_2-C=O), 2.49 (CH_2-C=O), 2.75 (CH_2-N), 2.85 (CH_2-N), 2.89 (CH_2-N), 3.00 (CH_2-N), 3.60 (CH_2-O), 4.04 (CH_2-O), 4.09 (CH_2-O), 4.09 (CH_2-O-P) ppm.

FTIR (ATR): 3398 (C-OH), 2935 (C-H), 1728 (C=O), 1205 (P=O), 1021, 965 (P-O) cm^{-1}.

3.4.2.3. [PEGDA:PA]-A1.

^{1}H-NMR (400 MHz, $CDCl_3$, TMS): δ = 0.84 (CH_3), 1.33 (CH_3), 1.42 (CH_2), 1.62 (CH_2), 1.95 (CH_2-P), 2.36 (CH_2-N), 2.46 (CH_2-C=O), 2.46 (CH_2-C=O), 2.53 (CH_2-N), 2.75 (CH_2-N), 2.89 (CH_2-N), 3.64 (CH_2-O), 3.68 (CH_2-O), 4.04 (CH_2-O), 4.10 (CH_2-O-P), 4.22 (CH_2-O), 4.22 (CH_2-O) ppm.

FTIR (ATR): 2868 (C-H), 1730 (C=O), 1247 (P=O), 1026, 951 (P-O) cm^{-1}.

3.4.2.4. [PEGDA:HP]-A1.

^{1}H-NMR (400 MHz, $CDCl_3$, TMS): δ = 1.32 (CH_2), 1.32 (CH_3), 1.43 (CH_2), 1.55 (CH_2), 1.94 (CH_2-P), 2.40 (CH_2-N), 2.46 (CH_2-C=O), 2.46 (CH_2-C=O), 2.54 (CH_2-N), 2.76 (CH_2-N), 2.89 (CH_2-N), 3.65 (CH_2-O), 3.65 (CH_2-O), 3.65 (CH_2-O), 4.10 (CH_2-O), 4.21 (CH_2-O), 4.21 (CH_2-O) ppm.

FTIR (ATR): 3436 (O-H), 2865 (C-H), 1730 (C=O), 1247 (P=O), 1027, 950 (P-O) cm^{-1}.

3.4.2.5. [HDDA:PA]-A2.

^{1}H-NMR (400 MHz, $CDCl_3$, TMS): δ = 0.85 (CH_3), 1.39 (CH_2), 1.42 (CH_2), 1.62 (CH_2), 2.35 (CH_2-N), 2.45 (CH_2-C=O), 2.75 (CH_2-N), 4.04 (CH_2-O), 4.14 (CH_2-O), 5.80 (CH=CH-*H*), 6.10 (C*H*=CH_2), 6.40 (CH=CH-*H*) ppm.

FTIR (ATR): 2935, 2962 (C-H), 1730 (C=O), 1680 (C=C), 1249 (P=O), 1024, 969 (P-O) cm^{-1}.

3.4.3. Measurement of pK_b

The pK_b values of the polymers were measured by titration method. 50 mg polymer or macromer were dissolved in 50 mL deionized water for each case and the pH of the medium was decreased to 3 by HCl solution. Then, the pH was tuned with the addition of 0.1 mL of 0.1 M NaOH solution. The pK_b was determined as the half neutralization of the amine group in the macromer or polymer.

3.4.4. pH-Dependent Light Transmittance

The light transmittance of the polymer solutions was measured at different pH values by UV-Vis spectrometer. In each case, polymer was dispersed in deionized water and pH values were adjusted to 3-8 by NaOH/HCl solutions, with a final concentration of 1.0 $mgmL^{-1}$. The exact pH value of the solutions measured with a pH meter and the turbidity of the polymer solutions was determined from the light transmittance at 550 nm.

3.4.5. Preparation of Micelles

The micelles were prepared by dialysis method. The polymer (20 mg) was dissolved in 1 mL of DMF and then 5 mL of PBS (pH = 7.4) was slowly added while stirring. The resulting solution was stirred for another 3 h and then transferred into the dialysis membrane (MWCO: 1kDa) and dialyzed against 1 L of deionized water for 24 h to remove DMF.

3.4.6. Characterization of Micelles

Sizes of the micelles before and after DOX loading were measured by DLS. The concentration of the micelle solutions was adjusted to 1 $mgmL^{-1}$ and the resultant solutions were filtered through a 450-nm syringe filter to remove the free DOX.

The morphology of unloaded and DOX loaded micelles was also determined by SEM. The micelle solutions prepared as above were dropped onto the gold coated surface and left to dry.

3.4.7. DOX Encapsulation and Release

DOX was loaded into the micelles by dialysis method. 2 mg DOX dissolved in 0.8 mL DMF was mixed with 3 equivalents of trimethylamine. Then 20 mg polymer in 0.2 mL DMF was added and the resulting solution was stirred for 1 h. At the end of this time, 10 mL PBS (pH=7.4) was added dropwise (12-13 second/drop) and the mixture was stirred for 3 h. The resulting solution was dialyzed using a 1 kDa molecular weight cutoff dialysis membrane against 1 L of deionized water for 24 h to remove free DOX. In order to calculate drug loading efficiency of DOX loaded polymeric micelles, 1 mL of DOX loaded micelle solution was lyophilized and dissolved in 4 mL of DMSO. The resultant solution was quantified by absorbance using UV-Vis spectroscopy at 480 nm.

$$DLE\ \% = \left(\frac{Weight\ of\ DOX\ in\ 1mL\ solution\ x\ V\ of\ total\ solution}{Weight\ of\ initial\ DOX}\right) \times 100 \qquad (3.1)$$

DOX loaded micelles (3 mL) prepared as described above were loaded in a dialysis membrane (MWCO: 1 kDa) and this membrane was incubated in 30 mL PBS (pH= 7.4 or 5.5) at 37 °C with a shaking rate of 100 rpm. At predetermined time intervals, 3 mL of the outside of the dialysis bag medium was withdrawn and the same volume of fresh PBS at the same pH was added to keep the total volume constant. The DOX content of the sample was determined by measuring the UV-Vis absorbance at 480 nm.

3.5. Polyethylenimines

3.5.1. Synthesis of Phosphonated PEIs

Polyethylenimines (M_n = 1.8 and 10 kDa) were reacted with diethyl vinylphosphonate (P1), tetraethyl vinylidene bisphosphonate (P2) and HDDA:A1 (1.2 mmol:1 mmol) macromer at different molar ratios (1:25, 1:7.5, 0.5:1, 1:1, 2:1, 4:1) in vials at room temperature for 24 h while stirring. The resulting polymers were washed with ether to remove unreacted monomers and dried under reduced pressure.

3.5.1.1. PEI-P1.

^{1}H-NMR (400 MHz, $CDCl_3$, TMS): δ = 1.18 (CH_3), 1.90 (CH_2-P), 2.98 (CH_2-CH_2-P), 3.98 (CH_2-O) ppm.

FTIR (ATR): 3290 (N-H), 2937, 2818 (C-H), 1221 (P=O), 1024, 961 (P-O) cm^{-1}.

3.5.1.2. PEI-P2.

^{1}H-NMR (400 MHz, $CDCl_3$, TMS): δ = 1.18 (CH_3), 2.50 (CH_2-N), 2.50 (CH-P), 2.98 (CH_2-CH-P), 4.05 (CH_2-O) ppm.

FTIR (ATR): 3290 (N-H), 2930, 2814 (C-H), 1235 (P=O), 1022, 966 (P-O) cm^{-1}.

3.5.1.3. PEI-(HDDA:A1).

^{1}H-NMR (400 MHz, $CDCl_3$, TMS): δ = 1.28 (CH_3), 1.34 (CH_2), 1.62 (CH_2), 1.90 (CH_2-P), 2.40 (CH_2-C=O), 2.48 (CH_2-C=O), 2.60 (CH_2-N), 2.72 (CH_2-N), 2.87 (CH_2-N), 2.90 (CH_2-N), 4.08 (CH_2-O), 4.08 (CH_2-O), 4.08 (CH_2-O-P) ppm.

FTIR (ATR): 3429 (N-H), 2937, 2860 (C-H), 1724 (C=O), 1637 (C=C), 1249 (P=O), 1024, 964 (P-O) cm^{-1}.

3.5.2. In Vitro Uptake of Synthesized Polymers/pDNA Complexes

This part of the study was performed by Hasan Uludağ from University of Alberta according to the literature example [47]. The uptake of PEI-P1/pDNA and PEI-P2/pDNA complexes was assessed in MDA-231 and MFC cells through flow cytometry and confocal microscopy using Cy^{TM3}-labelled pDNA. The cells were seeded 24 well plate and left overnight for growth. The complexes consisting of PEI-P1 and PEI-P2 polymers and Cy^{TM3}-labelled pDNA of different composition were prepared. After that, cells were treated with prepared complexes. After 24 h of treatment, cells were washed with Hank's balanced salt solution (3x), trysinized and fixed with formaldehyde and analyzed by flow cytometer. For confocal microscopy study, MDA-231 cells were seeded on cover slips attached into 6 well-plates and allowed to grow overnight. Prepared complexes were directly added to cells and incubated for 24 h under a humidified air. Then, cells were washed with Hank's balanced salt solution (3x) and fixed with 1 mL formaldehyde for 30 min and washed with distilled water. The nuclei of cells were stained with DAPI and cytoplasm with WGA. Lastly, prepared cover slips were mounted onto the slides and observed under 60 x 1.3 oil plan apochromat lenses in Laser Scanning Confocal Microscopy.

4. RESULTS AND DISCUSSION

4.1. PBAEs

4.1.1. Synthesis of Phosphonate and Bisphosphonate-Functionalized Amines

In this work, one primary (A1) and one secondary (A2) amine was used for the synthesis of phosphonate/bisphosphonate end-modified PBAEs.

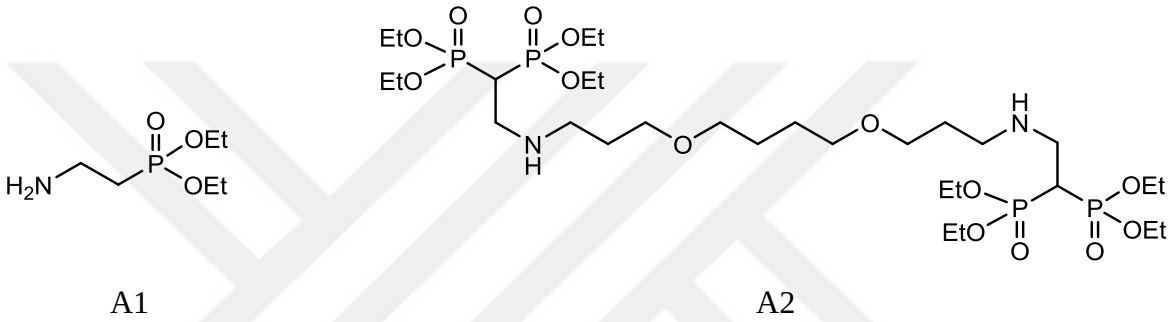

A1 A2

Figure 4.1. Structures of phosphonate and bisphosphonate-functionalized amines.

Diethyl 2-aminoethylphosphonate (A1) was synthesized from the reaction of diethyl vinyl phosphonate (P1) and ammonia [45] (Figure 4.2). ^{1}H-NMR spectrum of the product confirmed its structure (Figure 4.3). There were peaks at 2.03, 2.87 and 4.11 ppm because of methylene protons next to phosphorous, nitrogen and oxygen atoms (Figure 4.3). Also, FTIR spectrum shows peaks at around 3371, 2982, 1228, 1021 and 954 cm^{-1} due to N-H, C-H, P=O and P-O stretchings, respectively (Figure 4.4).

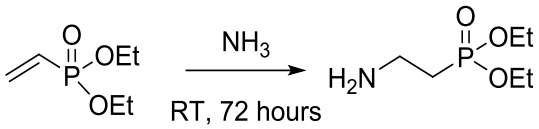

Figure 4.2. Synthesis of A1.

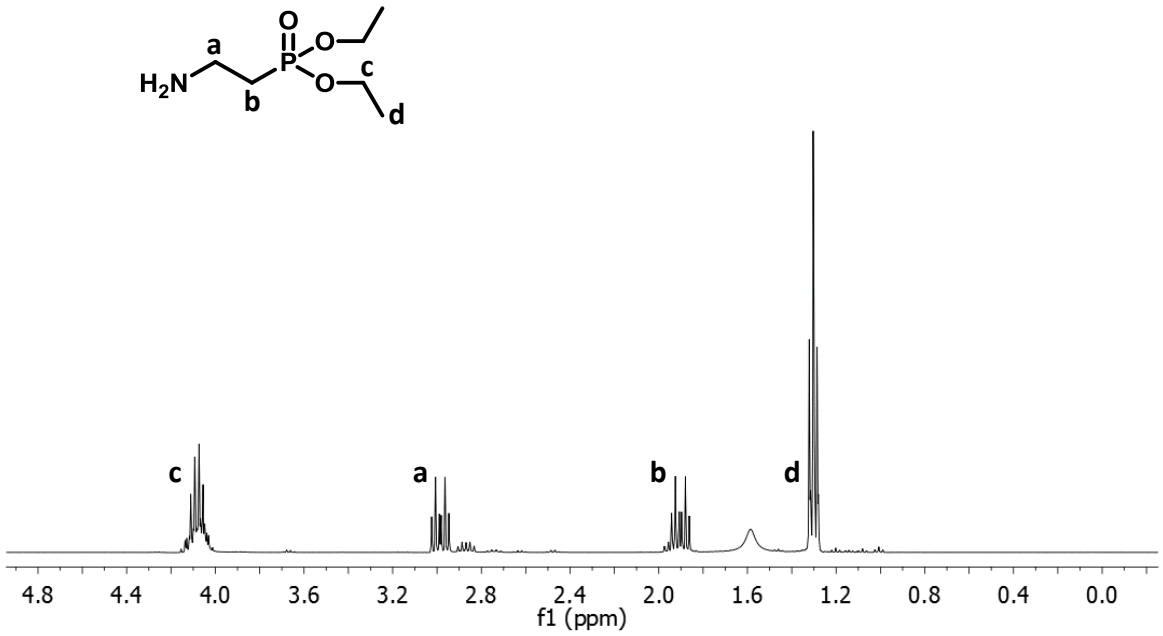

Figure 4.3. ^{1}H NMR spectrum of A1.

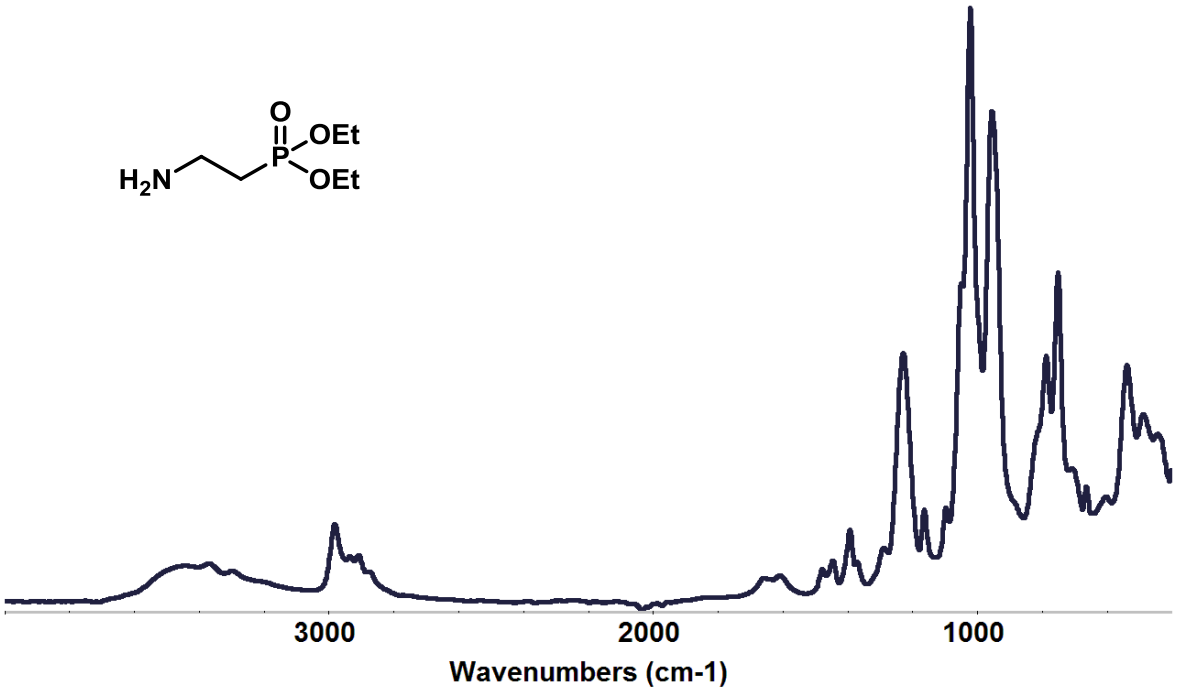

Figure 4.4. FTIR spectrum of A1.

The second amine, A2, was syntesized from Michael addition reaction of 4,9-dioxa-1,12-dodecanediamine and tetraethyl vinylidene bisphosphonate (P2) (Figure 4.5). Tetraethyl vinylidene bisphosphonate was synthesized according to a literature procedure

as shown in Figure 4.5 [46]. ^{1}H NMR spectrum of the product confirmed its structure (Figure 4.6).

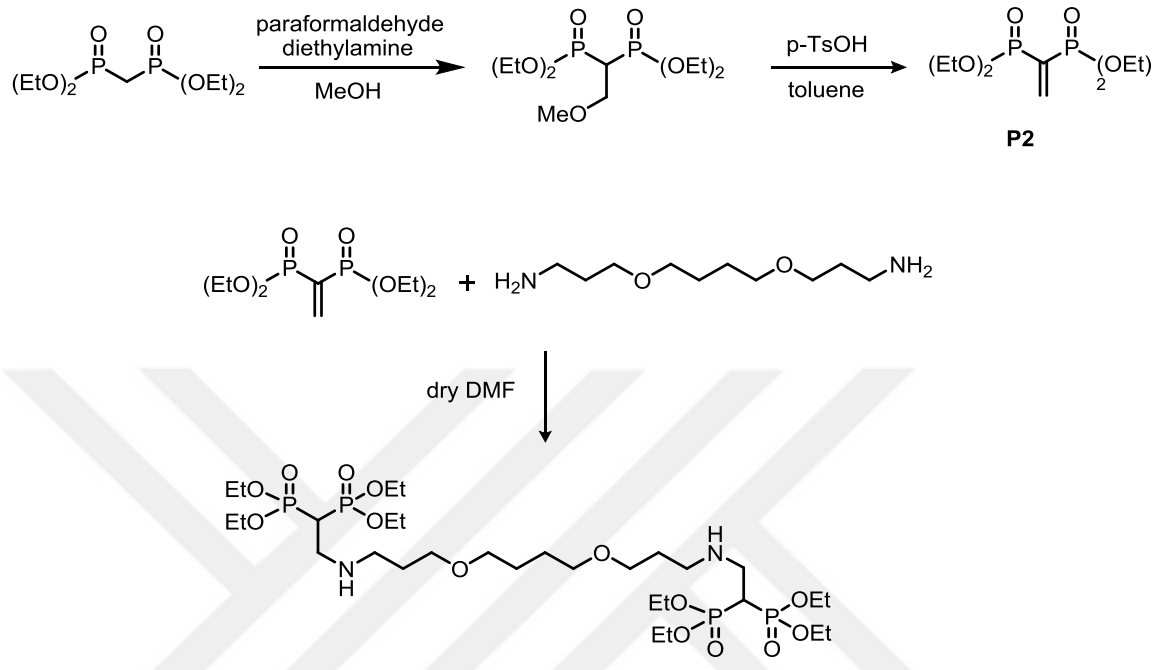

Figure 4.5. Synthesis of A2.

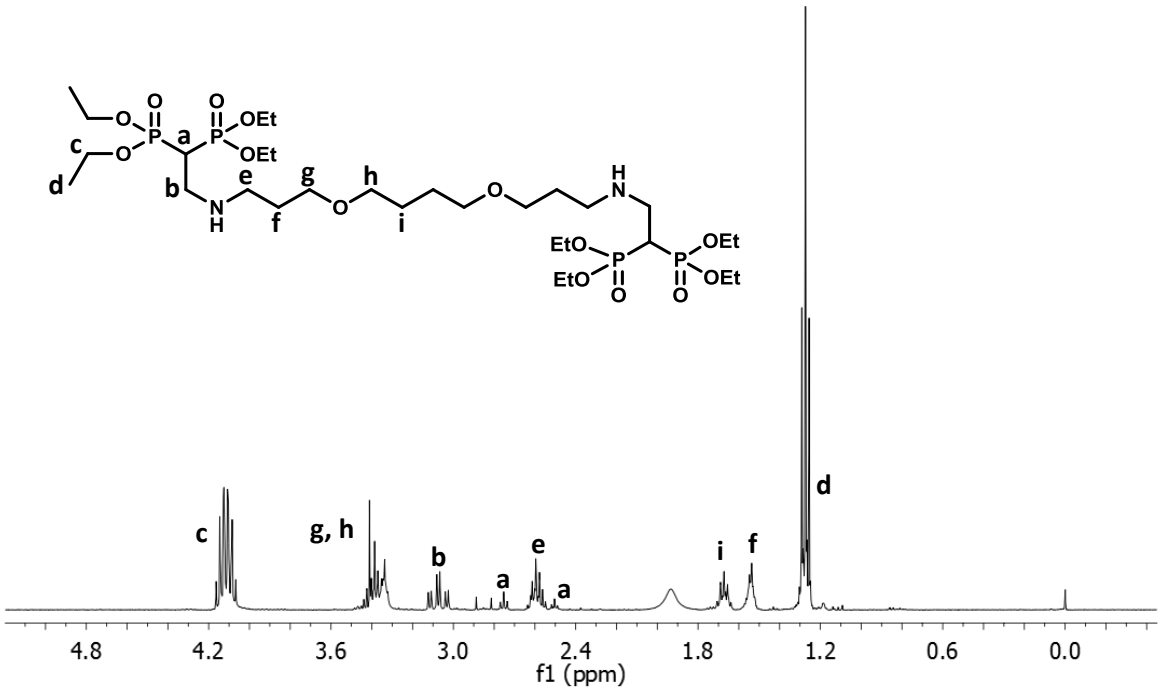

Figure 4.6. ^{1}H NMR spectrum of A2.

4.1.2. Synthesis of PBAE Macromers

Acrylate terminated PBAE macromers were synthesized by aza-Michael addition reaction of primary amines (PA and HP) with diacrylates (HDDA and PEGDA) without any solvent or catalyst (Figure 4.7). Two diacrylate to amine mol ratios 1:1 and 1.2:1 were used and the reactions were completed in 24 h at 90 °C. The macromers were washed with petroleum ether or diethyl ether to remove unreacted initial monomers or monosubstitution products. The products were obtained as yellowish viscous liquids. While PEGDA-based macromers were soluble in water, HDDA-based ones were soluble in organic solvents such as chloroform and THF (Table 1). All the macromers are soluble in water at acidic pH because of the quaternization of their amine groups. The macromers were characterized using their IR and ^{1}H NMR data. ^{1}H NMR spectra of macromers synthesized from PA showed methyl peak at around 0.85 ppm. HP based macromers showed peaks at 1.3, 1.42, 1.54 and 3.4 ppm due to the methylene groups of HP. Also, all macromers showed peaks between 2.4 and 2.8 ppm because of methylene attached to nitrogen and carbonyl groups (Figure 4.8.-4.11). The average number of repeating units of the macromers synthesized with 1.2:1 ratio were calculated from their ^{1}H NMR spectra by integrating acrylate protons (5.7-6.5 ppm) with respect to methyl protons (0.85 ppm) of PA or methylene protons attached to OH group (3.4-3.6 ppm) of HA (Table 2), which gives information about number average molecular weight (M_n). However, the macromers synthesized from 1:1 diacrylate to amine ratio may not have acrylate group at the both ends so their average molecular weight cannot be calculated by this technique. HDDA-based macromers had slightly higher number of repeating units compared to PEGDA-based macromers. This is probably because HDDA is a small monomer compared to PEGDA. The FTIR spectra of the macromers showed peaks at around 1725 and 1630 cm^{-1} due to C=O and C=C stretching. Also, macromers including HP showed a peak at around 3450 cm^{-1} because of O-H stretching (Figure 4.12).

Table 4.1. Solubilities of macromers.

Macromers	Water	Ether	Petroleum Ether	Chloroform	THF	Ethanol
HDDA:PA	-	+	-	+	+	+
HDDA:HP	-	+	-	+	+	+
PEGDA:PA	+	-	-	+	+	+
PEGDA:HP	+	-	-	+	+	+

Table 4.2. Repeating units (n) of macromers.

Macromer	n	M_n
HDDA:PA (1.2:1)	4-5	2335
HDDA:HP (1.2:1)	5-6	2554
PEGDA:PA (1.2:1)	2-3	2390
PEGDA:HP (1.2:1)	3-4	2795

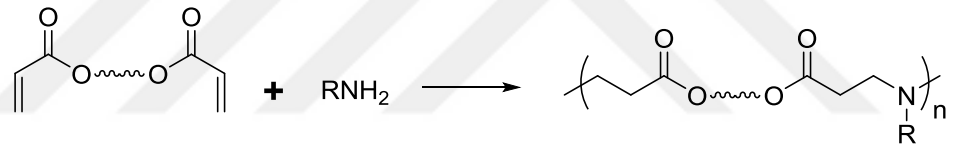

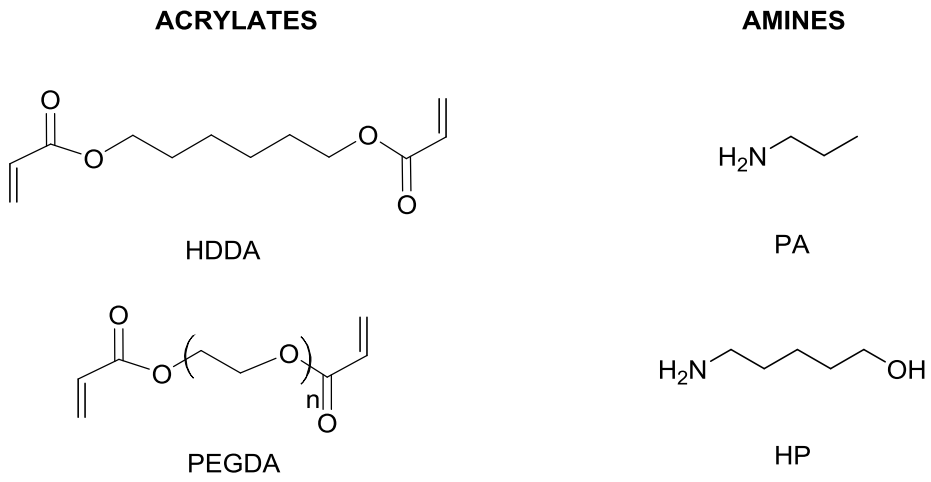

Figure 4.7. Synthesis route of macromers and structures of diacrylates and amines.

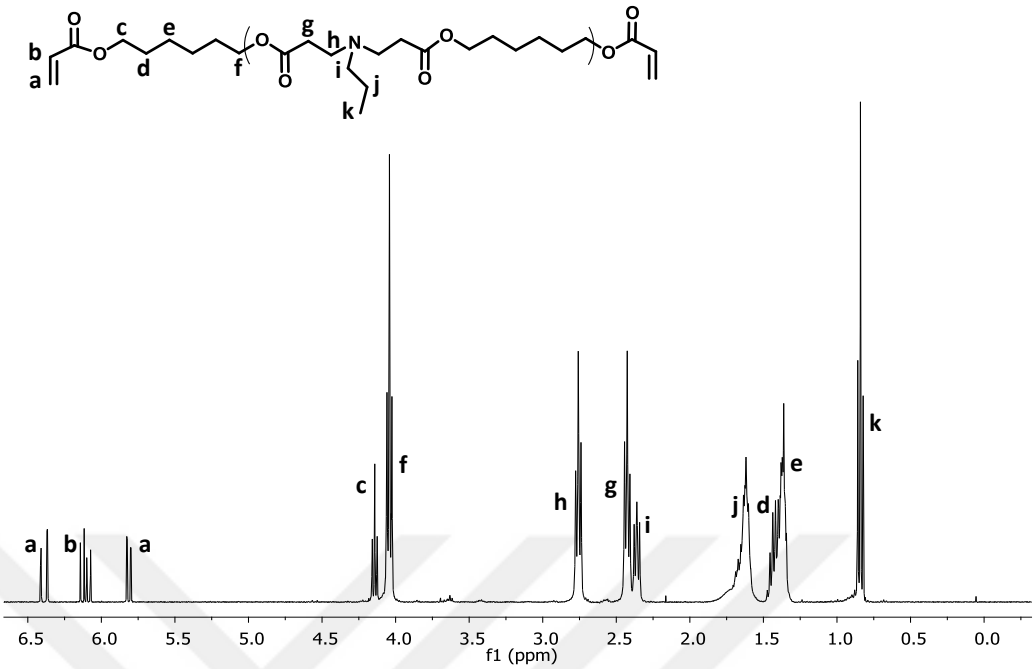

Figure 4.8. ^{1}H-NMR spectrum of HDDA:PA macromer (diacrylate to amine ratio is 1.2:1 mol).

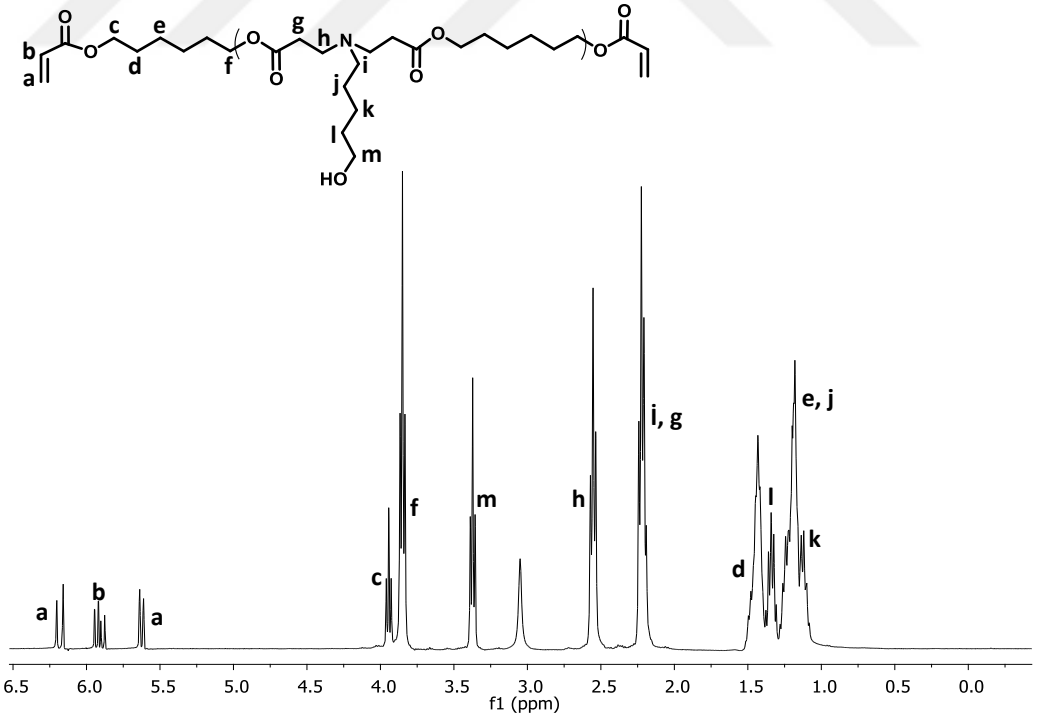

Figure 4.9. ^{1}H-NMR spectrum of HDDA:HP macromer (diacrylate to amine ratio is 1.2:1 mol).

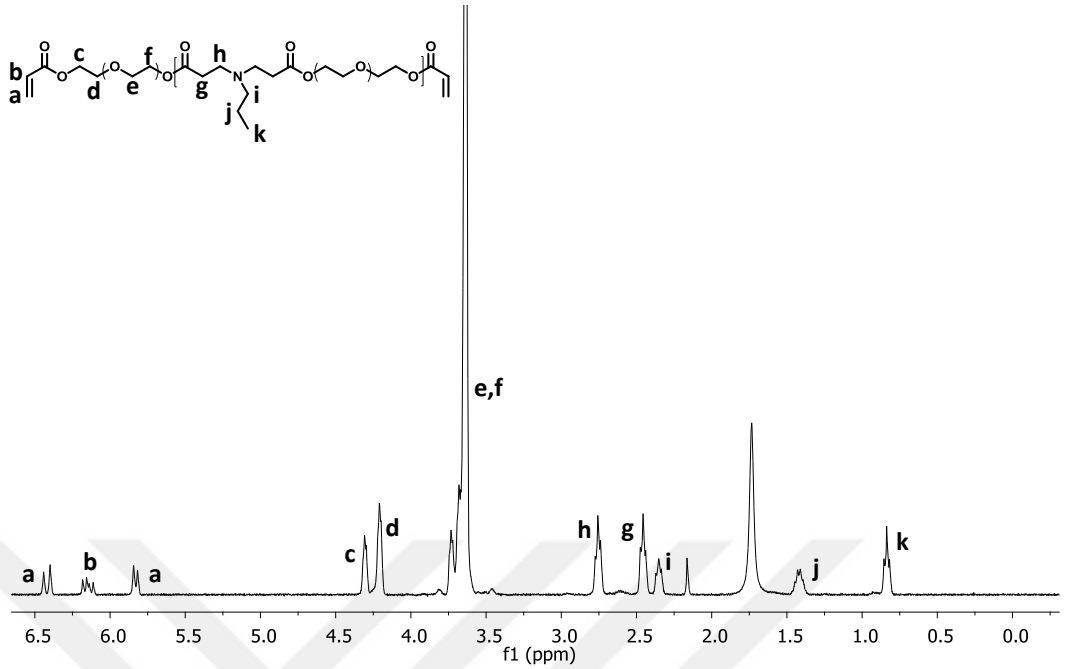

Figure 4.10. ^{1}H-NMR spectrum of PEGDA:PA macromer (diacrylate to amine ratio is 1.2:1 mol).

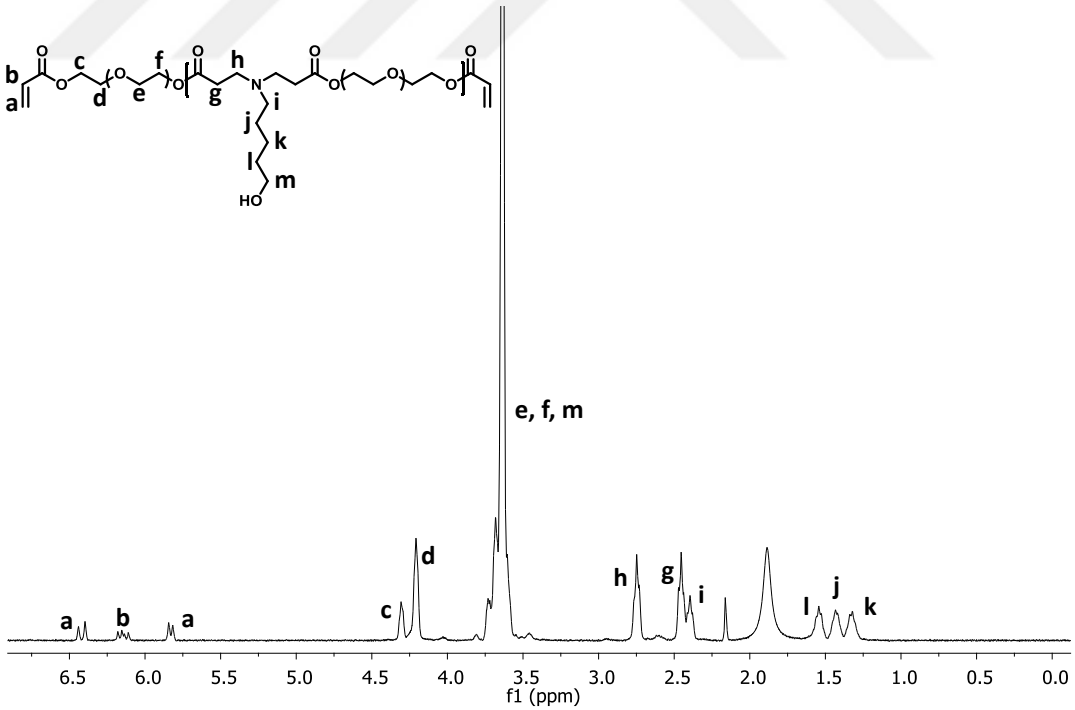

Figure 4.11. ^{1}H-NMR spectrum of PEGDA:HP macromer (diacrylate to amine ratio is 1.2:1 mol).

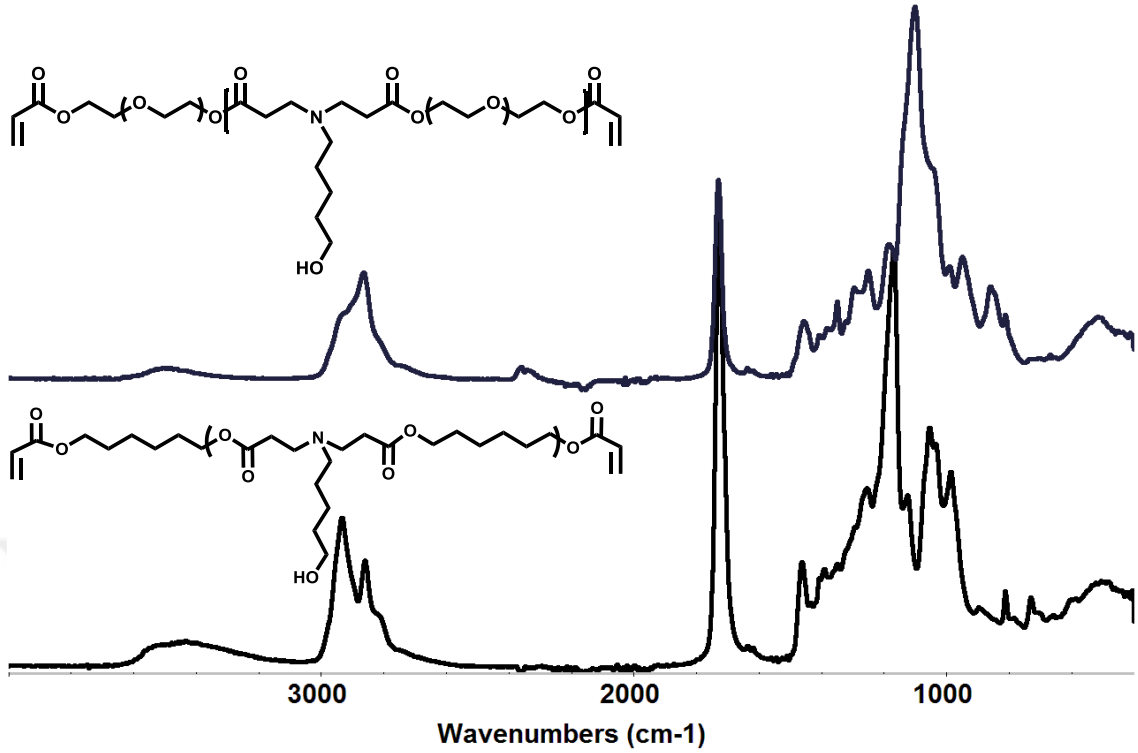

Figure 4.12. FTIR spectra of PEGDA:HP and HDDA:HP macromers.

4.1.3. Synthesis of Phosphonate and Bisphosphonate Functionalized PBAEs

Phosphonate end-functionalized PBAEs were synthesized by aza-Michael addition reaction of the amine A1 to the macromers (HDDA:PA, HDDA:HP, PEGDA:PA and PEGDA:HA) (Figure 4.13). The reactions were carried out with excess amine at room temperature for 3 days and the products were purified by washing with ether or petroleum ether to remove unreacted macromers or amines. PEGDA-based PBAEs were soluble in water but HDDA-based ones were soluble in organic solvents such as THF and DCM.

The polymers were characterized using their IR and ^{1}H NMR data. ^{1}H NMR spectra of polymers showed complex peaks at around 1.9 ppm due to methylene protons attached to phosphorus atom and acrylate peaks at around 5.7-6.5 ppm in the spectrum of the macromers disappeared because of addition of A1 amine (Figure 4.14-4.15). IR spectra of these polymers showed peaks at around 1720, 1245, 1025 and 960 cm^{-1} because of C=O, P=O, and P-O stretching (Figure 4.16-4.18).

A bisphosphonate end-functionalized PBAE was synthesized by aza-Michael addition reaction of the amine A2 to the macromer HDDA:PA (Figure 4.19). This reaction was carried out in 1:1 macromer:amine mol ratio at room temperature for 5 days to complete the functionalization reaction. The polymer was soluble in ether, DCM and THF but insoluble in petroleum ether and water.

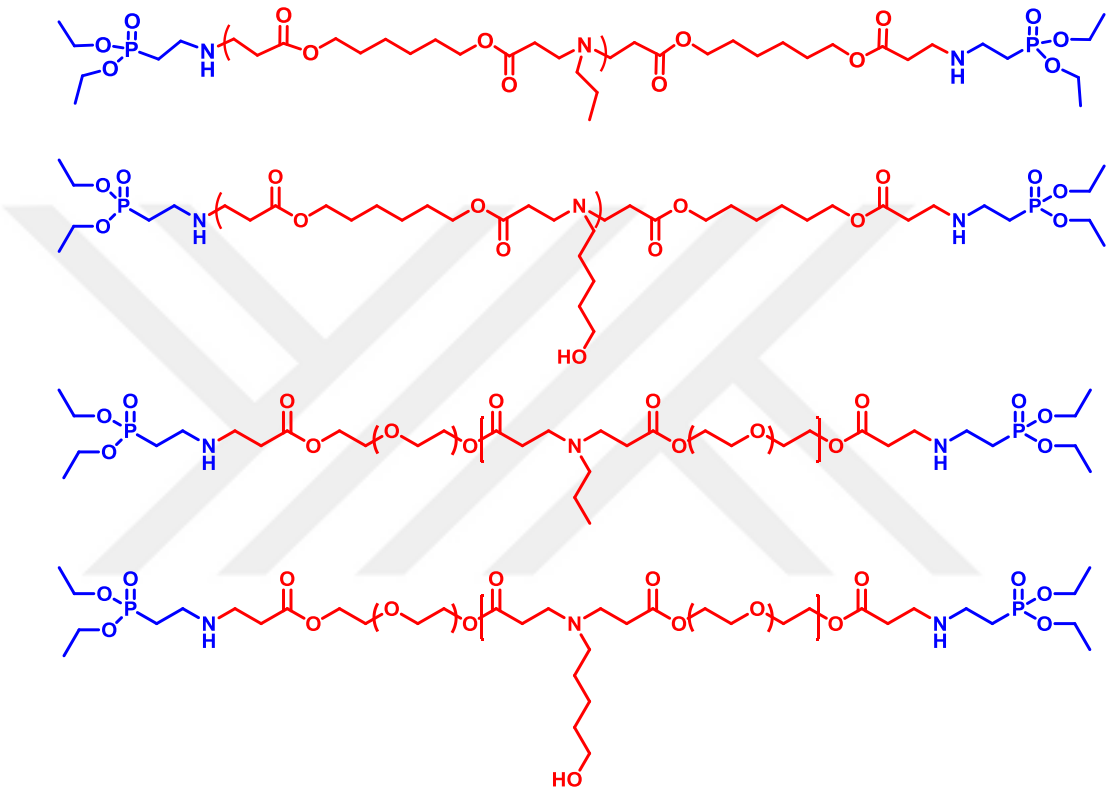

Figure 4.13. Structures of A1-based polymers.

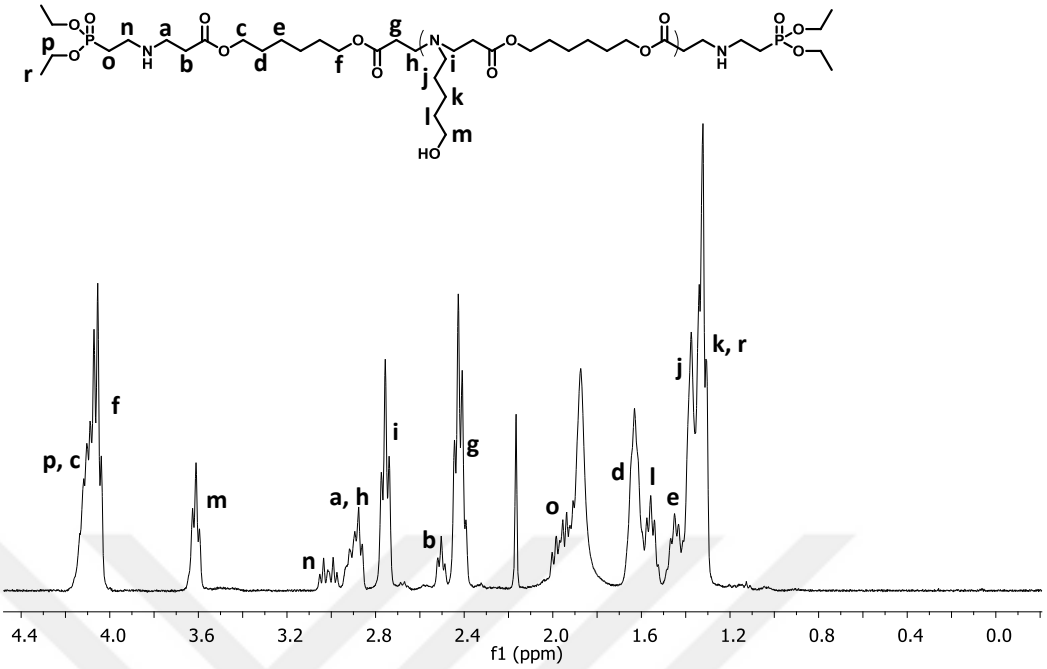

Figure 4.14. ^{1}H-NMR spectrum of [HDDA:HP]-A1 polymer.

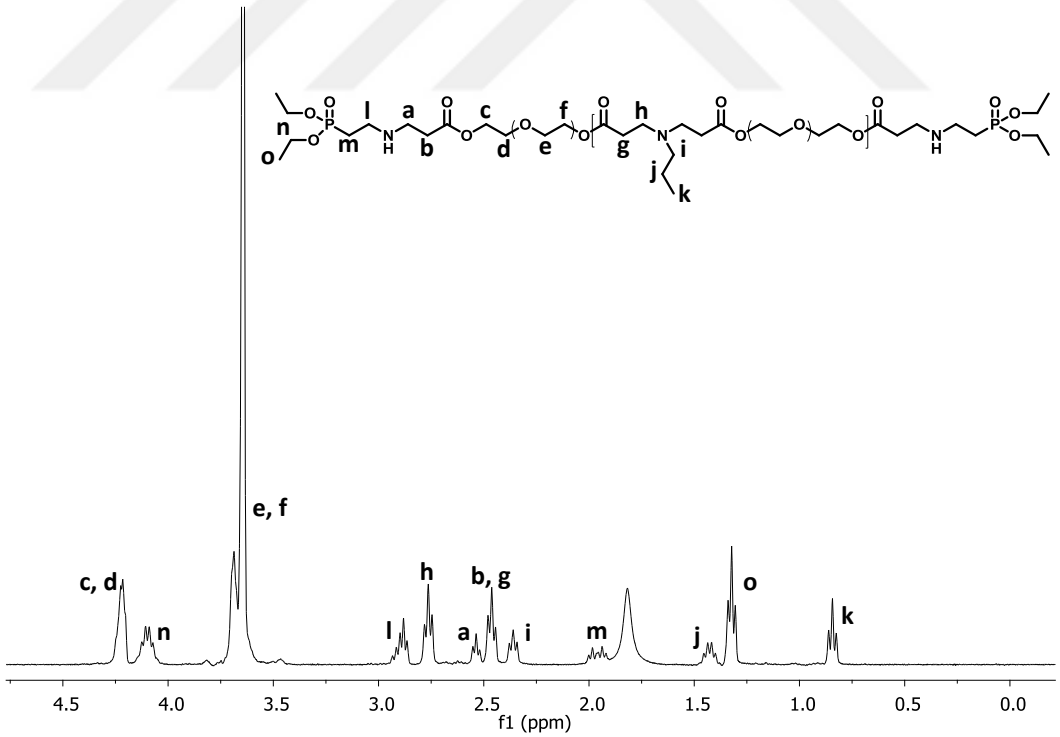

Figure 4.15. ^{1}H-NMR spectrum of [PEGDA:PA]-A1 polymer.

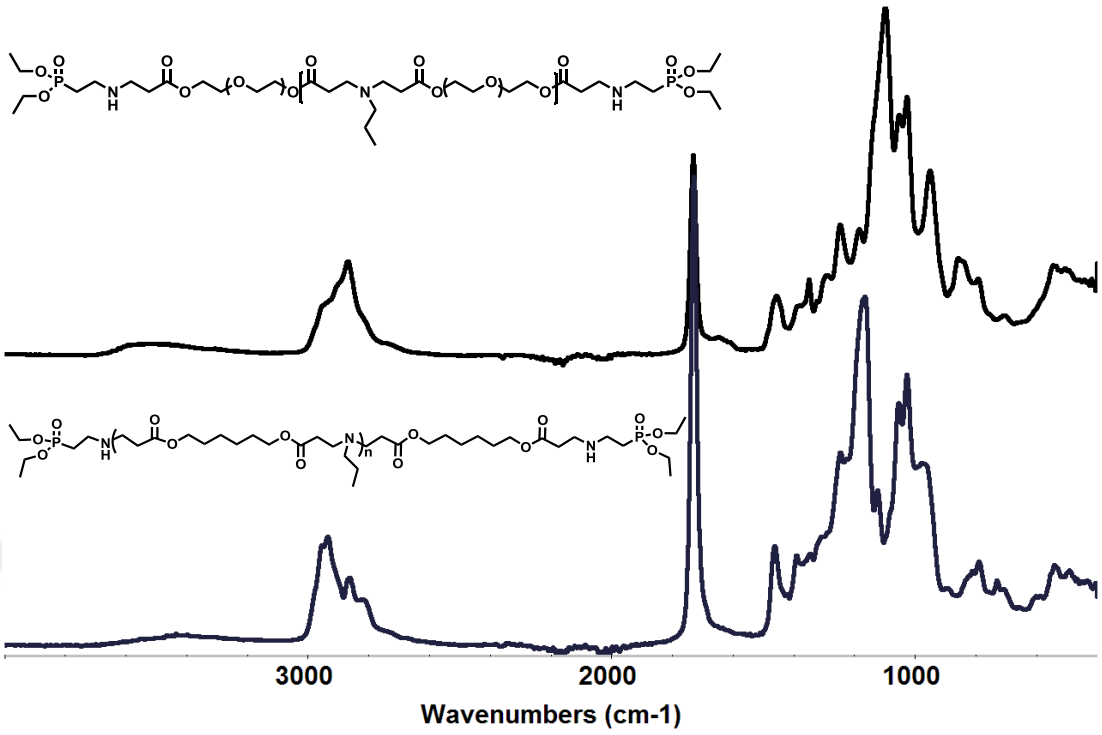

Figure 4.16. FTIR spectra of [HDDA:PA]-A1 and [PEGDA:PA]-A1.

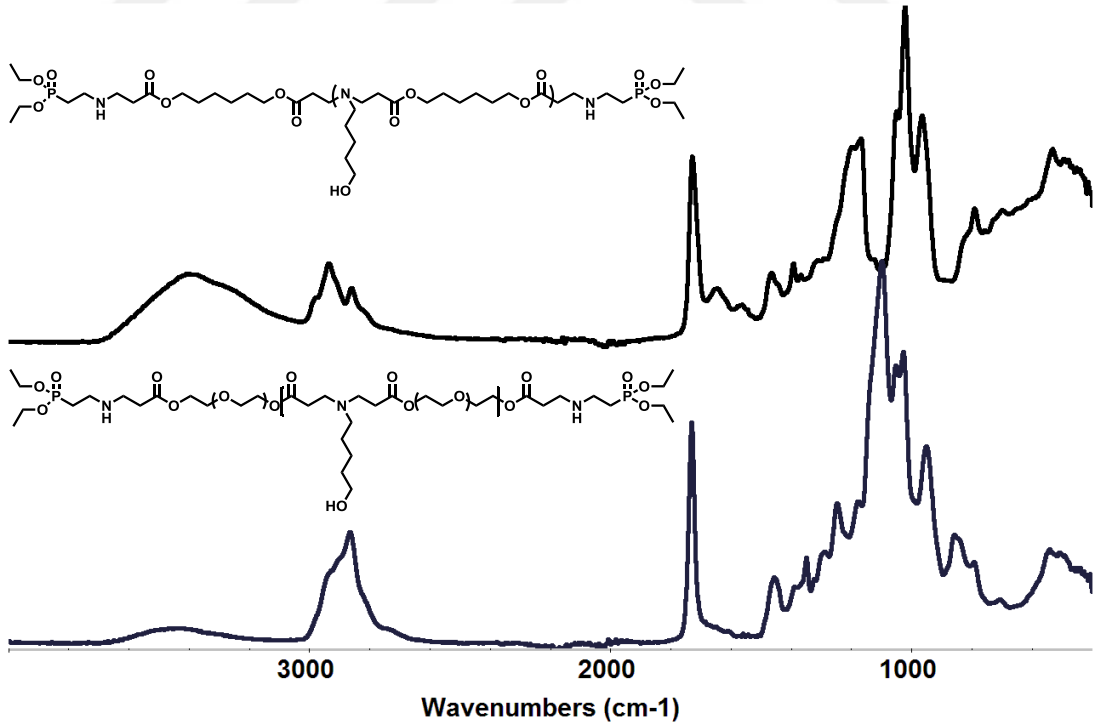

Figure 4.17. FTIR spectra of [HDDA:HP]-A1 and [PEGDA:HP]-A1.

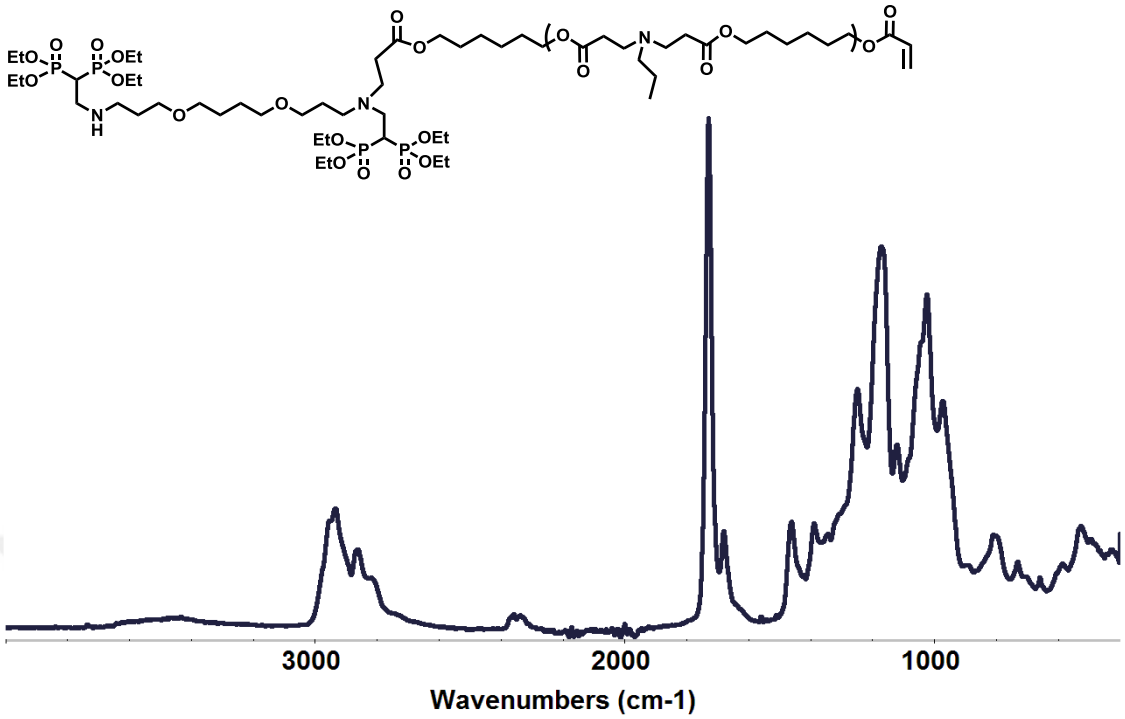

Figure 4.18. FTIR spectrum of [HDDA:PA]-A2.

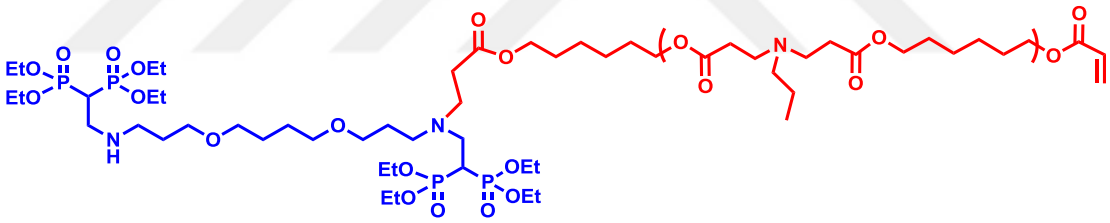

Figure 4.19. Structure of [HDDA:PA]-A2.

4.1.4. pH Sensitivity of PBAEs

The tunability of pH sensitivity of PBAEs is important for drug delivery systems because human body has different pH values in different tissues. In order to determine the pH sensitivity of the synthesized PBAE macromers and their phosphonate/bisphosphonate functionalized polymers, they were dissolved in deionized water at a final concentration of 1 mgmL^{-1} and titrated with 0.1 NaOH solution. The acid-base titration profiles are presented in Figures 4.20-4.23. It was observed that polymer structure has a strong influence on pH sensitivity. The pK_b values of polymers based on PEGDA were higher than those from HDDA (Figure 4.22 and 4.23). When hydrophilicity of the polymer is increased the pK_b values are observed to change to higher regions, as reported in other publication [7]. However, the effect of pendant groups (HA and PA) was not obvious. The

macromers prepared from 1.2:1 acrylate/amine ratios showed slightly lower pK_b values than those prepared from 1.1:1 ratios, indicating effect of molecular weight (Figure 4.20, 4.21 and Table 3). Also, polymers did not show much difference in titration curve from their macromer forms (Figure 4.20-4.23). Macromers consist of 1:1 ratio had a little lower pK_b values than 1.2:1 ratio ones (Figure 4.20 and 4.21). We can say that molecular weight has slight impact on pH titration curve. Repeating units of PEGDA-based macromers were less than HDDA-based ones so they contained fewer amine group. As a result of this, their plateaus in the titration curve were shorter than HDDA-based ones (Figure 4.20-4.21). Besides, HDDA-based macromers and polymers had straighter plateaus than PEGDA-based ones in the titration curve (Figure 4.20-4.23).

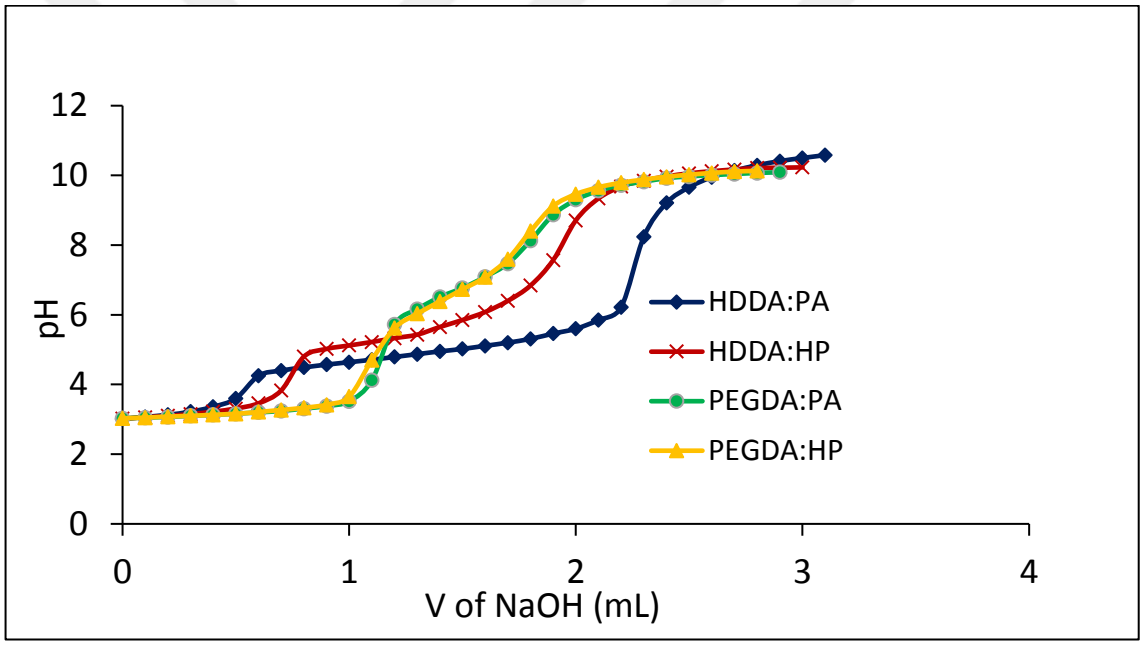

Figure 4.20. pH titration curve of macromers (1:1 ratio).

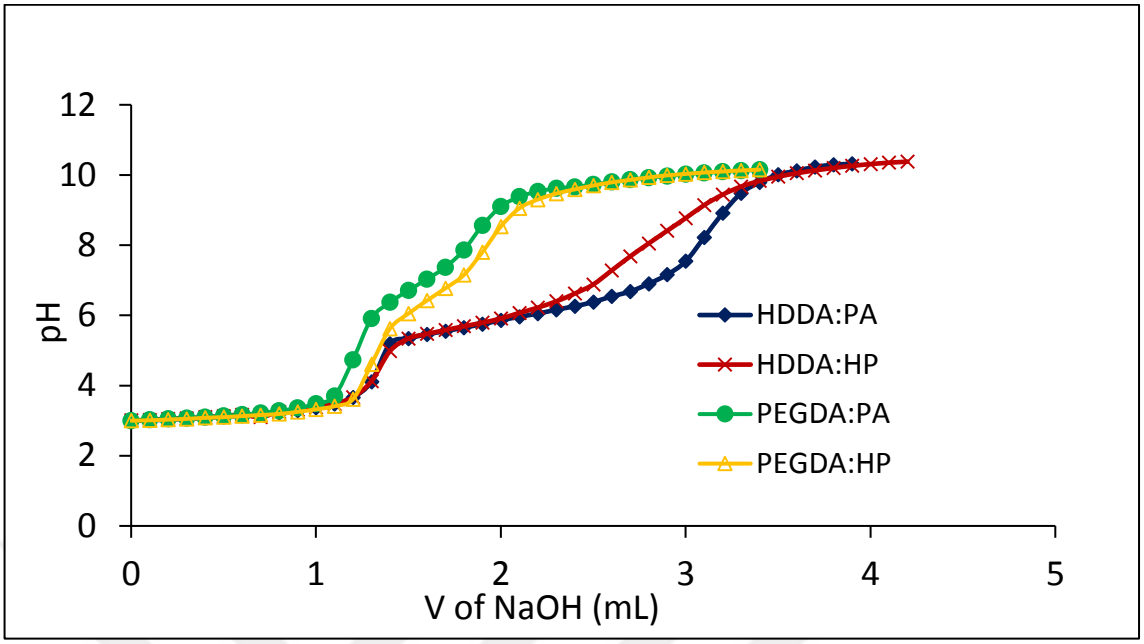

Figure 4.21. pH titration curve of macromers (1.2:1 ratio).

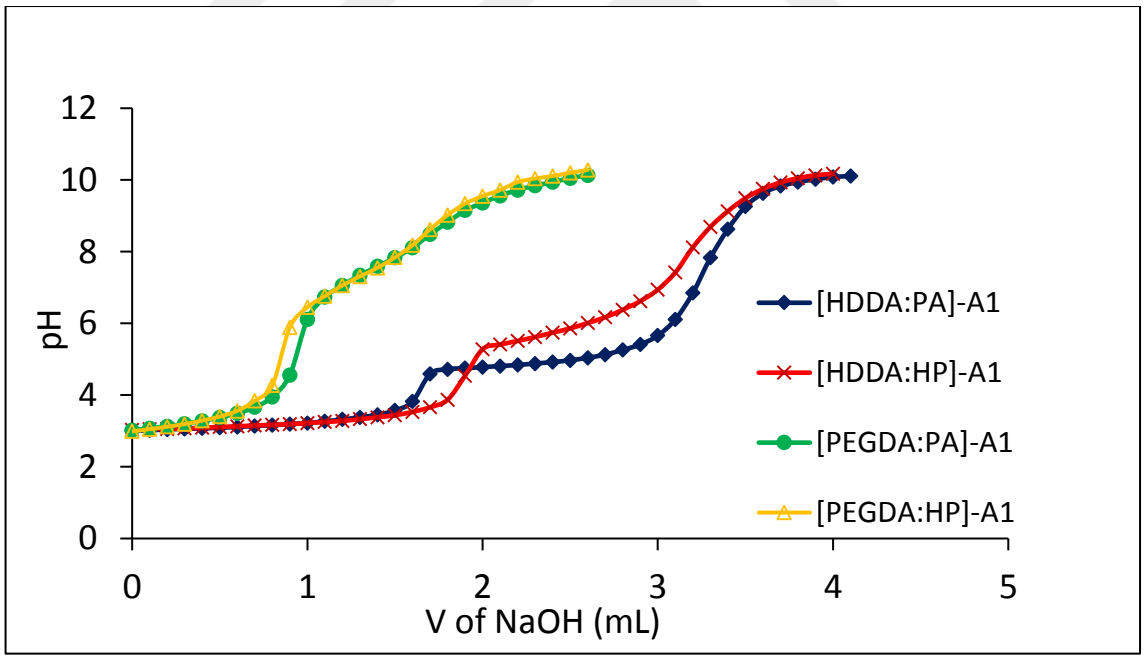

Figure 4.22. pH titration curve of polymers (1:1 ratio).

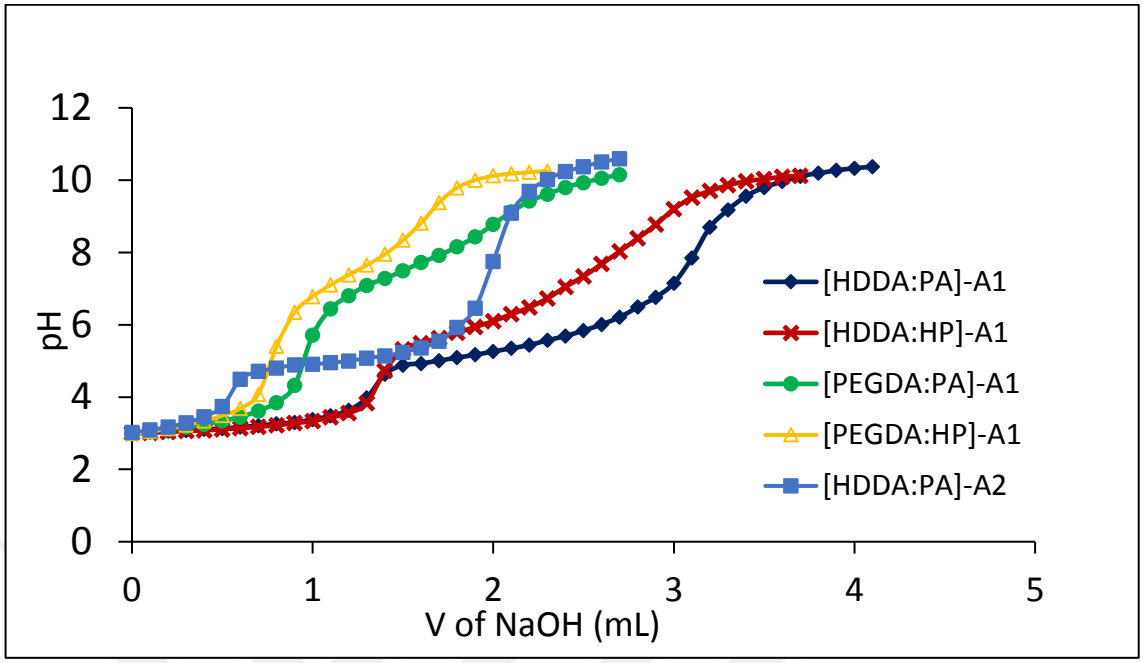

Figure 4.23. pH titration curve of polymers (1.2:1 ratio).

Table 4.3. pK_b values of macromers and polymers.

Macromers/polymers	**pK_b**
HDDA:PA (1.2:1)	6.05
HDDA:HP (1.2:1)	5.90
PEGDA:PA (1.2:1)	6.85
PEGDA:HP (1.2:1)	6.42
HDDA:PA (1:1)	4.95
HDDA:HP (1:1)	5.50
PEGDA:PA (1:1)	6.55
PEGDA:HP (1:1)	6.50
[HDDA(1.2):PA(1)]-A1	5.44
[HDDA(1.2):HP(1)]-A1	6.02
[PEGDA(1.2):PA(1)]-A1	7.50
[PEGDA(1.2):HP(1)]-A1	7.30
[HDDA(1):PA(1)]-A1	4.90
[HDDA(1):HP(1)]-A1	5.86
[PEGDA(1):PA(1)]-A1	7.34
[PEGDA(1):HP(1)]-A1	7.06
[HDDA(1.2):PA(1)]-A2	5.08

The pH sensitivity of the polymers was also tested by monitoring light transmittance properties (at 550 nm) of their dispersions in deionized water (Figure 4.24). PEGDA-based macromers were soluble in water so they did not show any turbidity.

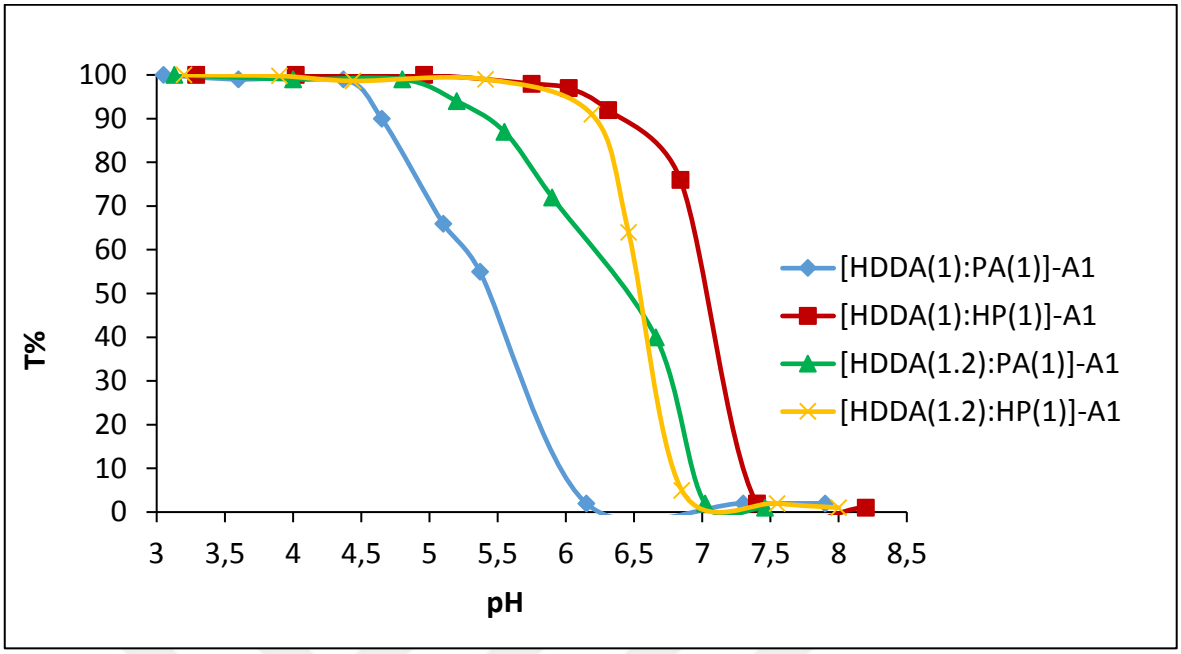

Figure 4.24. Transmittance curves of HDDA-based polymers.

4.1.5. Synthesis and Characterization of Micelles

An efficient drug delivery system requires stable drug encapsulation, capability of entering specific cells and rapidly releasing the drug in response to a biological trigger. Nanoparticles can be used as drug delivery systems due to their potential to improve circulation half-life, efficacy and drug tolerability [48]. For example, pH-responsive nanoparticles respond to changes in surface charge which can improve targeted delivery. Such pH-responsive drug delivery systems are usually prepared by using amphiphilic copolymers with hydrophilic and hydrophobic blocks. In this work, two of the phosphonate and bisphosphonate end functionalized polymers were evaluated for their capability of pH-sensitive drug delivery (Figure 4.25). They have quite similar pK_b values but the first polymer is like a triblock copolymer and second one may behave as a diblock copolymer. They will make micelles in different ways and it may affect properties of micelles such as stabiliy, size and drug loading efficiency. In this work, DOX was used to test drug delivery efficiency of the micelles in response to pH. Micelles with or without DOX were prepared by dialysis against water using DMF.

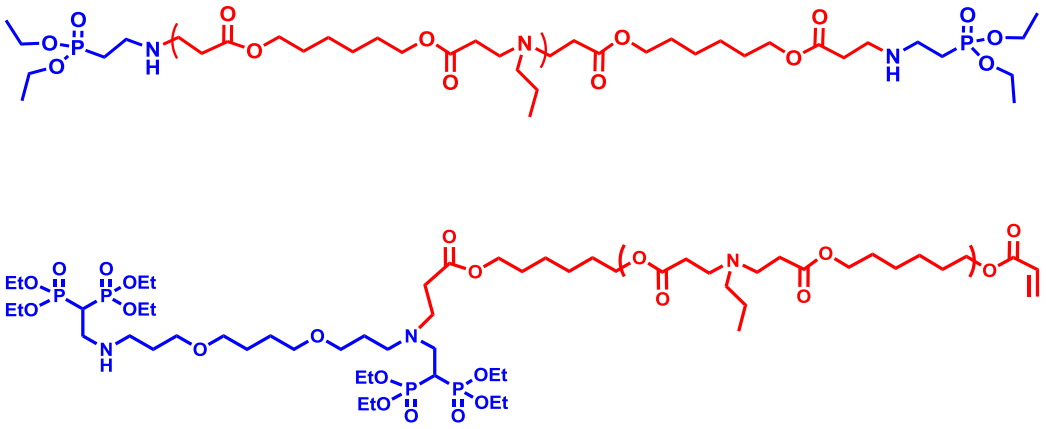

Figure 4.25. Structure of phosphonate and bisphosphonate end-functionalized polymers.

The morphology and the size distributions of the micelles in aqueous solutions, with and without DOX were investigated using DLS and SEM. The size of micelles prepared from [HDDA(1.2):PA(1)]-A1 were determined as 48 and 90 nm before and after DOX loading. Also, the size of the DOX-loaded [HDDA(1.2):PA(1)]-A2 micelles were found to be 96 nm (Figure 4.28). In general, polymeric micelles with small particle size (20–100 nm) have great potential for efficient drug delivery [49]. The micelles with larger sizes (>100 nm) may not be able to penetrate deeply into a tumor mass. Therefore, the synthesized micelles may have potential to be used in drug delivery systems.

Morphology of the DOX-loaded [HDDA(1.2):PA(1)]-A1 and [HDDA(1.2):PA(1)]-A2 micelles were determined by using SEM (Figure 4.29 and 4.30). The images show that micelles have a quite spherical shape and their sizes are consistent with DLS results.

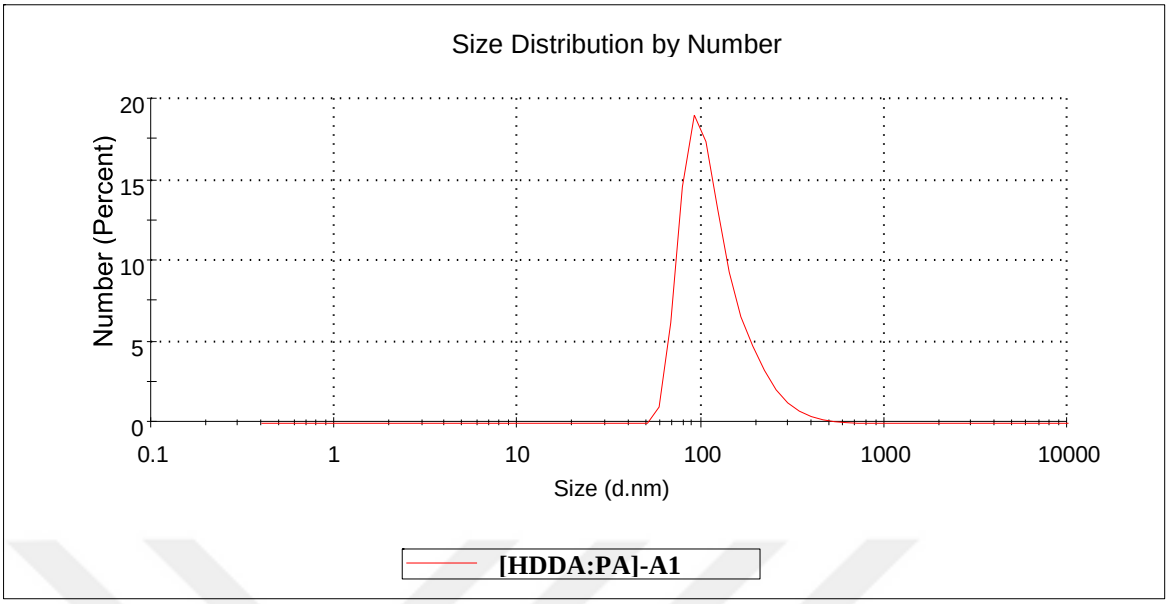

Figure 4.26. DLS result of DOX-loaded [HDDA(1.2):PA(1)]-A1 micelles.

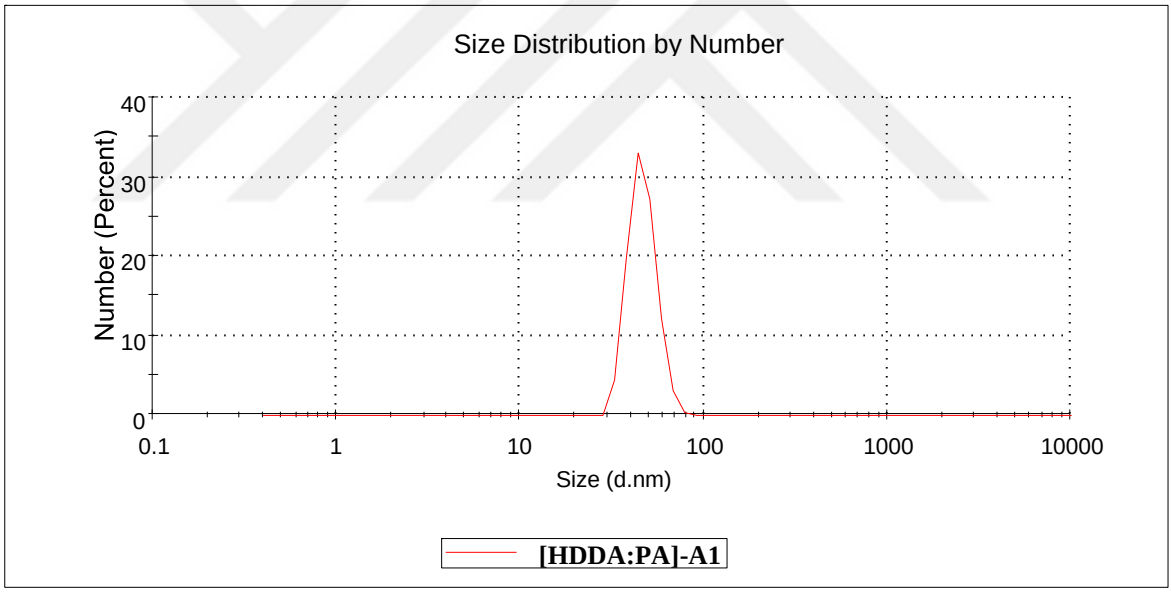

Figure 4.27. DLS result of unloaded [HDDA(1.2):PA(1)]-A1 micelles.

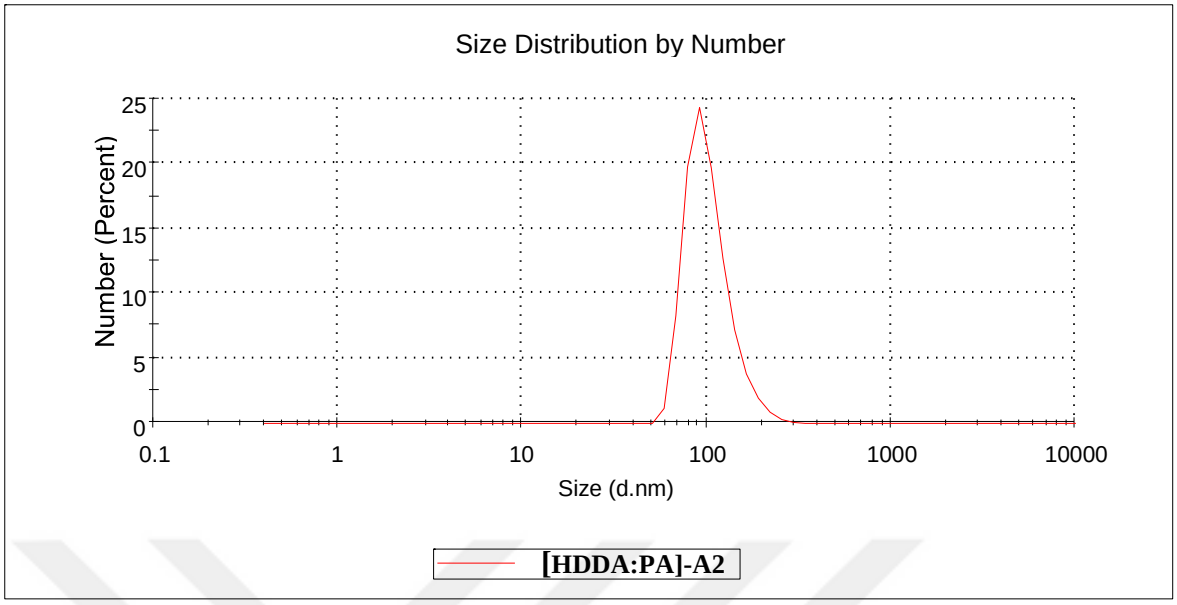

Figure 4.28. DLS result of DOX-loaded [HDDA(1.2):PA(1)]-A2 micelles.

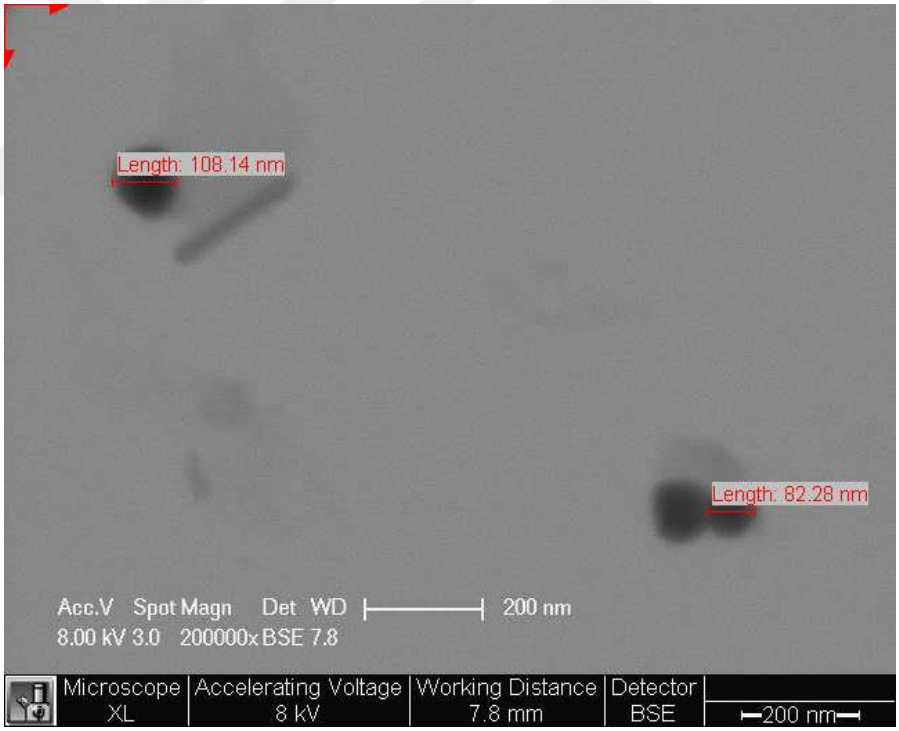

Figure 4.29. SEM image of DOX-loaded [HDDA(1.2):PA(1)]-A1 micelles.

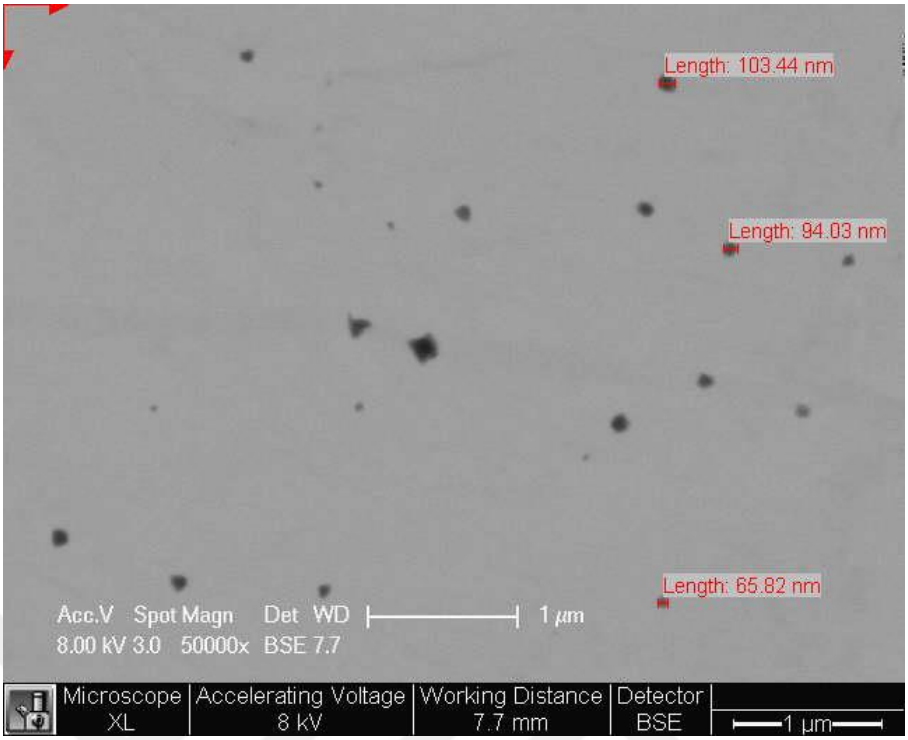

Figure 4.30. SEM image of DOX-loaded [HDDA(1.2):PA(1)]-A2 micelles.

4.1.6. DOX Encapsulation and Release

DOX release profiles from [HDDA(1.2):PA(1)]-A1 micelles are shown in Figure 4.31. It was observed that the release rate was less than 20% at pH 7.4 in 120 h. However, when pH was decreased to 5.5, the release rate becomes faster and 60% of DOX was released in 120 h. The release rate of [HDDA(1.2):PA(1)]-A2 micelles, was about 20% at pH 7.4 in 144 h. But release rate was increased to 63% in 144 h when the pH was decreased to 5.5. At pH 5.5, amine groups on the polymers get protonated and demicellization occurs. Thus, DOX is released from micelles and goes out of the dialysis membrane. These results showed that the synthesized micelles are able to minimize drug loss in circulation and extracellular environment. Also they can release their cargos inside acidic tumor cells.

Moreover, it was found that the concentration of triethylamine (TEA) used during DOX encapsulation has an important effect on drug loading efficiency. When TEA concentration was 3 times higher than that of DOX, drug loading efficiencies were 28% and 35% for [HDDA(1.2):PA(1)]-A1 and HDDA(1.2):PA(1)]-A2 micelles. However,

when TEA concentration was 13 times higher than that of DOX, drug loading efficiencies were around 43% for both micelles.

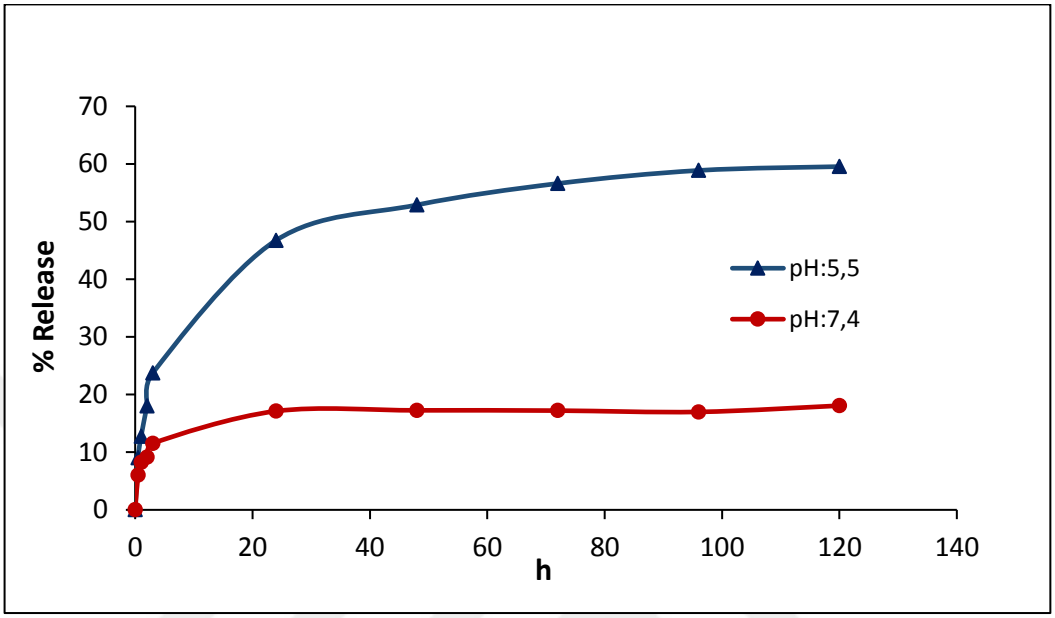

Figure 4.31. Release profiles of DOX-loaded [HDDA(1.2):PA(1)]-A1 micelles in different pH buffer solutions.

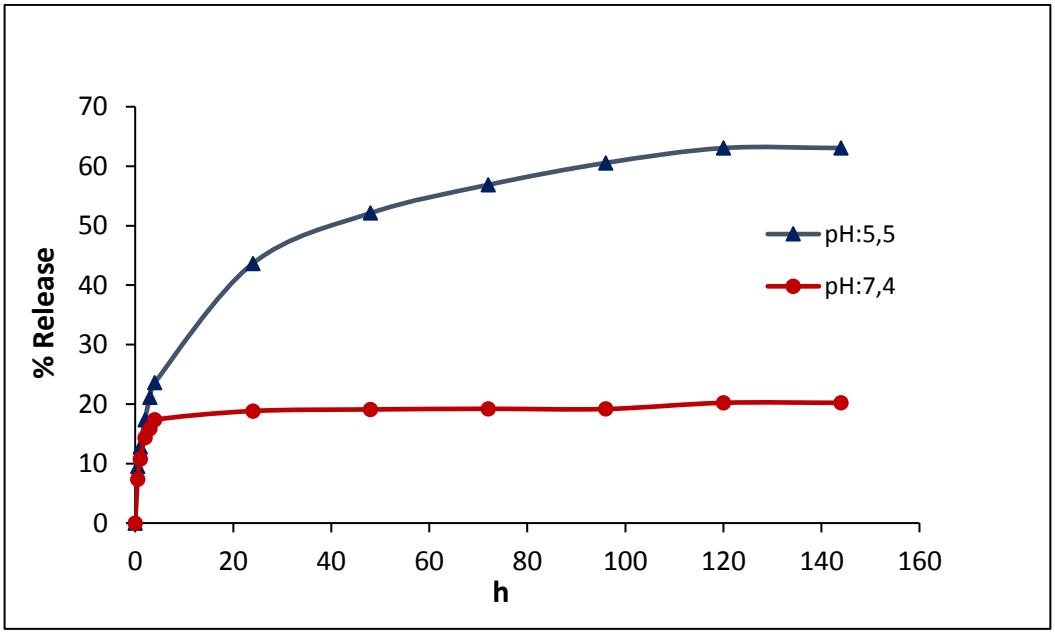

Figure 4.32. Release profiles of DOX-loaded [HDDA(1.2):PA(1)]-A2 micelles in different pH buffer solutions.

4.2. Polyethylenimines

4.2.1. Synthesis of Phosphonate and Bisphosphonate-Functionalized PEIs

Phosphonate and bisphosphonate-functionalized PEIs were synthesized by aza-Michael addition reaction of PEIs (1.8 and 10 kDa) and diethyl vinyl phosphonate (P1) and tetraethyl vinylidene bisphosphonate (P2) without any solvent or catalyst. The extent of substitution on PEIs was controlled by P1/P2:PEI feed ratio during the synthesis (Table 4) and the reactions were carried out room temperature for 2 days. The polymers were purified by washing with diethyl ether to remove unreacted P1 or P2 to give products as yellowish oils. They were soluble in water and methanol but insoluble in diethyl ether and petroleum ether. The polymers were characterized using their IR and ^{1}H NMR data. ^{1}H NMR spectra of PEI-P1 polymers showed methyl protons at 1.16 ppm and methylene protons attached to the P and O atoms at 1.95 and 3.98 ppm, respectively (Figure 4.33). The FTIR spectrum of PEI-P1 polymers showed peaks at around 3290, 2937-2818, 1227, 1023 and 961 cm^{-1} due to N-H, C-H, P=O and P-O stretching. ^{1}H NMR spectra of PEI-P2 polymers showed a methyl peak at 1.22 and a methylene peak attached to the O at 4.1 ppm (Figure 4.34). The FTIR spectrum of PEI-P2 polymers showed peaks at around 3293, 2934-2822, 1237, 1017 and 964 cm^{-1} due to N-H, C-H, P=O and P-O stretching (Figure 4.35). Also, there were broad peaks at around 2360 and 2430 cm^{-1} in the FTIR spectra of PEI-P1 and PEI-P2 polymers which are probably due to CO_2. These peaks were very weak in the FTIR spectrum of pure PEI kept in open air for two days. This result indicates that incorporation of P1 or P2 groups enhances CO_2 capturing ability of PEI. PEI substitution ratios were calculated from ^{1}H NMR spectrum by integrating methyl protons (1.16-1.22 ppm) with respect to methylene protons (2.4-2.8 ppm) of PEI (Table 4). It was observed that the substitution increased with increasing feed ratio. At the highest feed ratio of 4.0 the substitutions were 5.17 and 1.93 for P1 and P2.

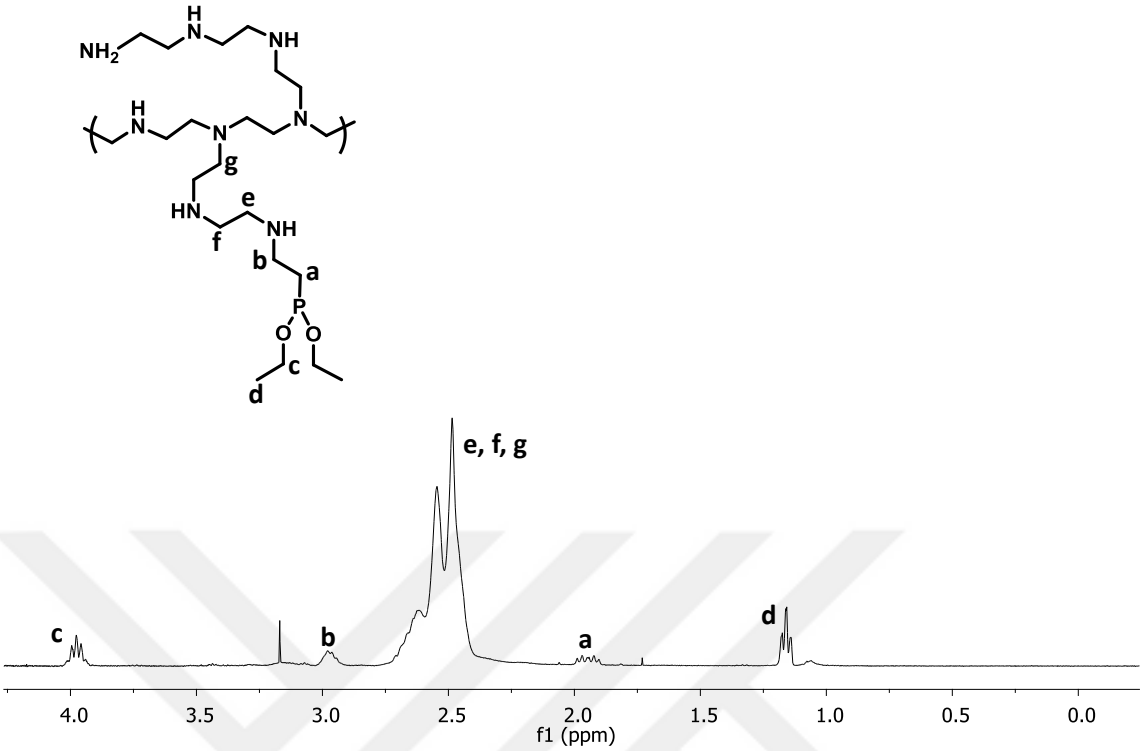

Figure 4.33. ^{1}H-NMR spectrum of PEI-P1-0.5.

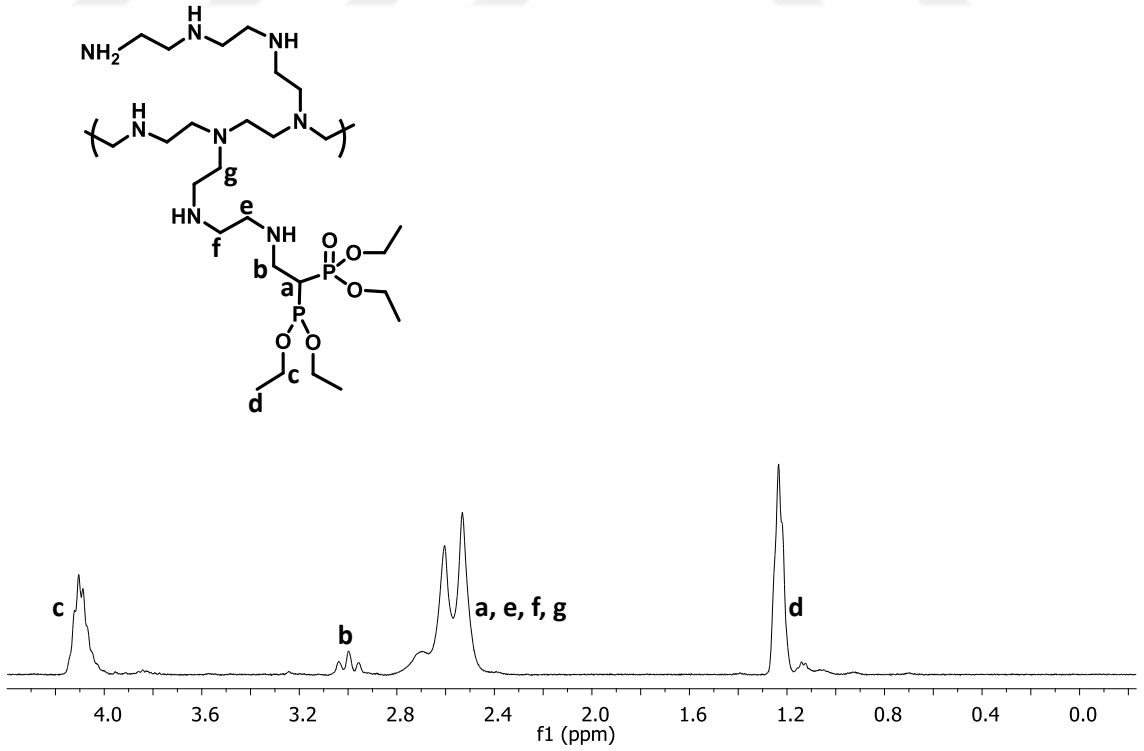

Figure 4.34. ^{1}H-NMR spectrum of PEI-P2-0.13.

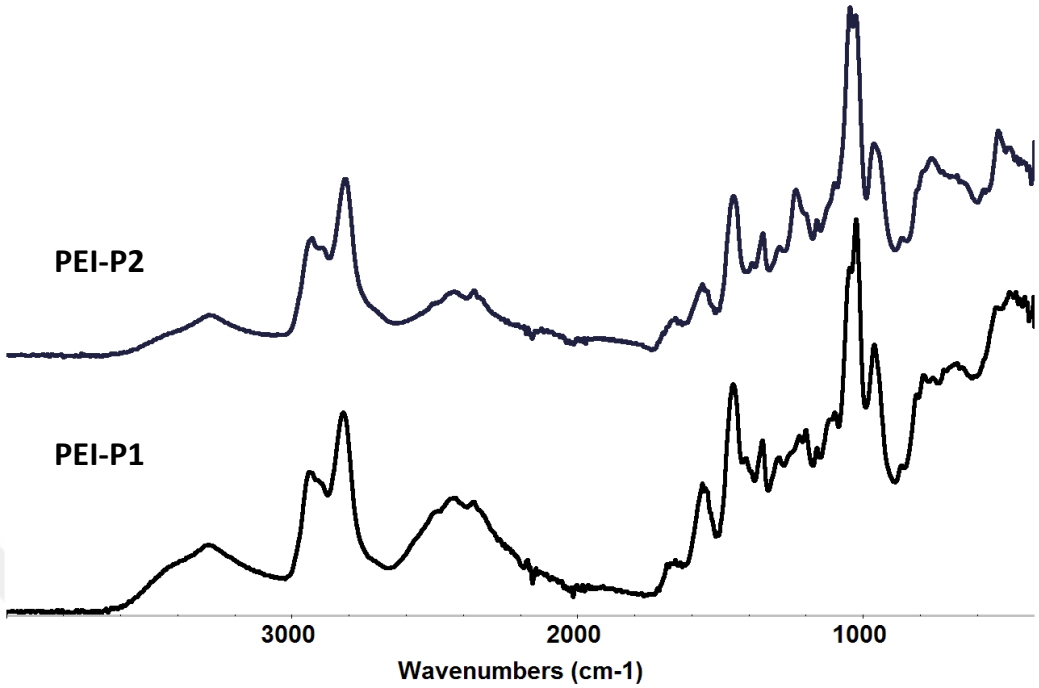

Figure 4.35. FTIR spectra of PEI-P1-0.5 and PEI-P2-0.5.

Table 4.4. Synthesized phosphonate and bisphosphonate-substituted 1.8 kDa PEIs.

Polymer designation	Substituent	PEI:Substituent ratio (feed)	PEI:Substituent ratio
PEI-P1-0.5	P1	0.5	0.49
PEI-P1-1.0	P1	1.0	1.20
PEI-P1-2.0	P1	2.0	1.83
PEI-P1-4.0	P1	4.0	5.17
PEI-P2-0.13	P2	0.13	0.135
PEI-P2-0.5	P2	0.5	0.68
PEI-P2-1.0	P2	1.0	1.00
PEI-P2-2.0	P2	2.0	3.00
PEI-P2-4.0	P2	4.0	4.93
PEI*-P2-0.04	P2	0.04	-

*10 kDa

4.2.2. Cellular Uptake and Transfection Efficiency of Polymers

This part of the study was carried out by Prof. Hasan Uludağ from University of Alberta. First, a series of bisphosphonate-functionalized PEIs (PEI-P2-1, PEI-P2-0.13 and PEI*-P2-0.04) were evaluated for transfection efficiency. Transfections were done at a DNA:polymer ratio of 1:5 and 1:10. Figure 4.36 shows the microscopic outcome on day 2. There was no efficiency for PEI-P2-0.13. High bisphosphonate substitution may be

reducing the ability of the polymers to complex DNA and/or the stability of the complexes. The other two polymers (PEI-P2-0.5 and PEI*-P2-0.04) showed some transfection efficiency but lower than PEI (25 kDa).

In order to find optimal substitution amount another series of this phosphonate and bisphosphonate substituted 1.8 kDa PEIs were evaluated for transfection efficiencies (Table 4). The polymers with a reasonable concentrations were screened by a microscope and it was found that PEI-P2-2 and PEI-P2-4 were the only ones that gave a positive response. Their transfection efficiencies were not as high as reference polymer but they had some transfection ability. Then, flow cytometry analysis of transfection was conducted for quantitative results. Reference polymer gave robust activity but our polymers did not show this activity. However, while reference polymer gave some toxicity, our polymers did not exhibit any toxicity even at high concentrations (Figure 4.36).

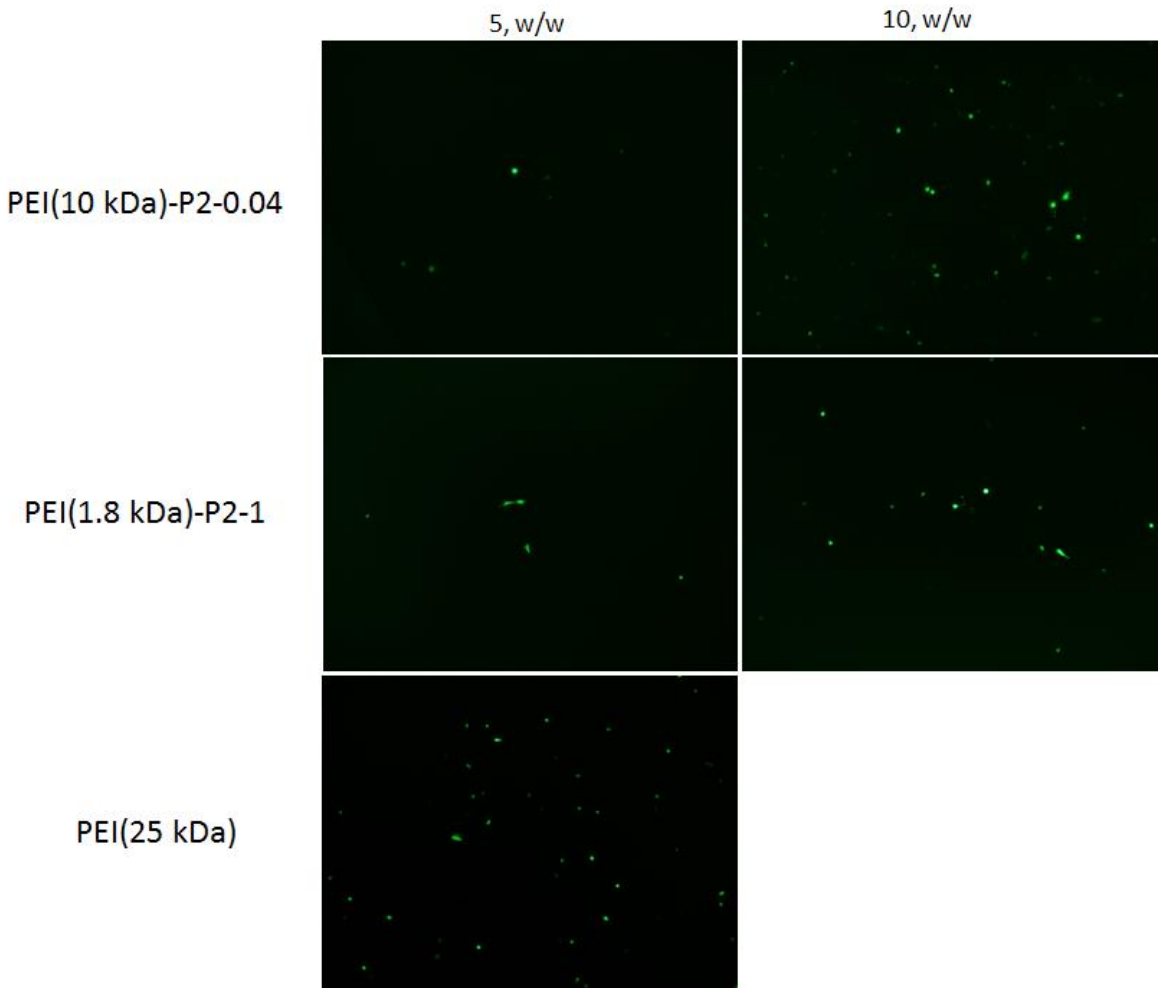

Figure 4.36. Transfection efficiencies of PEI (25 kDa) and the synthesized polymers at a DNA:polymer ratio of 1:5 and 1:10.

5. CONCLUSIONS

Four different phosphonate and one bisphosphonate end-modified PBAEs with ca. M_n = 2000-3000 were synthesized. All PBAEs showed different pK_b values depending on their chemical structure; HDDA-based PBAEs showed lower values than PEGDA-based ones. Two of the micelle forming PBAEs with micelle sizes of ca. 40-100 nm are investigated for the delivery of the chemotherapy drug Doxorubicin (DOX). The drug loading efficiencies were found to be 28-43% for both micelles. The micelles were quite stable at pH 7.4 and less than 20% of drug was released. When pH was decreased to 5.5, release rate was increased to 60%. These results showed that these polymers can be used for pH-sensitive drug delivery applications.

Novel phosphonate and bisphosphonate-functionalized PEIs were successfully synthesized and their structures were confirmed by ^{1}H-NMR and FTIR spectroscopy. Transfection ability of the synthesized polymers was evaluated and it was found that PEI-P2-1, PEI-P2-2 and PEI-P2-3 showed some transfection. Moreover, the polymers were found to be nontoxic at the concentration tested. Thus, transfection efficiency can be increased by increasing polymer concentration or by using higher molecular weight of PEI with the optimal substitution ratio. Also, PEI-P1 and PEI-P2 polymers showed higher CO_2 capturing ability than pure PEI.

REFERENCES

1. D. G. Anderson *et al.*, "A Polymer Library Approach to Suicide Gene Therapy for Cancer," *Proceedings of the National Academy of Sciences*, vol. 101, no. 45, pp. 16028–16033, 2004.

2. G. T. Zugates *et al.*, "Gene Delivery Properties of End-Modified Poly(beta-amino ester)s.," *Bioconjugate Chemistry*, vol. 18, no. 6, pp. 1887–1896, 2007.

3. Y. Gao *et al.*, "Highly Branched Poly(β-amino esters) for Non-Viral Gene Delivery: High Transfection Efficiency and Low Toxicity Achieved by Increasing Molecular Weight," *Biomacromolecules*, vol. 17, no. 11, pp. 3640–3647, 2016.

4. J. Zhao *et al.*, "Synthesis of Amphiphilic Poly(β-amino ester) for Efficiently Minicircle DNA Delivery in Vivo," *ACS Applied Material & Interfaces*, vol. 8, no. 30, pp. 19284–19290, 2016.

5. X. Deng, N. Zheng, Z. Song, L. Yin, and J. Cheng, "Trigger-Responsive, Fast-Degradable Poly(β-amino ester)s for Enhanced DNA Unpackaging and Reduced Toxicity," *Biomaterials*, vol. 35, no. 18, pp. 5006–5015, 2014.

6. K. Engin, D. B. Leeper, J. R. Cater, A. J. Thistlethwaite, L. Tupchong, and J. D. McFarlane, "Extracellular pH Distribution in Human Tumours," *International Journal of Hyperthermia*, vol. 11, no. 2, pp. 211–6, 1995.

7. W. Song *et al.*, "Tunable pH-Sensitive Poly(β-amino ester)s Synthesized from Primary Amines and Diacrylates for Intracellular Drug Delivery," *Macromolecular Bioscience*, vol. 12, no. 10, pp. 1375–1383, 2012.

8. K. H. Min *et al.*, "Tumoral Acidic pH-Responsive MPEG-poly(β-amino ester) Polymeric Micelles for Cancer Targeting Therapy," *Journal of Controlled Release*, vol. 144, no. 2, pp. 259–266, 2010.

9. S. Tang *et al.*, “Co-delivery of Doxorubicin and RNA Using pH-Sensitive Poly (β-amino ester) Nanoparticles for Reversal of Multidrug Resistance of Breast Cancer,” *Biomaterials*, vol. 35, no. 23, pp. 6047–6059, 2014.

10. J. Chen, X. Qiu, J. Ouyang, J. Kong, W. Zhong, and M. M. Q. Xing, “PH and Reduction Dual-Sensitive Copolymeric Micelles for Intracellular Doxorubicin Delivery,” *Biomacromolecules*, vol. 12, no. 10, pp. 3601–3611, 2011.

11. S. A. Meenach, C. G. Otu, K. W. Anderson, and J. Z. Hilt, “Controlled Synergistic Delivery of Paclitaxel and Heat from Poly(β-amino ester)/Iron Oxide-Based Hydrogel Nanocomposites,” *International Journal of Pharmaceutics*, vol. 427, no. 2, pp. 177–184, 2012.

12. A. Mozhi, I. Ahmad, C. I. Okeke, C. Li, and X.-J. Liang, “pH-Sensitive Polymeric Micelles for the Co-Delivery of Proapoptotic Peptide and Anticancer Drug for Synergistic Cancer Therapy,” *RSC Advances*, vol. 7, no. 21, pp. 12886–12896, 2017.

13. S. Perni and P. Prokopovich, “Poly-Beta-Amino-Esters Nano-Vehicles Based Drug Delivery System for Cartilage,” *Nanomedicine: Nanotechnology, Biology and Medicine*, vol. 13, no. 2, pp. 539–548, 2017.

14. Y. Zhang, R. Wang, Y. Hua, R. Baumgartner, and J. Cheng, “Trigger-Responsive Poly(β-amino ester) Hydrogels,” *ACS Macro Letters*, vol. 3, no. 7, pp. 693–697, 2014.

15. D. G. Anderson *et al.*, “A Combinatorial Library of Photocrosslinkable and Degradable Materials,” *Advanced Materials*, vol. 18, no. 19, pp. 2614–2618, October 2006.

16. D. M. Brey, J. L. Ifkovits, R. I. Mozia, J. S. Katz, and J. A. Burdick, “Controlling Poly(β-amino ester) Network Properties Through Macromer Branching,” *Acta Biomaterialia*, vol. 4, no. 2, pp. 207–217, 2008.

17. D. M. Brey, I. Erickson, and J. A. Burdick, “Influence of Macromer Molecular Weight and Chemistry on Poly(β-amino ester) Network Properties and Initial Cell Interactions,” *Journal of Biomedical Materials Research - Part A*, vol. 85, no. 3, pp. 731–741, 2008.

18. D. L. Safranski, M. A. Lesniewski, B. S. Caspersen, V. M. Uriarte, and K. Gall, “The Effect of Chemistry on the Polymerization, Thermo-Mechanical Properties and Degradation Rate of Poly(β-amino ester) Networks,” *Polymer*, vol. 51, no. 14, pp. 3130–3138, 2010.

19. D. L. Safranski, D. Weiss, J. B. Clark, W. R. Taylor, and K. Gall, “Semi-Degradable Poly(β-amino ester) Networks with Temporally Controlled Enhancement of Mechanical Properties,” *Acta Biomaterialia*, vol. 10, no. 8, pp. 3475–3483, 2014.

20. S. Monge *et al.*, “Phosphorus-Containing Polymers: Great Opportunity for the Biomedical Field,” *Biomacromolecules*, vol. 12, pp. 1973–1982, 2011.

21. G. Sahin, D. Avci, O. Karahan, and N. Moszner, “Synthesis and Photopolymerizations of New Phosphonated Methacrylates from Alkyl a-Hydroxymethacrylates and Glycidyl Methacrylate,” *Journal of Applied Polymer Science*, vol. 114, pp. 97–106, 2009.

22. B. Akgun and D. Avci, “Synthesis and Evaluations of Bisphosphonate-Containing Monomers for Dental Materials,” *Journal of Polymer Science Part A: Polymer Chemistry*, vol. 50, no. 23, pp. 4854–4863, 2012.

23. R. Erez, S. Ebner, B. Attali, and D. Shabat, “Chemotherapeutic Bone-Targeted Bisphosphonate Prodrugs with Hydrolytic Mode of Activation,” *Bioorganic & Medicinal Chemistry Letters*, vol. 18, no. 2, pp. 816–820, 2008.

24. H. Mahjoubi, J. M. Kinsella, M. Murshed, and M. Cerruti, “Surface Modification of Poly (D,L‐Lactic Acid) Scaffolds for Orthopedic Applications : A Biocompatible, Nondestructive Route via Diazonium Chemistry,” *ACS Applied Materials and*

Interfaces, vol. 6, no. 13, pp. 9975–9987, 2014.

25. X. Gao, K.-S. Kim, and D. Liu, "Nonviral Gene Delivery: What We Know and What is Next," The *AAPS Journal*, vol. 9, no. 1, pp. E92–E104, 2007.

26. C. N. Lungu, M. V. Diudea, M. V. Putz, and I. P. Grudzinski, "Linear and Branched PEIs (Polyethylenimines) and Their Property Space," *International Journal of Molecular Sciences*, vol. 17, no. 4, p. 555, 2016.

27. O. Yemul and T. Imae, "Synthesis and Characterization of Poly(ethyleneimine) Dendrimers," *Colloid and Polymer Science*, vol. 286, no. 6–7, pp. 747–752, 2008.

28. M. Khansarizadeh *et al.*, "Identification of Possible Cytotoxicity Mechanism of Polyethylenimine by Proteomics Analysis," *Human & Experimental Toxicology*, vol. 35, no. 4, pp. 377–387, 2016.

29. O. Boussif *et al.*, "A Versatile Vector for Gene and Oligonucleotide Transfer into Cells in Culture and in Vivo: Polyethylenimine.," *Proceedings of the National Academy of Sciences*, vol. 92, no. 16, pp. 7297–7301, 1995.

30. L. Jin, X. Zeng, M. Liu, Y. Deng, and N. He, "Current Progress in Gene Delivery Technology Based on Chemical Methods and Nano-Carriers," *Theranostics*, vol. 4, no. 3, pp. 240–255, 2014.

31. M. M. Mady, W. A. Mohammed, N. M. El-Guendy, and A. A. Elsayed, "Effect of Polymer Molecular Weight on the DNA/PEI Polyplexes Properties.," *Romanian Journal of Biophysics*, vol. 21, no. 2, pp. 151–165, 2011.

32. S. M. Moghimi, P. Symonds, J. C. Murray, A. C. Hunter, G. Debska, and A. Szewczyk, "A Two-Stage Poly(ethylenimine)-Mediated Cytotoxicity: Implications for Gene Transfer/Therapy," *Molecular Therapy*, vol. 11, no. 6, pp. 990–995, 2005.

33. S. Wen, F. Zheng, M. Shen, and X. Shi, "Surface Modification and PEGylation of

Branched Polyethyleneimine for Improved Biocompatibility," *Journal of Applied Polymer Science*, vol. 128, no. 6, pp. 3807–3813, 2013.

34. Y. Wang, M. Zheng, F. Meng, J. Zhang, R. Peng, and Z. Zhong, "Branched Polyethylenimine Derivatives with Reductively Cleavable Periphery for Safe and Efficient in Vitro Gene Transfer," *Biomacromolecules*, vol. 12, no. 4, pp. 1032–1040, 2011.

35. C. Song, "CO2 Conversion and Utilization: An Overview," *CO2 Conversion and Utilization*, vol. 809, no. 1, pp. 2–30, 2002.

36. C. Azar and H. Rodhe, "Targets for Stabilization of Atmospheric CO2," *Science*, vol. 276, no. 8, pp. 1818–1819, 1997.

37. Z. O. U. Yong and V. G. Mata, "Adsorption of Carbon Dioxide on Chemically Modified High Surface Area Carbon-Based Adsorbents at High Temperature," *Adsorption*, pp. 41–50, 2001.

38. Z. Yong, V. Mata, and A. E. Rodrigues, "Adsorption of Carbon Dioxide on Basic Alumina at High Temperatures," *Journal of Chemical and Engineering Data*, vol. 45, no. 6, pp. 1093–1095, 2000.

39. S. Satyapal, T. Filburn, J. Trela, and J. Strange, "Performance and Properties of a Solid Amine Sorbent for Carbon Dioxide Removal in Space Life Support Applications," *Energy and Fuels*, vol. 15, no. 2, pp. 250–255, 2001.

40. X. Xu, C. Song, J. M. Andresen, B. G. Miller, and A. W. Scaroni, "Novel Polyethylenimine-Modified Mesoporous Molecular Sieve of MCM-41 Type as High-Capacity Adsorbent for CO2 Capture," *Energy and Fuels*, vol. 16, no. 6, pp. 1463–1469, 2002.

41. N. Beyth, R. Pilo, and E. I. Weiss, "Antibacterial Activity of Dental Cements Containing Quaternary Ammonium Polyethylenimine Nanoparticles," *Journal of*

Nanomaterials, vol. 2012, Article ID 814763, 6 pages, 2012.

42. B. Gao, X. Zhang, and Y. Zhu, "Studies on the Preparation and Antibacterial Properties of Quaternized Polyethyleneimine," *Journal of Biomaterials Science*, vol. 18, no. 5, pp. 531–544, 2007.

43. A. V Briones, T. Sato, and U. G. Bigol, "Antibacterial Activity of Polyethylenimine /Carrageenan Multilayer Against Pathogenic Bacteria," *Advances in Chemical Engineering and Science*, vol. 4, no. 2, pp. 233–241, 2014.

44. G. A. Spoden *et al.*, "Polyethylenimine is a Strong Inhibitor of Human Papillomavirus and Cytomegalovirus Infection," *Antimicrobial Agents and Chemotherapy*, vol. 56, no. 1, pp. 75–82, 2012.

45. P. Bakó, T. Novák, K. Ludányi, B. Pete, L. Tõke, and G. Keglevich, "D-glucose-Based Azacrown Ethers with a Phosphonoalkyl Side Chain: Application as Enantioselective Phase Transfer Catalysts," *Tetrahedron Asymmetry*, vol. 10, no. 12, pp. 2373–2380, 1999.

46. M. N. Guven, M. Seckin Altuncu, F. Demir Duman, T. N. Eren, H. Yagci Acar, and D. Avci, "Bisphosphonate-Functionalized Poly(β-amino ester) Network Polymers," *Journal of Biomedical Materials Research Part A*, vol. 105, no. 5, pp. 1412–1421, 2017.

47. B. Thapa, S. Plianwong, K. Remant Bahadur, B. Rutherford, and H. Uludağ, "Small Hydrophobe Substitution on Polyethylenimine for Plasmid DNA Delivery: Optimal Substitution is Critical for Effective Delivery," *Acta Biomaterialia*, vol. 33, pp. 213–224, March 2016.

48. K. B. Sutradhar and M. L. Amin, "Nanotechnology in Cancer Drug Delivery and Selective Targeting," *ISRN Nanotechnology*, vol. 2014, Article ID 939378, 12 pages, 2014.

49. J. Luo *et al.*, “Well-Defined, Size-Tunable, Multifunctional Micelles for Efficient Paclitaxel Delivery for Cancer Treatment,” *Bioconjugate Chemistry*, vol. 21, no. 7, pp. 1216–1224, 2010.